

Dissertation zur Erlangung des Doktorgrades
der Fakultät für Chemie und Pharmazie
der Ludwig-Maximilians-Universität München

Investigation of the mechanism of toxicity in newly
established models of polyglutamine diseases

Niclas Wilhelm Schiffer

aus

Bad Hersfeld

2008

Erklärung

Diese Dissertation wurde im Sinne von §13 Abs. 3 bzw. 4 der Promotionsordnung vom 29. Januar 1998 von Prof. Dr. Franz-Ulrich Hartl betreut.

Ehrenwörtliche Versicherung

Diese Dissertation wurde selbständig, ohne unerlaubte Hilfe erarbeitet.

München, am 30. Januar 2008

Niclas W. Schiffer

Dissertation eingereicht am: 29.05.2008

1. Gutachter: Prof. Dr. Franz-Ulrich Hartl
2. Gutachter: Prof. Dr. Christian Haass

Mündliche Prüfung am: 15.07.2008

Danksagung

Ich möchte mich bei allen bedanken, die mich während meiner Doktorarbeit am Max-Planck-Institut für Biochemie unterstützt und ermuntert haben.

Mein besonderer Dank gilt Prof. Dr. F.-U. Hartl für die interessante Themenstellung und die Bereitstellung eines Laborplatzes, der der Forschung keine Grenzen setzt. Auch möchte ich mich für die Teilnahme an den Konferenzen in Berlin, Tomar und Eibsee bedanken, die nicht nur interessant sondern auch unheimlich motivierend waren. Seine Leidenschaft für die Wissenschaft ist bewundernswert. Vielen Dank auch an Dr. Manajit Hartl für ihre Ideen und wertvollen Ratschläge.

Dr. Sarah Broadley danke ich für die freundschaftliche Betreuung, ohne die diese Doktorarbeit so nicht zustande gekommen wäre. Sie hat immer ein offenes Ohr gehabt und mir selbstlos nicht nur bei wissenschaftlichen Problemen geholfen.

Prof. Dr. C. Haass danke ich nicht nur für die tolle Kooperation und die Erstellung des Zweitgutachtens sondern auch für seine großartige Unterstützung. Ebenfalls möchte ich mich bei Dr. Bettina Schmid für die freundschaftliche und produktive Zusammenarbeit bedanken. Das Jahr im Fischlabor war unvergesslich, was auch daran lag, dass ich mich nie als Außenständiger gefühlt habe. Deshalb vielen Dank auch an Frauke, Dominik, Sunita und vor allem Matthias und Alex, die unermüdlich Fische für mich angesetzt haben.

Auch möchte ich mich bei Dr. Thomas Hirschberger und vor allem Dr. Armin Giese für die exzellente Zusammenarbeit, Unterstützung und guten Ratschläge bedanken.

Dr. Christian Behrends, Dr. Annette Haacke, Dr. Zoya Ignatova, Dr. Leslie Ripaud, Dr. Gregor Schaffar sowie Dr. Martin Vabulas danke ich für ihre Hilfsbereitschaft und wertvollen Anregungen.

Allen momentanen und ehemaligen Mitarbeitern danke ich für die freundschaftliche und unterstützende Atmosphäre. Mein spezieller Dank gilt Alex, Annette, Carola, Florian, Manal, Kausik, Leslie, Markus, Raluca, Sae-Hun, Sathish, Shruti, Sladjana and Steph, die nicht nur mein Arbeitsalltag sondern auch mein Freizeitleben bereichern haben.

Abschließen möchte ich mit den Menschen, die das alles ermöglicht haben, meinen Eltern und Großeltern. Danke für die bedingungslose Unterstützung, die aufmunternden Worte, das Vertrauen und die Zuversicht. Danke für alles.

1	Summary	1
2	Introduction	3
2.1	Protein folding.....	3
2.1.1	General aspects of protein folding	4
2.1.2	Protein folding <i>in vivo</i>	6
2.2	Protein misfolding and conformational diseases	11
2.2.1	Factors that influence the aggregation of proteins.....	12
2.2.2	Amyloidosis.....	12
2.3	Polyglutamine diseases.....	18
2.3.1	Polyglutamine mediated pathogenesis.....	18
2.3.2	Huntington's disease.....	26
2.3.3	SBMA.....	29
2.4	Models of polyglutamine disease	34
2.4.1	Yeast	35
2.4.2	Zebrafish	36
2.5	Aim of thesis	38
3	Materials and Methods.....	39
3.1	Material.....	39
3.1.1	Instruments.....	39
3.1.2	Chemicals.....	40
3.1.3	Buffers and growth media.....	41
3.1.4	Bacterial and yeast strains, cell and zebrafish lines	45
3.1.5	Plasmids and Oligonucleotides	46
3.1.6	Antibodies.....	48
3.2	Methods.....	49
3.2.1	DNA subjected methods.....	49
3.2.2	Biochemical methods	51
3.2.3	<i>Escherichia coli</i> work.....	55
3.2.4	Yeast work	56
3.2.5	Cell culture work	60
3.2.6	Zebrafish work.....	62
4	Results.....	66
4.1	Development of a zebrafish model for polyglutamine disease suitable for whole organism validation of candidate compounds	67
4.1.1	The establishment and characterization of a zebrafish model of HD.....	67
4.1.2	Identification of compounds that inhibit polyglutamine aggregation.....	77
4.2	N-terminal polyglutamine-containing fragments inhibit androgen receptor transactivation function in a yeast model of SBMA	83

4.2.1	Development and characterization of a yeast model for SBMA	84
4.2.2	A newly established reporter system to evaluate the effect of the polyglutamine stretch on AR transactivation capacity	94
4.2.3	Analysis of the effect of N-terminal polyglutamine-containing AR fragments on AR transactivation capacity	97
4.2.4	Analysis of the effect of polyglutamine-expanded huntingtin exon 1 on AR transactivation capacity	104
5	Discussion	110
5.1	<i>Danio rerio</i> , a new model organism to identify inhibitors of polyglutamine aggregation	112
5.1.1	Zebrafish model for HD	112
5.1.2	The anti-prion compounds inhibit the aggregation of polyglutamine-expanded fragments	115
5.2	<i>Saccharomyces cerevisiae</i> , a model organism to study mechanisms of polyglutamine mediated toxicity	119
5.2.1	A yeast model for SBMA	119
5.2.2	N-terminal polyglutamine-expanded AR fragments decrease AR transactivation capacity	122
5.3	Perspective	127
6	References	129
7	Appendix.....	154
7.1	Abbreviations	154
7.2	Publications and Conference abstracts	156
7.2.1	Publications	156
7.2.2	Conference abstracts.....	157
7.3	Curriculum vitae	158
7.3.1	Personal details	158
7.3.2	Education	158

1 Summary

Several neurodegenerative diseases, including Huntington's disease (HD) and spinal and bulbar muscular atrophy (SBMA), are associated with aberrant folding and aggregation of polyglutamine-expansion proteins. In the first part of this work the zebrafish, *Danio rerio*, was established as a vertebrate HD model permitting the screening for chemical suppressors of polyglutamine aggregation and toxicity. Upon expression in zebrafish embryos, polyglutamine-expanded fragments of huntingtin (htt) accumulated in large SDS-insoluble inclusions, reproducing a key feature of HD pathology. Real-time monitoring of inclusion formation in the living zebrafish indicated that inclusions grow by rapid incorporation of soluble htt species. Expression of mutant htt increased the frequency of embryos with abnormal morphology and the occurrence of apoptosis. Strikingly, apoptotic cells were largely devoid of visible aggregates, suggesting that soluble oligomeric precursors may instead be responsible for toxicity. As in non-vertebrate polyglutamine disease models, the molecular chaperones, Hsp40 and Hsp70, suppressed both polyglutamine aggregation and toxicity. Using the newly established zebrafish model, two compounds of the *N'*-benzylidene-benzohydrazide class directed against mammalian prion proved to be potent inhibitors of polyglutamine aggregation, suggesting common structural mechanisms of aggregation for prion and polyglutamine disease proteins.

In the second part, a novel yeast model of SBMA was set up, which was used to investigate the molecular mechanism behind SBMA and its associated androgen insensitivity syndrome (AIS). SBMA is caused by a polyglutamine-expansion in androgen receptor (AR), a key player in male sexual differentiation. Interestingly, more than 80% of SBMA patients show signs of mild-to-moderate AIS. Upon expression in yeast, polyglutamine-expanded N-terminal fragments of AR aggregate and cause toxicity, reproducing key features of SBMA pathology. Pronounced toxicity was associated with nuclearly-localized AR fragments with 102 Q, which primarily accumulated as soluble oligomers in

the 200 – 500 kDa size range. Analysis using a luciferase reporter system revealed that full-length polyglutamine-expanded AR is fully functional in transactivation, but becomes inactivated in the additional presence of aggregating N-terminal fragments. Furthermore, greatest impairment of full-length AR activity correlated with its interaction with soluble oligomers of AR fragments. Taken together, the polyglutamine-expansion mutation in AR promotes a gain-of-function mechanism that results in the formation of toxic oligomers, which in turn cause loss-of-function through direct interaction with full-length AR perhaps by inducing its misfolding. These results provide new mechanistic insight into the loss-of-function mechanism behind AIS in SBMA.

2 Introduction

In 1854 the German physician scientist Rudolph Virchow introduced the term 'amyloid', derived from the Latin and Greek terms for starch (amylum and amylo, respectively), to describe a substance in the cerebral corpora amyloidea that caused an abnormal macroscopic appearance of the latter. He was misled by the observation that the substance stained positive at a iodine staining reaction, a common test to identify cellulose or starch. Later, it was shown that not carbohydrates but proteins with a propensity to undergo changes in conformation form amyloidogenic fibrils (Sipe and Cohen, 2000). Nowadays, the term amyloid is associated with a growing number of human diseases, for example Alzheimer's, Parkinson's and Polyglutamine diseases but also Spongiform encephalopathies, that are associated with misfolded proteins that form such amyloidogenic fibrils. Why do proteins 'misfold' and how is this process linked to disease?

2.1 Protein folding

Proteins ('prota', greek, meaning 'of primary importance') are, like other biological macromolecules such as polysaccharides and nucleic acids, essential parts of all living organisms. They participate in every process within the cell and are involved in biochemical reactions, have structural or mechanical functions and are also important in cell signaling, immune responses, cell adhesion, and the cell cycle.

Proteins are composed of amino acids, which consist of an amino group, a carboxyl group, a hydrogen atom and a variable side chain bound to a carbon atom. Twenty standard amino acids exist that differ in the side chain and as a result thereof, contribute unique properties. The amino acids are arranged in a linear chain and joined together by peptide bonds between the α -carboxyl group of one amino acid and the α -amino group of another. However, to become functionally active the amino acid sequence has to adopt a unique three-

dimensional structure, which is achieved via sterical limits and complex interactions between the amino acids. This condition is regarded as native state or physiologically folded providing the energetically most stable structure.

2.1.1 General aspects of protein folding

One of the most fundamental phenomena in nature is the ability of proteins to fold *de novo* to their functional *i.e.* native states in a physiologically-relevant time (Jahn and Radford, 2005). Anfinsen demonstrated that the information required to reach the native state is encoded in the primary structure of a protein (Anfinsen, 1973). Theoretically, a small polypeptide would require at least a period of time equivalent to the age of the universe to arrive at its correct native conformation if it is to attain its correctly folded configuration by sequentially sampling all the possible conformations (Levinthal, 1969). In reality however, an average-sized protein folds usually in less than one second (Karplus, 1997). Thus, it seems likely that proteins do not fold randomly but rather according to specific, defined pathways.

It is easy to imagine that there may not be just a single route to the native state. Towards the native structure, random fluctuations occur, and different native as well as non-native contacts form. Native interactions between residues are assumed to be more stable than non-native contacts, and as such contacts form, the number of available conformations is reduced. As a consequence thereof, the folding of the polypeptide chains is driven towards the native state (Jahn and Radford, 2005).

Energy landscapes are used to describe the search of the unfolded polypeptide down a funnel-like energy profile towards the native structure (Figure 1). Each polypeptide sequence follows its own energy landscape that is unique like a fingerprint. Partially folded states on this landscape can be intrinsically prone to aggregation, and favorable intermolecular contacts may lead to their association and ultimately to protein-misfolding diseases. Since the number of possible interactions increases with the size of the polypeptide chain, small single domain proteins, usually less than 100 amino acids in length fold

relatively fast (sub-second timescale). The folding landscape of these proteins is usually relatively smooth, with only a small number of possible kinetic traps (Daggett and Fersht, 2003; Fersht, 2000). However, the larger the proteins are (more than 100 residues), the more they face a much rougher landscape in which states of folding intermediates are commonly populated on the way to the native protein. A possible explanation for this is that larger chains have a higher tendency to collapse in aqueous solution forming more compact states. These compact states include both, native and non-native interactions and the reorganization of the interresidual contacts may include high free-energy barriers. As a result thereof, partially folded or 'intermediate' states accumulate. This can be beneficial, if the intermediate is productive for folding, so-called 'on-pathway,' or unprofitable if the native state cannot be reached without substantial re-organizational events (off-pathway). Parallel folding of different regions also exists, as it is the case in large multidomain proteins, where a final folding step establishes all native intra- and interdomain contacts resulting in the final functional form (Radford *et al.*, 1992).

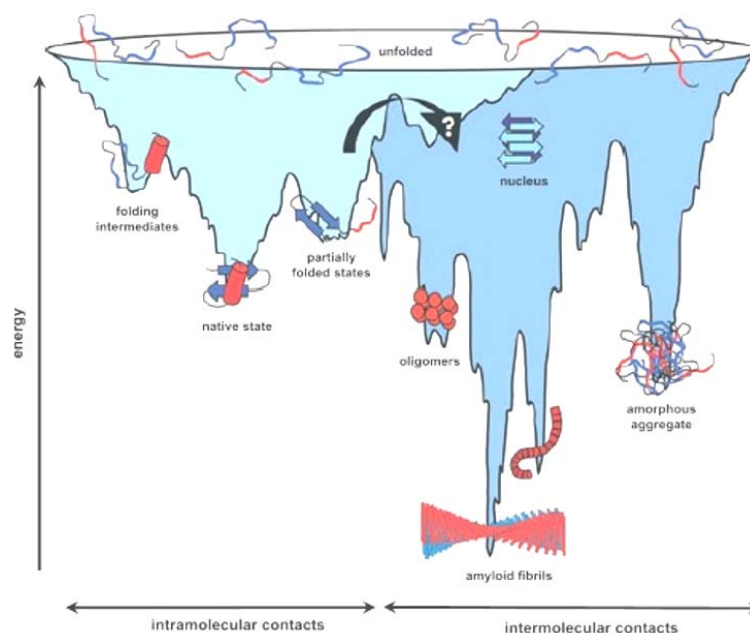


Figure 1: Schematic energy landscape of protein folding and aggregation.

Rugged surface that shows kinetic traps and energy barriers leading to a multitude of conformations towards the native state by intramolecular contact formation, or, upon intermolecular contacts towards the formation of amyloid fibrils (adapted from Jahn and Radford, 2005).

2.1.2 Protein folding *in vivo*

In a living cell, the folding of a polypeptide into its native conformation is not an issue that is left to chance. The *in vivo* situation is much more complex than the *in vitro* situation. For instance, the interior of a cell is a crowded and dynamic environment. The protein concentration in a cell has been estimated to be as high as 300 mg/ml, which equals approximately 20 - 30% of the total cellular volume (Zimmerman and Trach, 1991). As a consequence thereof, the mutual impenetrability of all solute molecules implicates a non-specific steric repulsion. This phenomenon has been described as 'molecular crowding' or 'excluded volume' effect (Ellis, 2001; Minton, 2001). Steric exclusion results in an increase in the effective concentration of each macromolecular species and since aggregation is highly concentration dependent, molecular crowding promotes the aggregation of partially folded and misfolded polypeptides. Molecular crowding favors association of macromolecules in biochemical equilibrium as the available volume increases upon association of macromolecules (Zimmerman and Trach, 1991). Concomitantly, small structures are favored over large. Applied to macromolecules, the collapse of nascent polypeptide chains into compact functional proteins or the aggregation of unfolded polypeptides into ordered structures is the logical consequence.

Another obstacle that has to be overcome *in vivo* i.e. in the cell is the vectorial synthesis of the polypeptides. In eukaryotes, translation occurs on a timescale up to several minutes. Since stable folding of a domain (100 - 300 amino acids) can only occur after its complete synthesis, parts of nascent polypeptides chains permanently face misfolding and aggregation because hydrophobic stretches cannot immediately be buried upon folding (Creighton, 1990; Jaenicke, 1991). The close proximity to other nascent chains (of the same type as it is the case in polyribosomes) additionally increases the tendency to aggregate (Hartl and Hayer-Hartl, 2002).

Because of the challenges posed by the *in vivo* folding environment, a large network of proteins, including molecular chaperones and proteases, has evolved as a quality control system to promote the correct folding of proteins on one hand and the rapid degradation of mutated or misfolded polypeptides on

the other. Protein homeostasis is therefore maintained by continuously subjecting the entirety of proteins in the cell to this quality-control system (Kleizen and Braakman, 2004; Young *et al.*, 2004).

2.1.2.1 Molecular chaperones

The folding of newly synthesized proteins is assisted by molecular chaperones. They guide the polypeptides through the landscape of folding to their native state by multiple, sequential interactions thereby preventing aggregation (Maier *et al.*, 2005; Young *et al.*, 2004). Importantly, they do not contribute conformational information to the folding process (Hartl and Hayer-Hartl, 2002).

The cytosol provides a well-developed network of chaperones which cooperate in a topologically and timely ordered manner (Figure 2; Ellis and Hartl, 1996; Frydman and Hartl, 1996; Hartl and Hayer-Hartl, 2002; Young *et al.*, 2004). In eukaryotes, the emerging nascent chain is received by NAC (nascent chain-associated complex), a ribosome-associated heterodimeric complex. Although not yet fully elucidated NAC probably binds to and therefore protects hydrophobic peptide stretches (Young *et al.*, 2004).

The cytosolic Hsp70s (heat shock protein 70) *i.e.* nonribosome-binding, form part of the so-called Hsp70 system that is highly conserved in prokaryotes as well as in eukaryotes. With cochaperones of the Hsp40 family, the Hsp70s function by binding and releasing extended polypeptides segments of proteins that are in a non-native state (Hartl and Hayer-Hartl, 2002). Thereby, the carboxy-terminal domain of Hsp40s shows a high affinity for hydrophobic peptides and can thus recruit Hsp70s to nascent chains (Langer *et al.*, 1992; Rudiger *et al.*, 2001; Sha *et al.*, 2000). The interaction of the unfolded protein and Hsp70 is not restricted to a single event and unfolded polypeptides can undergo multiple rounds of binding and release. In particular, nascent chains expose multiple hydrophobic stretches requesting the binding of several Hsp70 chaperone to the same polypeptide.

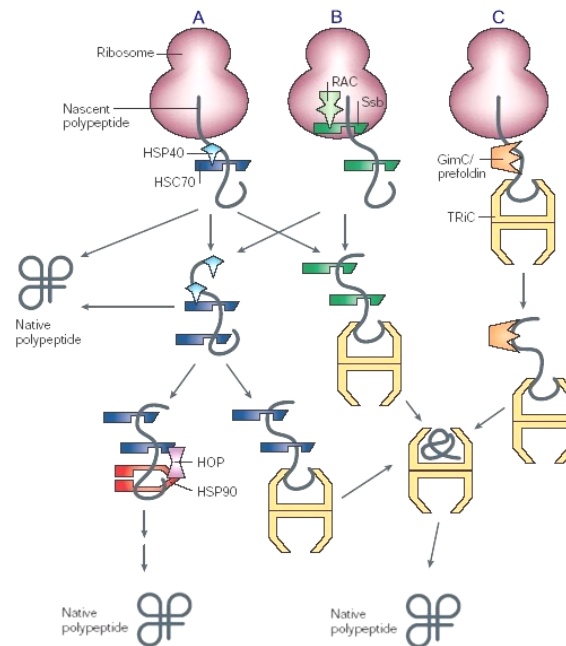


Figure 2: Schematic representation of the chaperone network of the eukaryotic cytosol.

(A) In mammals, Hsc70 and Hsp40 interact with the nascent polypeptide chain emerging from the ribosome. (B) In *Saccharomyces cerevisiae*, RAC recruits Ssb to bind nascent chains. (C) The folding to the native states of actin and tubulin nascent chains is assisted by GimC/prefoldin and TRiC. In addition, Hsc70 and Ssb also cooperate with TRiC in the folding. Other nascent chains can fold spontaneously, are assisted by Hsc70 or are passed to Hsp90 via the co-chaperone HOP that mediates the transfer from Hsc70 to Hsp90 (adapted from Young *et al.*, 2004).

Additional complexes that recognize hydrophobic stretches and are involved in nascent polypeptide binding, particularly of actin and tubulin, are GimC in *S. cerevisiae* and prefoldin in mammals, respectively (Geissler *et al.*, 1998; Vainberg *et al.*, 1998). In an ATP-independent manner, hydrophobic extensions enable recognition of substrates and probably mediate the transfer of polypeptides to chaperonin TRiC (Martin-Benito *et al.*, 2002). The chaperonins differ from the other cytosolic chaperones with regard to the folding mechanism. Chaperonins are relatively large, cylindrical complexes that provide a physically defined compartment inside. Unfolded polypeptides get captured through hydrophobic interactions with multiple chaperonin subunits and are subsequently relocated into the central ring cavity. The latter enables complete proteins or domains to fold while being sequestered from the cytosol. This way, the chaperonins prevent non-productive interactions with other unfolded

polypeptides (Hartl and Hayer-Hartl, 2002; Meyer *et al.*, 2003). The activity of all chaperonins is ATP-dependent and folding cycles are repeated until the protein reaches its native state.

Another ATP-regulated chaperone in the eukaryotic cytosol is the highly abundant and essential chaperone Hsp90. (Richter and Buchner, 2001; Young and Hartl, 2000; Young *et al.*, 2001). The homodimeric Hsp90 is involved in the folding of a diverse set of proteins, including transcription factors *e.g.* steroid hormone receptors, regulatory kinases and other proteins, often in cooperation with Hsc70 (Young *et al.*, 2004).

Lastly, chaperones of the Hsp100 family unfold proteins or disrupt protein aggregates in an ATP-dependent manner (Ben-Zvi and Goloubinoff, 2001). That was shown for *e.g.* Hsp104 which upon co-expression reduced the formation of polyglutamine aggregates in yeast and *Caenorhabditis elegans* (Krobitsch and Lindquist, 2000; Satyal *et al.*, 2000).

2.1.2.2 Cellular quality control

Proteins that become useless, as is the case for regulatory proteins as well as misfolded proteins, undergo a sophisticated system for protein degradation. This is particularly important for misfolded proteins since they might exert harmful properties. Whenever chaperones fail to refold misfolded proteins, another system has to become responsible for their disposal.

The ubiquitin-proteasome system (UPS) is probably the most prominent mechanism for disposing of faulty proteins. In this system, multimers of the ubiquitin polypeptide (Ub) are covalently attached to proteins and are thereby labelled for targeting to and degradation by the 26S proteasome (Hershko and Ciechanover, 1998). The 26S proteasome is a multi-subunit, self-compartmentalized protease composed of a 20S core complex bearing rather non-specific proteolytic sites within its cavity and two axial 19S regulatory caps (Pickart and Cohen, 2004). Subsequent to deubiquitylation and unfolding, the substrates are translocated into the 20S catalytic chamber where they are digested to peptides that are 2-24 residues long (Goldberg, 2003; Kisselev *et al.*, 1999). The

peptides released by the proteasome are digested by cellular endopeptidases and finally hydrolyzed to amino acids by aminopeptidases (Saric *et al.*, 2004).

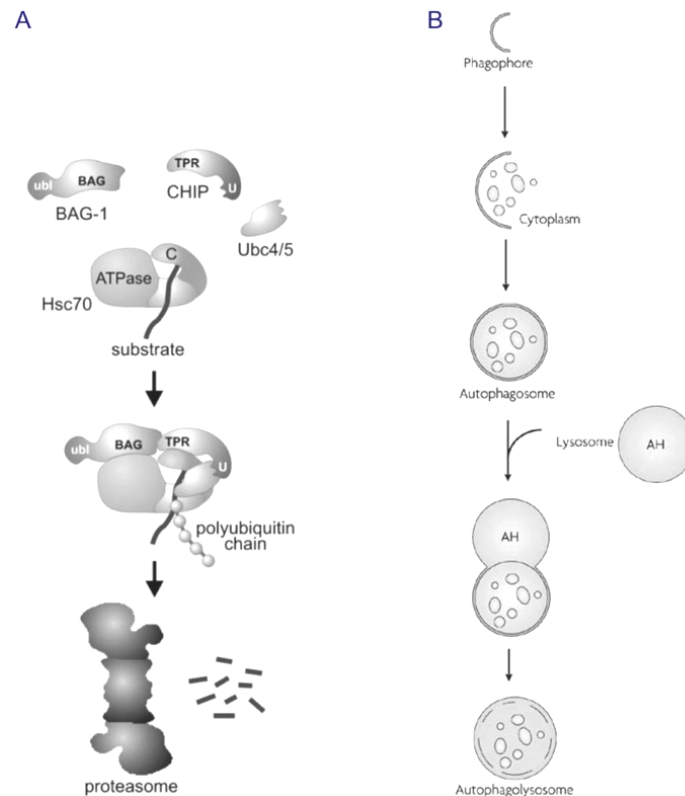


Figure 3: Cellular mechanism of protein degradation

(A) Schematic overview of proteasomal degradation. BAG-1, CHIP and ubiquitin-conjugating enzymes of the Ubc4/5 family associate with substrate-bound Hsc70. Thereby, BAG-1 binds to the adenosine triphosphatase domain of peptide-bound Hsc70, Ubc4/5 is thought to bind to the carboxyl terminal U-box (u) of CHIP which associates with the carboxyl terminal domain of Hsc70 (c). The ubiquitin-like domain of BAG-1 (ubl) remains exposed in the formed complex and serves as a proteasomal sorting signal for the ubiquitinated substrate which finally gets degraded by the proteasome. (B) Schematic overview of macroautophagy. The initial phagophore that is formed by a membrane of unknown origin expands to sequester cytoplasm and closes to form the double-membrane autophagosome. The latter fuses with a lysosome to form the autophagolysosome and the acid hydrolases therein (AH) degrade its content. The resulting macromolecules are released back into the cytosol (Alberti *et al.*, 2003; Rubinsztein *et al.*, 2007).

Since a large number of proteins (approx. 25% of total proteome) are destined to enter secretory pathways and herein, the endoplasmic reticulum (ER) is responsible for their structural maturation, the ER harbors two distinct mechanisms to handle misfolded proteins. The first one, the unfolded protein

response (UPR), increases the folding capacity of the ER in response to ER-directed stress (Schroder and Kaufman, 2005; van Anken and Braakman, 2005a; van Anken and Braakman, 2005b). The second one, termed ER-associated degradation (ERAD), recognizes and targets terminally misfolded proteins across the ER membrane into the cytosol. There they meet the fate of all cytosolic misfolded proteins, degradation by the UPS (Romisch, 2005).

Aggregates however, seem to undergo another way of clearance. Although it was shown that aggregates are to a large extent reactive with anti-ubiquitin antibodies, as they are recognized by the ubiquitin conjugation system as misfolded species, they seem to be an insurmountable obstacle for the proteasome. They may even inhibit proteasomal function, possibly by “choking” the proteasome chamber (Bence *et al.*, 2001; Bennett *et al.*, 2005; Venkatraman *et al.*, 2004). More complex substrates including protein complexes and organelles are degraded via autophagy (Figure 3). This process is characterized by the recognition and engulfment of targeted proteins or organelles into autophagosome vesicles, double membrane structures, that become fused with lysosomes. As a consequence thereof, the vesicles including their contents are broken down by the lysosomal hydrolases (Levine and Klionsky, 2004). Autophagy was also shown to degrade large aggregates composed of a polyglutamine-expanded huntingtin fragment (Ravikumar *et al.*, 2002; Ravikumar *et al.*, 2004; Yamamoto *et al.*, 2000) and also the clearance of mutated forms of α -synuclein that cause Parkinson’s disease, seems to be highly dependent on autophagy (Webb *et al.*, 2003). Thus peptides may become inaccessible to the proteasome when they oligomerise.

2.2 Protein misfolding and conformational diseases

Since the native conformation of proteins is not rigid, random conformational fluctuations can lead to the transient formation of aggregation-prone intermediate states that can initiate aggregation (Jahn and Radford, 2005). It is easy to imagine that the function of the cellular quality-control system is essential and hence, small irregularities have detrimental consequences. Large

quantities of partially folded proteins can accumulate, the capacity of the quality-control system gets overwhelmed and intracellular aggregates can form before refolding or degradation is possible (Barral *et al.*, 2004).

2.2.1 Factors that influence the aggregation of proteins

Although it was shown that many proteins not known to be involved in misfolding diseases can aggregate *in vitro*, the propensity to undergo aggregation varies between molecules (Guijarro *et al.*, 1998). It is mostly dependent on the physicochemical features of the molecules such as charge, secondary-structure propensities and hydrophobicity (Chiti *et al.*, 2003). In addition, external factors that promote exposure of hydrophobic side chains for example, low pH or fragmentation can facilitate aggregation (Dobson, 2003).

2.2.2 Amyloidosis

Incorrectly folded better known as misfolded proteins are polypeptides that are trapped somewhere in the folding pathway and did not achieve native conformation. These misfolded proteins stress the cell not only due to the reduction in the quantity of functional protein but also they often gain characteristics that cause toxicity. This is reflected in grave human disorders that are caused by such proteins that failed to adopt, or remain in, their native functional conformational state (Chiti and Dobson, 2006). A very prominent class among those are the so-called 'amyloidosis' (Stefani, 2004).

2.2.2.1 Common aspects

The name amyloidosis derives from the characteristic fibrils these aggregated proteins form, 'amyloid fibrils' *in vitro* and 'intracellular inclusions' *in vivo*, respectively (Westermarck *et al.*, 2005), that can be stained with the dye Congo red in a manner similar to starch (amylose) (Sipe and Cohen, 2000). Remarkably, although the precursor proteins that comprise the fibrils are structurally very diverse, they do not share any obvious sequence identity nor a

similar secondary structure composition, the associated fibrils however, are very similar in their overall properties and appearance (Sunde and Blake, 1997; Tycko, 2004).

In addition to non-neuropathic systemic amyloidoses, the so-called neuropathic amyloidoses exist in which aggregation occurs in the brain (Table 1:). Well known examples are Alzheimer's, Parkinson's and polyglutamine disease but also Spongiform encephalopathies (Chiti and Dobson, 2006; Westermarck *et al.*, 2005). A pathological hallmark all these diseases have in common are the proteinaceous deposits found in patients. These deposits are made of a major protein component that forms the core and then additional associated species, including metal ions, glycosaminoglycans, collagen and many others (Alexandrescu, 2005; Hirschfield and Hawkins, 2003). Interestingly, the toxicity is most likely independent of the function of the normal protein, but instead dependent on aggregates or their precursors in the aggregation pathway, thus toxicity is, at least in part, the result of a 'gain of function' mechanism.

Table 1: A summary of the main neuropathic amyloidoses and the proteins or peptides involved.

Clinical syndrome	Fibril component
Alzheimer's disease	A β peptides (1–40, 1–41, 1–42, 1–43); Tau
Spongiform encephalopathies	Prion protein (full-length or fragments)
Parkinson's disease	α -synuclein (wild type or mutant)
Fronto-temporal dementias	Tau (wild type or mutant)
Familial Danish dementia	ADan peptide
Familial British dementia	ABri peptide
Hereditary cerebral haemorrhage with amyloidoses	Cystatin C (minus a 10-residue fragment); A β peptides
Amyotrophic lateral sclerosis	Superoxide dismutase (wild type or mutant)

Clinical syndrome	Fibril component
Dentatorubro-pallido-Luysian atrophy	Atrophin 1 (polyglutamine expansion)
Huntington's disease	Huntingtin (polyglutamine expansion)
Cerebellar ataxias	Ataxins (polyglutamine expansion)
Kennedy's disease	Androgen receptor (polyglutamine expansion)
Spino cerebellar ataxia 17	TATA box-binding protein (polyglutamine expansion)

2.2.2.2 Structure and formation of amyloid fibrils

Much effort was spent to elucidate the aggregation pathway towards the final amyloid fibril (Figure 4). Transmission electron microscopy (TEM) and atomic force microscopy revealed, that the fibrils, composed of proteins of very different size and native structure, usually consist of a number (typically 2-6) of protofilaments, each about 2-5 nm in diameter (Serpell *et al.*, 2000). These protofilaments twist together to form rope-like fibrils that are typically 7-13 nm wide (Serpell *et al.*, 2000; Sunde and Blake, 1997) or associate laterally to form long ribbons that are up to 30 nm wide and 2-5 nm thick (Bauer *et al.*, 1995; Pedersen *et al.*, 2006; Saiki *et al.*, 2005). In each protofilament the protein or peptide molecules are arranged so that the polypeptide chain forms β -strands that run perpendicular to the long axis of the fibril structure (Sunde and Blake, 1997), a feature that confers outstanding stability and insolubility. Thereby, the fraction of the residues that are incorporated in the core structure can vary substantially and the influence of the side chains results in significant differences in detail (Fandrich and Dobson, 2002).

Since it was shown that many proteins not known to be involved in amyloid disease can aggregate *in vitro* into amyloid-like structures, it seems that the formation of the cross- β fold is an inherent property of the polypeptide chain (Guijarro *et al.*, 1998). Interestingly, the major driving forces for aggregation and correct folding are the same, namely the formation of hydrogen bonds and the

burial of hydrophobic surface area. The key residues however, that drive either aggregation or correct folding are different (Chiti *et al.*, 2002b).

Amyloid fibril formation has many characteristics of a nucleated growth mechanism, which means, that a lag phase is followed by a rapid exponential growth phase. In this process, the lag phase is the time required for nuclei formation, which is followed rapidly by further association of either monomers or oligomers with the nucleus. (Naiki *et al.*, 1997; Pedersen *et al.*, 2004; Serio *et al.*, 2000; Uversky *et al.*, 2002).

The formation of the amyloid fibrils is preceded by the formation of a series of metastable, nonfibrillar species which have been termed protofibrils (Harper *et al.*, 1997a; Harper *et al.*, 1997b; Walsh *et al.*, 1999; Walsh *et al.*, 1997). The latter differ in their appearance and can adopt a spherical bead structure or beaded chains that again can form annular structures upon circularization. All of these structures which have been observed amongst others for A β peptide, α -synuclein or polyglutamine-containing proteins, have the bead-like units of 2-5 nm in diameter in common (Conway *et al.*, 2000; Harper *et al.*, 1997a; Harper *et al.*, 1997b; Kaye *et al.*, 2004; Walsh *et al.*, 1999; Walsh *et al.*, 1997). These species are characterized by extensive β -structure as well as the ability to bind Congo red and interestingly, a specific antibody can bind to protofibrillar species from different sources but not to their corresponding monomeric or fibrillar states. This suggests, that similar to the amyloid fibrils, already these soluble amyloid oligomers have important common structural elements independent of the primary structure (Kaye *et al.*, 2003). Since the β -strands within in the sheets of the protofibrils are initially misaligned they have to undergo several detachment and re-annealing events or internal structural reorganization within the sheets is necessary towards the formation of the final amyloid fibrils (Petty *et al.*, 2005). Not many details are known about the formation of the protofibrils but it was suggested that structured protofibrillar species can form from the assembly of small and relatively disorganized oligomers (Nguyen and Hall, 2004). Hence, large, globular proteins need to (partially) unfold to aggregate into amyloid fibrils (Dobson, 1999; Kelly, 1998; Uversky and Fink, 2004). Thus, it is not surprising that among the familial forms of disease often mutations can be found,

that destabilize the native structure and as a consequence thereof, increase the population of nonnative states (Canet *et al.*, 2002; Ferrao-Gonzales *et al.*, 2000; Raffin *et al.*, 1999). Also fragments of globular proteins generated by proteolysis, as it is the case *e.g.* in several polyglutamine diseases, tend to aggregate most likely because of their inability to fold in the absence of the remainder of the polypeptide chain (Chiti and Dobson, 2006).

The polyglutamine fibrils are of particular interest because of the possibility that the additional array of hydrogen-bonding interactions involving the side chains results in a structure significantly different from that of the classical amyloid fibrils (Chiti and Dobson, 2006).

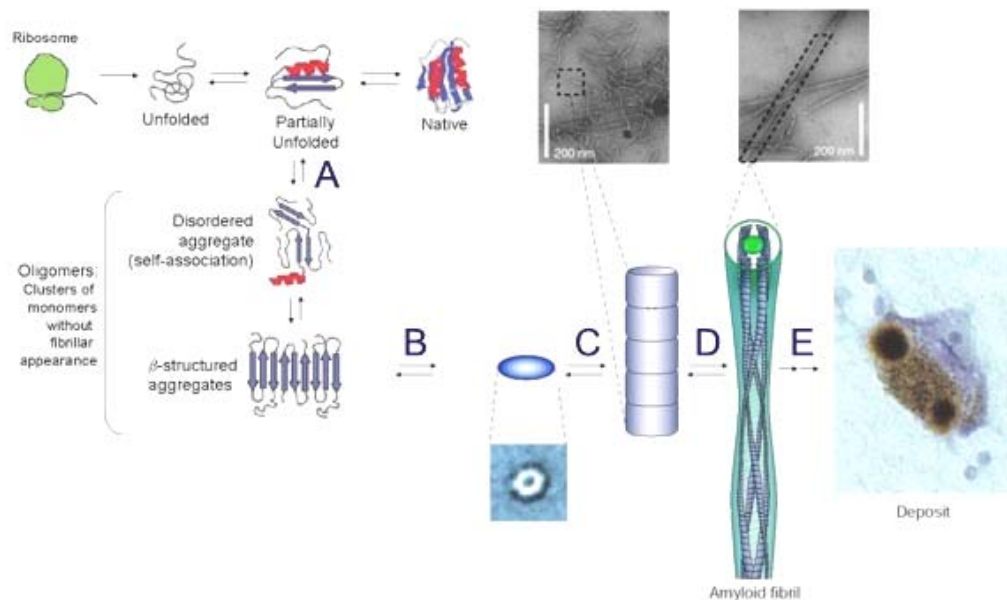


Figure 4: Schematic representation of the general mechanism of amyloid fibril formation

(A) Aggregation-prone folding intermediates, often rich in β -sheet structure, associate with each other to form soluble oligomers, (B) which assemble into amorphous or ring-shaped structures. (C) These undergo further assembly into protofibrils or protofilaments and finally (D), mature amyloid fibrils which often accumulate in plaques or inclusion bodies (E) (adapted from Chiti and Dobson, 2006; Dobson, 2003).

For the sake of completeness, it should be mentioned that aggregation of globular proteins is not restricted to partial unfolding. Thermodynamic studies revealed that for some proteins *e.g.* the pathogenic variant of ataxin-3,

aggregation occurs via the formation of native-like oligomers, that undergo structural reorganization to form amyloid protofibrils that have extensive β -structure (Chow *et al.*, 2004; Plakoutsi *et al.*, 2005). In terms of determinants that favour the aggregation of an unfolded polypeptide, hydrophobicity of the side chains, low net charge and a high propensity to form β -sheets must be noted (Broome and Hecht, 2000; Chiti *et al.*, 2002a; Chiti *et al.*, 2002b; Otzen *et al.*, 2000; Schmittschmitt and Scholtz, 2003; Wurth *et al.*, 2002).

2.2.2.3 Aggregation mediated toxicity

Recent findings suggest that not the intracellular inclusions but more likely precursors to amyloid fibrils, such as low-molecular-weight oligomers and/or structured protofibrils are the pathogenic species (Arrasate *et al.*, 2004; Behrends *et al.*, 2006). This would explain the observed onset of toxic manifestations before intracellular deposits of the respective protein were detectable in either Alzheimer's disease, Parkinson's disease or Huntington's disease (Bennett *et al.*, 2005; Kitada *et al.*, 1998; Larson *et al.*, 1999; Moechars *et al.*, 1999). Concomitantly, prefibrillar forms of non-disease-related proteins turned out to be highly toxic to cultured fibroblasts and neurons, whereas the monomeric native states and the amyloid-like fibrils displayed little toxicity (Bucciantini *et al.*, 2002; Malisauskas *et al.*, 2005; Sirangelo *et al.*, 2004). Why do these prefibrillar forms cause toxicity? Unfortunately, only little is known about how these prefibrillar forms mediate toxic effects. Most likely, toxicity results from the exposure of an array of groups on their surface that are normally buried in globular proteins or dispersed in highly unfolded peptides. This probably results in a set of inappropriate interactions with cellular components, such as membranes or proteins what leads to the malfunctioning of crucial aspects of the cellular machinery and ultimately to cell death (Chiti and Dobson, 2006). The fact that small aggregates have a higher proportion of residues on their surface in comparison to larger aggregates, such as amyloid fibrils, could explain the increased toxicity of the former.

2.3 Polyglutamine diseases

The polyglutamine disorders represent the most common form of inherited neurodegenerative disease (Riley and Orr, 2006). They are caused by expansion of a translated CAG repeat that results in an extended stretch of glutamine residues in the disease protein. Actually, nine neurodegenerative disorders are known to be caused by expansion of an translated CAG repeat Huntington's disease (HD), Dentatorubral-pallidoluysian atrophy (DRPLA), Spinocerebellar ataxias SCA1, SCA2, SCA3/MJD, SCA6, SCA7 and SCA17 and Spinal bulbar muscular atrophy (SBMA, or Kennedy's disease). Apart from the polyglutamine stretch, the proteins involved are structurally unrelated but are thought to share common pathogenic mechanisms (Orr and Zoghbi, 2001).

Interestingly, the polyglutamine stretch seems to be unique to the human genome although genes were identified that are highly homologous to the polyglutamine ones. The fact that the polyglutamine stretch itself however is not conserved within these genes suggests that it is not necessary for normal function (Hardy and Orr, 2006). The length of a non-expanded polyglutamine tract is polymorphic and usually ranges from 10 to 35 glutamines in normal individuals. Independent of the protein involved in polyglutamine disease, an extension beyond this threshold causes the respective disease. This seems to be a result of a conformational change in the protein, which promotes aggregation of the latter (Scherzinger *et al.*, 1997). The CAG sequence is an unstable repetitive element and since mutant CAG repeats show both somatic and germline instability the repeat grows upon passage from generation to generation. As a consequence thereof affected members in successive generations have an earlier age of onset and a more rapidly progressing form of the disease, a phenomenon that is known as genetic anticipation (Gatchel and Zoghbi, 2005).

2.3.1 Polyglutamine mediated pathogenesis

The group of polyglutamine diseases which are with the exception of the X-linked androgen receptor inherited autosomal dominantly share many features with other families of neurodegenerative diseases (Zoghbi and Orr,

2000). All of these disorders are progressive, typically strike at midlife and have a course that consists of an extended period of neuronal dysfunction followed by neuronal loss and eventually death 10–20 years after onset (Hardy and Orr, 2006). The age of onset and the severity of the disease is inversely related to the length of the polyglutamine tract, a characteristic of this group of neurodegenerative disorders. The propensity to aggregate however, increases with the number of glutamines. Thus, a hallmark of the diseases is the accumulation of insoluble material within neurons but also peripheral tissue.

In the beginning it was thought that the genetic similarities among these polyglutamine mediated neurological disorders share a common mechanism of pathogenesis entirely dependent on the toxic properties of the polyglutamine tract. This was associated with the enhanced ability of polyglutamine peptides to form extra- and intranuclear aggregates. The concept of large inclusions of mutant polyglutamine being closely associated with neurodegenerative disease, has become suspect. Increasing evidence suggests that IBs, and the fibrillar aggregates therein, may not represent the primary neurotoxic agent (Arrasate *et al.*, 2004; Behrends *et al.*, 2006; Cleary *et al.*, 2005; Ross and Poirier, 2005; Walsh *et al.*, 2002). Instead, soluble intermediates in the aggregation pathway are likely to be the key toxic species, giving rise to neurodegeneration through various mechanisms. (Bennett *et al.*, 2005; Schaffar *et al.*, 2004).

Another fact that suggests more complicated pathologic mechanism is that although the disease-causing proteins are widely expressed in the central nervous system and also in peripheral tissues, nevertheless specific collections of neurons degenerate in each disease. This in turn results in characteristic patterns of pathology and clinical symptoms. For instance, the region mainly affected in SBMA includes the spinal and bulbar motor neurons whereas in HD it is the caudate nucleus, putamen and the cerebral cortex (Table 2:). This might be due to very specific interactions of polyglutamine-expanded proteins with other cellular constituents during the aggregation process which can even result in recruitment of the latter into the aggregates (McC Campbell *et al.*, 2000; Nucifora *et al.*, 2001; Preisinger *et al.*, 1999). Presumably, exposed β -sheets in intracellular

polyglutamine monomers or oligomers interact unfavorably with the surface of other proteins thereby disturbing various cellular functions (Sakahira *et al.*, 2002b). But also the protein context of the expanded polyglutamine is hypothesized to have key roles in disease-specific processes since it was shown that the flanking regions affect the toxicity of the polyglutamine stretch (Dehay and Bertolotti, 2006; Duennwald *et al.*, 2006a). Interestingly, cell specificity declines with the progression and severity of disease for instance juvenile-onset or large polyglutamine expansions, respectively (Zoghbi and Orr, 2000).

Several non-exclusive hypotheses were proposed to explain polyglutamine mediated neurodegeneration. Thereby, the most prominent include the inactivation of essential transcription factors and inhibition of the ubiquitin proteasome system. It was shown that glutamine-rich regions trigger the transient association of transcriptional regulators into their transcriptional complexes (Gerber *et al.*, 1994). Being presumably flexible and unstructured they probably recruit additional factors or bridge large distances, as it is required in transcription (Faux *et al.*, 2005). Thus it seems possible that polyglutamine expanded species, monomers but also oligomers, interact with such glutamine-rich regions of transcriptional regulators and as a consequence thereof the activity of the latter is disturbed (Cha, 2000; Sakahira *et al.*, 2002b; Schaffar *et al.*, 2004).

Inhibition of the ubiquitin proteasome system is considered as the second major explanation for polyglutamine mediated toxicity due to the fact that polyglutamine containing fragments accumulate and form inclusions which were shown to be relatively stable. It was observed that these inclusions contain not only molecular chaperones but also components of the ubiquitin proteasome system (Ciechanover and Brundin, 2003; Sakahira *et al.*, 2002b). Since they were also tested ubiquitin-positive it seems that these polyglutamine expanded proteins are recognized as misfolded species that have to be degraded by the ubiquitin proteasome system (Li *et al.*, 1998a). If impairment of the ubiquitin proteasome system contributes to the polyglutamine diseases is still under discussion but recent studies support this hypothesis (Bennett *et al.*, 2007; Pandey *et al.*, 2007).

Table 2: Molecular characteristics of polyglutamine neurodegenerative diseases

Disease	Gene product	Normal CAG(n)	Expanded CAG(n)	Protein localization	Brain regions most affected
SBMA	Androgen receptor	9–36	38–62	Nuclear and cytoplasmic	Anterior horn and bulbar neurons, dorsal root ganglia
HD	Huntingtin	6–34	36–121	Cytoplasmic	Striatum, cerebral cortex
SCA1	Ataxin-1	6–44	39–82	Nuclear in neurons	Cerebellar Purkinje cells, dentate nucleus; brainstem
SCA2	Ataxin-2	15–31	36–63	Cytoplasmic	Cerebellar Purkinje cells, brain stem, fronto-temporal lobes
SCA3	Ataxin-3	12–41	62–84	Cytoplasmic	Cerebellar dentate neurons, basal ganglia, brain stem, spinal cord
SCA6	CACNA1A	4–18	21–33	Cell membrane	Cerebellar Purkinje cells, dentate nucleus, inferior olive
SCA7	Ataxin-7	4–35	37–306	Nuclear	Cerebellum, brain stem, macula, visual cortex
SCA17	TATA-BP	29–42	47–55	Nuclear	Cerebellum, cerebral cortex
DRPLA	Atrophin-1	6–36	49–84	Cytoplasmic	Cerebellum, cerebral cortex, basal ganglia, Luys body

However, other hypotheses came up in order to explain the toxicity of the polyglutamine expanded proteins. In concordance with the inactivation of nuclear transcription factors the functions of many additional cytoplasmic and

nuclear proteins that were found in aggregates are altered (Harjes and Wanker, 2003; Li and Li, 2004). It was also suggested that polyglutamine expanded proteins may damage cells via a channel mechanism since they were shown to form ion channels in planar lipid bilayers. This mechanism could cause damage to the plasma membrane by running down ionic gradients, discharging membrane potential; or allowing influx of toxic ions such as Ca^{2+} (Hirakura *et al.*, 2000; Monoi *et al.*, 2000; Trushina and McMurray, 2007). Other groups postulated mitochondrial dysfunction that again causes oxidative stress due to ATP deficits, Ca^{2+} release, loss of antioxidants and overproduction of reactive oxygen species (reviewed in Trushina and McMurray, 2007). There is also evidence that axonal and dendritic trafficking is impaired as it was observed that polyglutamine aggregates are able to physically block and as a consequence thereof alter neurite transport and thus deprive neuronal processes of factors or components that are important for axonal and dendritic functions. The soma may then be affected, leading to neuronal dysfunctions and possibly to cell death (Lee *et al.*, 2004; Piccioni *et al.*, 2002). Although it is unknown what process is responsible for the pathological cascade in the polyglutamine diseases, it seems likely that all contribute to some extent to the pathophysiology.

2.3.1.1 Toxic species

As already mentioned, a hallmark of polyglutamine diseases is the formation of inclusion bodies. Since the size of the polyglutamine stretch was shown to correlate with an enhanced ability of polyglutamine peptides to form extra- and intranuclear aggregates as well as with an earlier onset of disease the aggregates were suspected of mediating toxicity. There is indeed evidence supporting this hypothesis as it was shown that inhibition of aggregate formation by peptides, chemical compounds, intrabodies against huntingtin or molecular chaperones leads to suppression of both, inclusion body formation and cytotoxicity of polyglutamine peptides *in vivo* (Colby *et al.*, 2004; Cummings *et al.*, 1998; Muchowski *et al.*, 2000; Nagai *et al.*, 2003; Sanchez *et al.*, 2003; Warrick *et al.*, 1999). Nevertheless, the concept of large inclusions of mutant polyglutamine

being the toxic species, has become suspect and the idea came up that they might be even beneficial and neuroprotective (Arrasate *et al.*, 2004; Bates, 2003; Sakahira *et al.*, 2002a). This hypothesis is based on the observation that the regions in the brain that show the highest density of inclusions do not overlap with those undergoing massive degeneration (Gutekunst *et al.*, 1995; Kuemmerle *et al.*, 1999). Studies on transgenic mouse models as well as cell culture models revealed no or only little correlation between inclusion bodies and neurodegeneration or dysfunction (Arrasate *et al.*, 2004; Saudou *et al.*, 1998; Slow *et al.*, 2005). Enhancing inclusion body formation even resulted in suppression of toxicity (Bodner *et al.*, 2006). Consequently, it was suggested that inclusion body formation is an active cellular regulation mechanism for handling misfolded or aggregated proteins promoting neuronal survival (Kopito, 2000). As the level of diffuse polyglutamine peptide was recently shown to correlate with toxicity, the expanded polyglutamine peptides probably gain cytotoxicity during the aggregation process, before inclusion body formation (Arrasate *et al.*, 2004). Extensive study on this topic was carried out but the difficult handling of the in aqueous solution highly insoluble polyglutamine peptides impedes with clear results. So far amorphous oligomers were suspected of gaining characteristics that mediate toxicity and a recent study demonstrated that already a polyglutamine expanded peptide monomer exerts toxic effects upon a β -sheet conformational transition (Bennett *et al.*, 2005; DiFiglia *et al.*, 1997; Li *et al.*, 2007; Nagai *et al.*, 2007; Schaffar *et al.*, 2004).

Notably, in addition to the polyglutamine expanded proteins also polyglutamine containing fragments of the respective full-length proteins were found in the inclusion bodies (Becher *et al.*, 1998; Butler *et al.*, 1998; DiFiglia *et al.*, 1997; Li *et al.*, 1998b). Studies on these fragments revealed that they are more prone to aggregate and are substantially more toxic, in most cell culture and mouse models, than their full-length counterparts (de Almeida *et al.*, 2002; Peters *et al.*, 1999; Saudou *et al.*, 1998). Probably, they are even crucial for aggregation and cytotoxicity as it was recently suggested (Graham *et al.*, 2006). Caspases are thought to be responsible for the cleavage of polyglutamine containing proteins since masking of the predicted cleavage sites suppressed both aggregation as

well as toxicity and the rate of cleavage was shown to be polyglutamine length dependent (Ellerby *et al.*, 1999; Graham *et al.*, 2006; Kobayashi *et al.*, 1998; Wellington *et al.*, 1998). The activity of the caspases necessary for the initial cleavage of the polyglutamine peptide may reside in the inherent low-level activity of the zymogen. Accumulation and aggregation of toxic fragments may trigger additional caspase activity (such as caspase-8) that may activate additional effector caspase activity and contribute to cell death (Wellington and Hayden, 2000; Wellington *et al.*, 2000). This could also explain the late onset of the disease as the quality control system of the cell might cope with the formation of fragments under normal conditions. But as the quality control system becomes compromised as it is likely the case in aging cells, toxic fragments accumulate to toxic levels.

2.3.1.2 Gain of function versus loss of function

It is widely accepted that neuronal dysfunction and death in all polyglutamine diseases is due to a toxic gain-of-function mechanism associated with an expanded polyglutamine repeat in the respective protein. This is supported by the dominant inheritance pattern of all polyglutamine diseases, together with an extensive studies on cell culture and animal models of these diseases (Piccioni *et al.*, 2001; Zoghbi and Orr, 2000).

The proposed toxic gain-of-function mechanism becomes particularly apparent in SBMA. Unlike most other polyglutamine repeat diseases, the function of the protein mutated in SBMA, the androgen receptor, is well established. Patients with androgen resistance syndromes, *e.g.* due to mutations in the androgen receptor, do not develop signs of neurodegeneration. Thus, it is likely that the SBMA neurological phenotype is due to a newly-gained toxic effect of the expanded polyglutamine repeat, rather than to a loss of androgen receptor function (Brooks and Fischbeck, 1995; Piccioni *et al.*, 2001).

Although polyglutamine expansion mutations produce a dominant gain-of-function toxicity, it seems obvious that the overall activity of the disease causing protein is altered either due to intrinsic properties of the elongated

polyglutamine stretch or to a reduction in the total amount of the respective protein due to aggregation. This might contribute to disease pathogenesis and explain differences in pathology among the polyglutamine diseases. As most polyglutamine disease proteins are widely expressed throughout the neuraxis but only cause degeneration in select regions of the central nervous system, partial loss of disease protein function could render particular neurons exquisitely sensitive to the toxic gain-of-function effects that a polyglutamine expansion imparts to the disease protein (Thomas *et al.*, 2006). Although a mechanistic explanation for how loss-of-function of a polyglutamine protein contributes to polyglutamine disease pathogenesis is lacking, studies on HD but also on SBMA revealed considerable evidence for a pathogenic role of diminished normal function of disease proteins containing polyglutamine repeat expansions (Dragatsis *et al.*, 2000; Leavitt *et al.*, 2001; Leavitt *et al.*, 2006b; Thomas *et al.*, 2006).

2.3.1.3 Advances towards medical treatment

Up to now, there is no known cure for polyglutamine diseases and existing pharmacological therapies are targeted at managing, rather than preventing, symptoms. Currently, a wide variety of research towards establishing therapies targeting each step in the pathogenesis of the polyglutamine diseases is in progress, which includes suppressing mutant gene expression by RNAi (Boado *et al.*, 2000; Gonzalez-Alegre, 2007; Haque and Isacson, 1997; Haque *et al.*, 1997; Hasholt *et al.*, 2003; Nellesmann *et al.*, 2000; Yen *et al.*, 1999), inhibiting protein misfolding/aggregation (Cummings *et al.*, 1998; Kobayashi *et al.*, 2000; Muchowski and Wacker, 2005; Warrick *et al.*, 1999; Wyttenbach, 2004; Wyttenbach *et al.*, 2000), promoting protein degradation (Adachi *et al.*, 2007; Janknecht, 2002; Jia *et al.*, 2007; Seo *et al.*, 2007; Waza *et al.*, 2005; Yang *et al.*, 2007), activating transcription (Janknecht, 2002; Shimohata *et al.*, 2005), restore mitochondrial deficits (Kim *et al.*, 1999; Oliveira *et al.*, 2006; Oliveira *et al.*, 2007), inhibiting neuronal cell death (Kim *et al.*, 1999), and neuroprotection by neurotrophic factors (Anderson *et al.*, 1996; Perez-Navarro *et al.*, 2000; Petersen and Brundin, 1999; Saudou *et al.*, 1998; Ventimiglia *et al.*, 1995). Certainly, the

most powerful approach would be the prevention of the toxic species since it appears that independent of the protein context the toxic mechanism is shared by all polyglutamine diseases. However, the lack of knowledge with regard to the toxic species impedes with the identification of powerful drugs. Nevertheless, several compounds or antibodies with anti-aggregation activity have been identified, such as small molecules, but their benefits remain questionable (Bonelli and Hofmann, 2007; Heiser *et al.*, 2002; Hockly *et al.*, 2006; Sanchez *et al.*, 2003; Wang *et al.*, 2005; Wolfgang *et al.*, 2005; Wood *et al.*, 2007). Similarly, the idea to promote aggregation revealed promising results, however, an approved drug is still missing (Bodner *et al.*, 2006).

2.3.2 Huntington's disease

Huntington's disease is the most prevalent of the nine polyglutamine diseases. In Europe and North America the risk to develop Huntington's disease is approximately 1:10,000. Thereby, both sexes are affected with the same frequency. Huntington's disease is inherited in an autosomal dominant manner and is characterized by irrepressible motor dysfunction, cognitive decline and psychiatric disturbance, which lead to progressive dementia and death approximately 15-20 years after disease onset (Bates, 2000; Martin and Gusella, 1986). To date there is no effective treatment to prevent or delay disease progression (Borrell-Pages *et al.*, 2006).

2.3.2.1 Huntingtin

Huntingtin is an essential ~350-kDa protein that contains a polymorphic glutamine/proline-rich domain at its amino terminus (Figure 5). Although the gene was discovered more than a decade ago, its role has not been fully elucidated yet. Apart from the polyglutamine stretch it shares no sequence homology to other known human proteins. Huntingtin is ubiquitously expressed but the highest levels are found in the testis and brain (Difiglia *et al.*, 1995; Gutekunst *et al.*, 1995; Trottier *et al.*, 1995). Within the brain, the neocortex, the cerebellar cortex, the striatum and the hippocampus were identified as main

expression sites, a pattern that only partially overlaps with the regions most affected in Huntington's disease (Figure 6; Fusco *et al.*, 1999). The cellular distribution is as diverse. It is mainly found in the cytoplasm, but is also located in the nucleus, within neurites and at synapses. But it was also shown to associate with organelles and structures, such as clathrin coated vesicles, endosomal and endoplasmic compartments, mitochondrial, microtubules as well as plasma membrane (Difiglia *et al.*, 1995; Gutekunst *et al.*, 1995; Hoogeveen *et al.*, 1993; Kegel *et al.*, 2002; Kegel *et al.*, 2005; Trottier *et al.*, 1995).

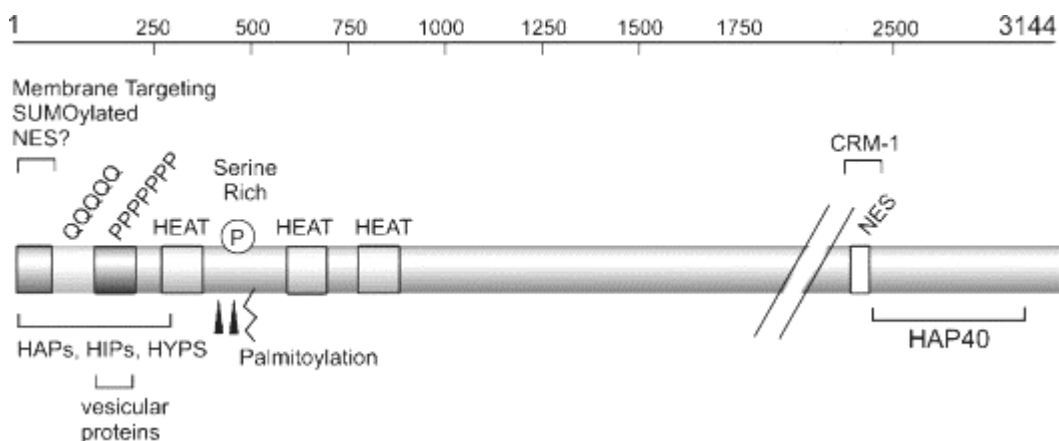


Figure 5: Major interaction domains of the huntingtin protein (Truant *et al.*, 2007).

Huntingtin was shown to interact with a variety of proteins involved in gene expression, intracellular transport, intracellular signalling and metabolism (Borrell-Pages *et al.*, 2006; Harjes and Wanker, 2003; Li and Li, 2004). It appears that huntingtin regulates transcription by shuttling transcription factors between the nucleus and the cytoplasm (Cattaneo, 2003; Charrin *et al.*, 2005; Sugars and Rubinsztein, 2003; Zuccato *et al.*, 2003). Huntingtin is suggested to be involved in trafficking since it interacts with many proteins that regulate intracellular transport or endocytosis. (Gauthier *et al.*, 2004; Kalchman *et al.*, 1997; Li *et al.*, 1995; Modregger *et al.*, 2002; Singaraja *et al.*, 2002; Wanker *et al.*, 1997). Interestingly, it confers anti-apoptotic properties and protects against polyglutamine expanded huntingtin-induced cell death (Cattaneo *et al.*, 2001;

Gervais *et al.*, 2002; Hackam *et al.*, 2000; Ho *et al.*, 2001; Leavitt *et al.*, 2001; Leavitt *et al.*, 2006a; Rigamonti *et al.*, 2000; Zhang *et al.*, 2003).

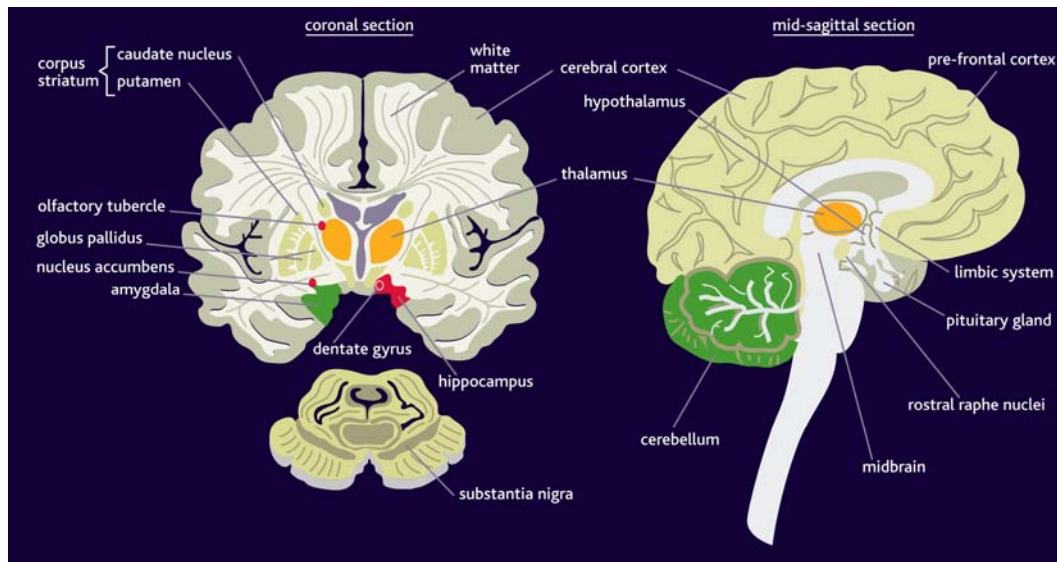


Figure 6: Coronal and mid-sagittal section through the human cerebrum (adapted from www.CNSforum.com).

2.3.2.2 Characteristics, affected region, phenotype

The first symptoms of Huntington's disease usually appear in middle age. Most of the patients show involuntary movements of the face, fingers, feet or thorax in the beginning which at the same time act as an indicator for Huntington's disease (Folstein *et al.*, 1986). In addition to the physical symptoms patients also develop psychiatric disturbances, for instance depression, anxiety, apathy and irritability which usually occur 10-20 years before onset of the choreiform movements (Craufurd *et al.*, 2001). At a later stage, the patients suffer from choreiform movements of the head, neck, arms and legs as well as cognitive deficits such as impairments of memory and language comprehension (Bachoud-Levi *et al.*, 2001). Males in addition, become frequently sexually dysfunctional and have testicular abnormalities (Fedoroff *et al.*, 1994; Van Raamsdonk *et al.*, 2007). At the final stage of the disease, patients become severely rigid and akinetic and present severe dementia. 15-20 years after the first symptoms appear the patient usually dies.

At the cellular level, Huntington's disease causes the selective dysfunction and death of specific neuronal subpopulations within the central

nervous system. The gamma-aminobutyric acid-releasing spiny-projecting neurons of the striatum and the subcortical brain structure that controls body movement are mainly affected and to a lesser extent, neurons within the cerebral cortex (Vonsattel *et al.*, 1985). With the progression of the disease, a general neuronal loss in several brain regions such as the globus pallidus, the subthalamic nuclei, the substantia nigra, the cerebellum and the thalamus is observed.

2.3.3 SBMA

Spinal and bulbar muscular atrophy (SBMA; Kennedy's disease) is an X-linked dominant neurodegenerative disorder that results from expanded glutamine repeats in the amino terminus of the androgen receptor (AR) protein (La Spada *et al.*, 1991). In Europe the risk of being affected by SBMA is about 1:10,000 to 1:50,000. The onset of the disease is usually between 30 and 60 years and is characterized by progressive lower motor neuron degeneration in the spinal cord and bulbar nuclei of the brain stem (Katsuno *et al.*, 2006; Kennedy *et al.*, 1968; Li *et al.*, 1998a). It mainly affects males and SBMA is frequently associated with gynaecomastia, testicular failure and other feminized signs. Female carriers of SBMA, even homozygous, usually do not show disease phenotypes (Abou-Sleymane *et al.*, 2006; Schmidt *et al.*, 2002; Sobue *et al.*, 1993). Presumably, this is due to low concentrations of testosterone, a ligand of the AR protein which is a steroid hormone transcription factor.

2.3.3.1 AR

Of all proteins associated with polyglutamine disease the AR protein is probably the best investigated. The AR is a member of the steroid and nuclear receptor superfamily and is regulated by the binding of androgens. The AR gene consists of eight exons and encodes a protein with 919 amino acid residues. Exon 1 of the gene consists of two polymorphic repeat motifs (CAG and GGN), encoding variable lengths of polyglutamine and polyglycine stretches,

respectively, which are separated by 248 amino acids of non-polymorphic sequence (Faber *et al.*, 1989; Lubahn *et al.*, 1988). The AR protein consists of an N-terminal transactivation domain (TAD), a central DNA-binding domain (DBD), a C-terminal ligand-binding domain (LBD), and a hinge region connecting the LBD and the DBD (Figure 7). The LBD is in addition to ligand binding also involved in dimerization of the receptors and contains a ligand-dependent activation function (AF2) (Brinkmann *et al.*, 1989; Gelmann, 2002). In contrast to other nuclear receptors, the NTD of AR harbors one or more transcriptional activation function (AF1) and is known to strongly interact with the LBD in a hormone dependent manner (Brinkmann, 2001; Singh *et al.*, 2006). But also a number of co-regulators modulate the actions of AR (Chamberlain *et al.*, 1994; Faber *et al.*, 1989; Kazemi-Esfarjani *et al.*, 1995).

The AR is a key player in male sexual differentiation since AR transcription mediates muscle and bone growth, spermatogenesis and the development of secondary sexual characteristics (Mooradian *et al.*, 1987). Since AR is present in the brain in areas critical for learning and memory such as the thalamus and hippocampus, it is also thought to be important for cognitive function but similar to Huntington's disease a lack of correlation between the AR protein expression levels and pathological involvement in SBMA is seen (Li *et al.*, 1998a; Li *et al.*, 1998b; Yaffe *et al.*, 2003). In non-neural tissues AR protein is mainly expressed in the testis, skin, and muscle, whereas it is low in the kidney, spleen, and liver (Li *et al.*, 1998a; Li *et al.*, 1998b).

At the cellular level, AR is predominantly cytoplasmic and rapidly translocates into the nucleus upon binding of the ligand (Simental *et al.*, 1991). This is mediated by a large dynamic heterocomplex composed of heat shock proteins, co-chaperones, and tetratricopeptide repeat (TRP)-containing proteins (Pratt and Toft, 1997). Unbound to ligand, the AR is maintained in a partially unfolded, inactive conformation that allows efficient ligand binding (Pratt *et al.*, 2004). Involved in folding of the nascent peptide and assembly of the final chaperone complex are Hsp70, Ydj1, Hip (hsc70 interacting protein) and Hop (Hsp organizer protein). The chaperone-complex that finally ensures a high affinity for ligand binding consists of Hsp90, p23 and TPR-containing

immunophilin (Davies *et al.*, 2002; Fan *et al.*, 2005; Freeman *et al.*, 2000; Frydman and Hohfeld, 1997; Georget *et al.*, 2002; Hohfeld *et al.*, 1995). Since the interactions between steroid hormone receptors and molecular chaperones are transient there is an ongoing dynamic folding/refolding cycle (Jakob and Buchner, 1994; Pratt *et al.*, 2004; Smith, 1993). Upon addition of androgens, the TPR-containing immunophilin gets substituted for another, which is thought to guide the receptor in a retrograde direction along microtubules (Davies *et al.*, 2002). Hsp70 and Ydj1 presumably assist AR in crossing the nuclear membrane (Caplan and Douglas, 1991; Rassow *et al.*, 1995; Smith and Toft, 1993). Inside the nucleus, Bag-1L is believed to facilitate transactivation mediating the recruitment of AR and Hsp70 to its promoter (Froesch *et al.*, 1998; Shatkina *et al.*, 2003). Once bound to specific elements on the DNA, the so-called androgen response elements (AREs), transcription of the respective target genes leads to an androgen response that physiologically involves genes responsible for male sexual differentiation in utero and for male pubertal changes. In adult males, androgen is mainly responsible for maintaining libido, spermatogenesis, muscle mass and strength, bone mineral density, and erythropoiesis (Johansen, 2004). As long as androgens are present, there is a molecular chaperone-mediated continuous disassembly/reassembly of the complex and transcriptional activation continues (Freeman and Yamamoto, 2001; Pratt *et al.*, 2004). The degradation of AR occurs via the ubiquitin-proteasome pathway (Pratt *et al.*, 2004). This process is mediated by CHIP (carboxyl terminus of Hsc70-interacting protein), which interacts with ARs that are unable to successfully transition into the high-affinity ligand-binding conformation (He *et al.*, 2004).

AR dysfunction is not only associated with SBMA. Since androgen pathways are integrated with several other pathways regulating metabolic processes in the human body alterations in AR transactivation capacity may lead to disturbances in the secondary sexual differentiation as well as in the physiology of numerous other organs. Extensive research revealed that AR dysfunction is implicated in reproductive disorders, in neurological disorders, in disorders of aero-digestive tract and digestive system as well as in disorders related to general body health and fitness (reviewed in Rajender *et al.*, 2007).

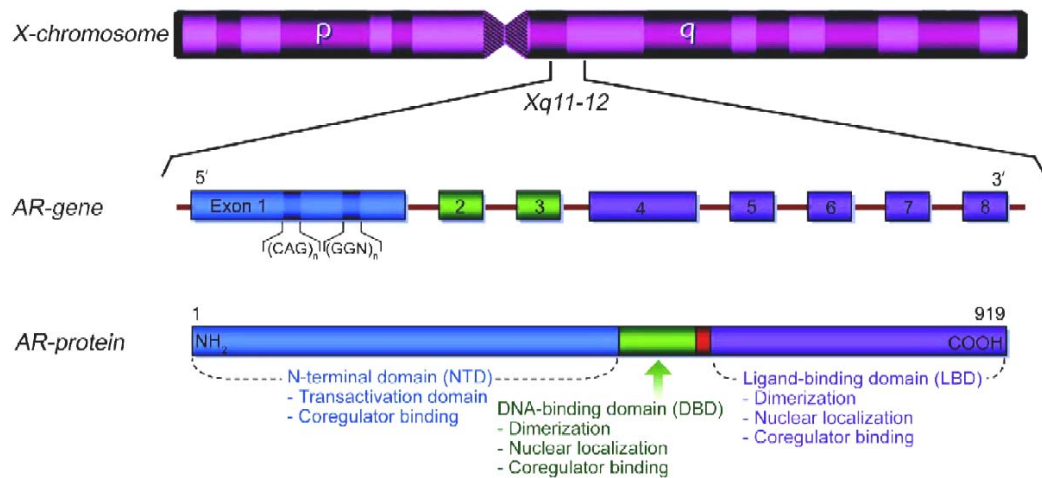


Figure 7: Genetic organization of the AR gene on the X-chromosome and major functional domains of the encoded protein (Rajender *et al.*, 2007).

2.3.3.2 Characteristics, affected region, phenotype

The major symptoms of SBMA are weakness, atrophy, and fasciculations of bulbar, facial and limb muscles (Katsuno *et al.*, 2004). First symptoms are often postural tremor such as tremor of the outstretched hands, muscle cramps, and in the early stage of the disease contraction fasciculations are noticeable in the face, neck, and tongue. Eventually, individuals develop limb weakness which usually begins in the pelvic or shoulder regions. Later, weakness of the facial and tongue muscles may occur and often leads to dysphagia (difficulty in swallowing), dysarthria (slurring of speech), and recurrent aspiration pneumonia. Although symptoms usually show up in the 30's patients reach a near-normal lifespan.

At the cellular level, SBMA patients show degeneration of anterior horn cells, bulbar neurons, and dorsal root ganglion cells, hence, motor nerves that control breathing, swallowing, talking and moving (Sobue *et al.*, 1989).

The majority of patients show also signs of androgen insensitivity such as gynaecomastia, impaired spermatogenesis, testicular atrophy, impotence and decreased fertility, some of which are detected before the onset of motor symptoms (Dejager *et al.*, 2002). This observation suggests that the polyglutamine

expansion mutation in SBMA imparts a partial loss-of-function in tissues important for the expression of male secondary sexual characteristics.

2.3.3.3 AIS

Impaired AR function causes the androgen insensitivity syndrome (AIS) which is most severe in the absence of functional AR, known as testicular feminization. Patients of the latter, fail to develop male external genitalia, have a female appearance and are infertile whereas patients with reduced AR activity often express phenotypic signs of gynaecomastia, testicular atrophy and reduced fertility (Brinkmann, 2001; Lyon and Hawkes, 1970; Pinsky *et al.*, 1992). AIS patients usually suffer from various types of mutations in the AR gene that devastate the functionality of AR protein (Brinkmann, 2001). Interestingly, more than 80% of SBMA patients show in addition to neurodegeneration also signs of mild-to-moderate AIS, for instance varying degrees of testicular atrophy, impaired fertility and gynecomastia (Dejager *et al.*, 2002). But unlike other AIS patients, the AIS in SBMA is not a fixed feature of the disease; sex differentiation proceeds normally and characteristics of AIS develop slowly progressive, similar to the neurological symptoms that appear later in life (Brinkmann, 2001; Dejager *et al.*, 2002).

To elucidate the molecular mechanism of this non-classic form of mild, late-onset AIS in SBMA, several studies were carried out with contradicting results. Some groups propose decreased levels of AR protein expression to be the cause of the loss of AR function in SBMA (Brooks *et al.*, 1997; Choong *et al.*, 1996) but this was not observed by others (Ellerby *et al.*, 1999; LaFevre-Bernt and Ellerby, 2003; Sopher *et al.*, 2004; Stenoien *et al.*, 1999). A decrease in AR apparent ligand binding affinity in subjects with SBMA was reported (Danek *et al.*, 1994; MacLean *et al.*, 1995; Warner *et al.*, 1992) but cell line studies could not confirm this result (Brooks *et al.*, 1997; Chamberlain *et al.*, 1994; Kazemi-Esfarjani *et al.*, 1995). The majority of researchers favors a linear decrease of transactivation function with progressive expansion of the polyglutamine repeat (Chamberlain *et al.*, 1994; Dejager *et al.*, 2002; Kazemi-Esfarjani *et al.*, 1995; Thomas *et al.*, 2006; Tut

et al., 1997), whereas Brooks *et al.* observed no differences in transactivation capacity comparing AR proteins with either 24Q or 65Q in a stably transfected motor neuron hybrid cell line (Brooks *et al.*, 1997). Two studies suggest impaired interaction of polyglutamine expanded AR protein with AR co-activators (Hsiao *et al.*, 1999; Irvine *et al.*, 2000). Regardless of the high grade of contradictory observations these hypotheses are based on, they seem to be inappropriate to explain the slowly progressive, late-onset AIS in SBMA, since, for instance, altered ligand binding affinity or decreased transactivation function of polyglutamine expanded AR are intrinsic properties and do not develop over the years.

An alternative attempt to explain the loss of AR function in SBMA, that takes into consideration the progressive development of AIS which resembles the appearance of neurological symptoms in SBMA (Dejager *et al.*, 2002), was given by Butler *et al.* and Stenoien *et al.* (Butler *et al.*, 1998; Stenoien *et al.*, 1999). They hypothesize that the reduction in transcriptional activity of AR protein in SBMA is due to aggregated and sequestered polyglutamine AR protein. Hence, the amount of active AR protein would decrease and furthermore it is possible, that the aggregates sequester other transcriptional components (Stenoien *et al.*, 1999). However other studies ruled out sequestration of AR protein into aggregates to be the cause of impaired AR transactivation (Piccioni *et al.*, 2001; Thomas *et al.*, 2006). Summarizing, the underlying mechanism of AIS in SBMA still remains far from clear.

2.4 Models of polyglutamine disease

In the last decade a variety of different models of polyglutamine disease came up with major contributions towards the understanding of molecular mechanisms that cause toxicity but also therapeutic strategies. These models encompass a variety of assays in which the mutant gene or some portion of it has been introduced into living organisms which experience a phenotypic response in some measure indicative of the respective human polyglutamine disease. Thereby, the key features which are thought to be requisite for any

model of polyglutamine disease are aggregation and toxicity of the polyglutamine-expanded species.

For high-throughput screening cell culture models were established, in which the outcome measure is cytotoxicity or some structural or biochemical measure related to pathogenesis. Lower organisms such as yeast, *Drosophila*, or *Caenorhabditis elegans*, provide a more salient context for the genetic mutation and opportunity for genetic analyses. They enable suppressor screens to identify genes that alleviate or modify the disease, therefore a powerful approach to identifying pathways involved in polyglutamine disease pathology and possible protective strategies (Hersch and Ferrante, 2004; Rubinsztein, 2002). However, these organisms could have important differences in the pathways that regulate and are perturbed by the polyglutamine disease mutation in humans. In addition, these simpler models do not express the mutant protein in neuronal types that degenerate in human polyglutamine disease and as a consequence thereof, cell-specific effects could be overlooked. Thus, ultimately such candidates from lower model organisms or screening of high-throughput assays using libraries containing thousands to millions of small molecules will need confirmation in mammalian models since disease expression and response to potential therapies can be quite close to what occurs in humans. The proof of efficacy in mammalian models is considered a requisite before considering possible testing in humans (Hersch and Ferrante, 2004; Rubinsztein, 2002).

2.4.1 Yeast

Yeast, *Saccharomyces cerevisiae*, is probably the best understood eukaryotic organism at the molecular and cellular levels. It was the first eukaryotic model organism whose genome has been completely sequenced. Its experimental tractability, combined with the remarkable conservation of gene function throughout evolution, makes yeast the ideal model genetic organism. Since many core cellular processes and metabolic pathways are conserved between yeast and mammals, yeast can in many cases serve as a model of human disease, focusing on functional analyses of whole genomes (Ma, 2001). In terms

of handling and maintenance the short generation time and the ease of manipulating the genome allows biochemical studies from a single genetically defined cell (Drubin, 1989). The low genomic complexity in comparison to higher eukaryotic organism makes it less suitable for research on processes involved in differentiation and development, integration of tissues and organ systems, and activities of specialized cells and tissues (Drubin, 1989; Ma, 2001).

Yeast has been also used to investigate the mechanisms of polyglutamine cytotoxicity and the formation and accumulation of polyglutamine aggregates. Thereby, investigations were focused on Huntington's disease using yeast strains that express the first exon of the huntingtin gene with various numbers of glutamine codons. Studies in yeast cells unanimously confirmed the correlation between the size of the polyglutamine stretch and aggregation propensity (Krobitsch and Lindquist, 2000; Muchowski *et al.*, 2000). The toxic effect of expanded polyglutamine fragments however, was shown to vary with the amino acid sequences flanking the polyglutamine tract and to be dependent on the [PIN⁺] prion determinant (Dehay and Bertolotti, 2006; Duennwald *et al.*, 2006a; Meriin *et al.*, 2002).

2.4.2 Zebrafish

The zebrafish, *Danio rerio*, is a common and useful model organism for studies of vertebrate development as well as gene function and it becomes more and more prominent for drug screening. It has several key advantages over other *in vivo* models of polyglutamine disease. It is a vertebrate organism and contains homologues to many human genes, including the htt gene (Figure 8; Karlovich *et al.*, 1998), making it a valuable tool to model human diseases such as HD. Additional important advantages include: the ease and cost efficiency with which *in vivo* drug tests can be performed; the robustness of the embryos that facilitates experimental manipulation; the transparency of zebrafish embryos allowing for visualization of morphological and physiological features in the live embryo; and the aqueous environment of the zebrafish, which facilitates drug administration (Zon and Peterson, 2005). Importantly, the zebrafish model system allows for the

evaluation of drug effectiveness in a whole organism, taking into account the stability and cellular targeting of the tested compound, as well as the assessment of potential side effects of the drug at active concentrations. Up to date, manipulation of the zebrafish genome pose a weak point of zebrafish as a model (van der Sar *et al.*, 2004). With regard to neurodegenerative diseases, zebrafish have only recently been explored as a model (Miller *et al.*, 2005; Rubinstein, 2003).

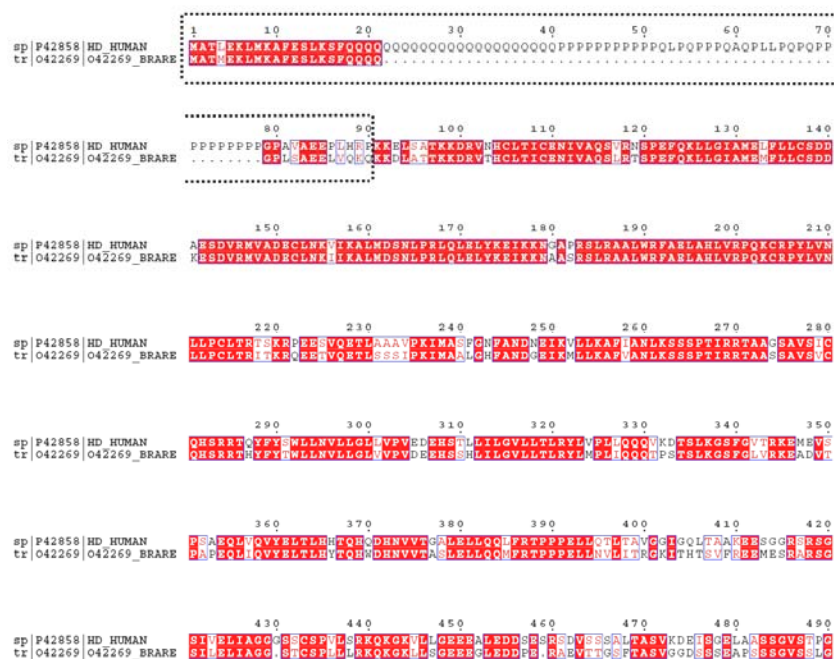


Figure 8: Huntingtin but not the polyglutamine/polyproline stretch is conserved among zebrafish and human.

An alignment of the human and zebrafish huntingtin protein showing the first ~500 amino acids. Exon 1 is framed with a dashed line, and identical amino acids are outlined in red.

2.5 Aim of thesis

Though the polyglutamine stretch was shown to mediate toxicity in all of the polyglutamine diseases, neither the key toxic species along the aggregation pathway nor the exact molecular mechanisms leading to toxicity were uncovered.

The overall goal of this study was to establish models of polyglutamine diseases to obtain new insights into the nature of the key toxic species and the molecular mechanisms of polyglutamine-mediated toxicity as well as to identify compounds that disrupt or alter the polyglutamine aggregation pathway as potential therapeutic agents.

A first aim was to establish a zebrafish HD model capable of whole organism validation of candidate therapeutic compounds. It was expected that the transparency of the zebrafish embryo would also allow for the determination of whether inclusion bodies of polyglutamine-expanded huntingtin directly contribute to toxicity.

A second aim was to establish a yeast model of SBMA to characterize polyglutamine containing AR fragments in terms of gain-of-function toxic effects. To shed light on AIS in SBMA, it was hoped that this model would also allow for the monitoring of AR function under conditions mimicking pathogenesis.

3 Materials and Methods

3.1 Material

3.1.1 Instruments

Abimed (Langenfeld, Germany): Gilson Pipetman (2, 10, 20, 100, 200, 1000 μ l).

Amersham Pharmacia Biotech (Freiburg, Germany): electrophoresis power supply EPS 600, FPLC systems, prepacked chromatography column Superdex200.

Beckman (München, Germany): DU 640 UV/VIS spectrophotometer;

Avanti J-25, Avanti 30 and GS-6R centrifuge; Optima TLX ultracentrifuge.

Biometra (Göttingen, Germany): T3 PCR-Thermocycler.

Bio-Rad (München, Germany): electrophoresis chambers MiniProtean 2 and 3; electrophoresis power supply Power PAC 300, GelAirDryer.

BioTek Instruments (Winooski, USA): Synergy HT Fluorescence Microplate Reader.

Eppendorf (Hamburg, Germany): centrifuges 5415C and 5417R, Thermomixer Comfort, Microinjector FemtoJet.

EG&G Berthold (Bad Wildbad, Germany): Lumat LB9507.

Fisher Scientific (Schwerte, Germany): pH meter Accumet Basic.

Fujifilm (Düsseldorf, Germany): Image Reader LAS 3000.

Hoefer Scientific Instruments (San Francisco, USA): SemiPhore blotting transfer unit.

Leitz (Wetzlar, Germany): Microscope Diavert

Mettler Toledo (Gießen, Germany): balances AG285, PB602.

Millipore (Eschborn, Germany): deionization system MilliQ plus PF, Millix-HA filters 0.22 μ m.

NanoDrop Technologies Inc. (Wilmington, USA): NanoDrop-1000 Spectrophotometer

New Brunswick Scientific (Nürtingen, Germany): orbital shaker and incubator Innova 4430.

Sartorius (Goettingen, Germany): vacuum filtration unit (0.2 μ m).

WTW (Weilheim, Germany): pH meter pH535.

Zeiss (Jena, Germany): Microscope Axiovert 200M, inverted confocal microscope LSM510 META.

3.1.2 Chemicals

All chemicals were of quality *pro analysis* and purchased from *Sigma-Aldrich* (Deisenhofen, Germany) if not stated otherwise. Solutions were prepared with deionised, double distilled and sterile-filtered water. Concentration in percent of liquids are given as (v/v) and of solid chemicals as (w/v).

Ambion (Austin, USA): MessageMachine Kit

Amersham Pharmacia Biotech (Freiburg, Germany): LMW and HMW gel filtration calibration kits, protein G-Sepharose beads, ECL⁺ Detection Kit.

BioMol (Hamburg, Germany): HEPES.

BioRad (München, Germany): ethidiumbromide, Protein Assay Kit.

BD Bioscience (Heidelberg Germany): doxycycline.

Calbiochem (Bad Soden, Germany): TWEEN-20.

Difco (Heidelberg, Germany): Bacto agar, Bacto yeast extract, Bacto peptone, Bacto tryptone, Yeast nitrogen base w/o amino acids.

Fermentas (St. Leon-Rot, Germany): PageRuler™ Prestained Protein Ladder Plus, GeneRuler™ 100bp and 1 kb DNA Ladder.

Fluka (Deisenhofen, Germany): DMSO.

Invitrogen (Karlsruhe, Germany): Lipofectamine™-reagent.

New England Biolabs (Frankfurt/Main, Germany), T4 DNA Ligase, DNA polymerase I (Klenow fragment), CIP, restriction endonucleases, prestained protein marker broad range.

Merck (Darmstadt, Germany): Benzonase, EDTA, 2-Mercaptoethanol, paraformaldehyde.

Molecular Probes (Karlsruhe, Germany): DAPI, TOPRO-3, Acridine Orange, ProLong®.

Qiagen (Hilden, Germany): QIAprep spin miniprep Kit, QIAGEN Plasmid Midi Kit, QIAprepEndoFree Plasmid Maxi kit, QIAquick PCR purification and gel extraction kits.

Pierce (Bonn, Germany): Coomassie protein assay reagent.

Promega (Mannheim, Germany): Wizard®PlusSV Minipreps, PureYield™ Plasmid Midiprep system, Wizard®SV gel and PCR clean-up system, Beetle Luciferin-potassium salt, Luciferase Assay System.

Roche (Basel, Switzerland): ampicillin, Complete Protease inhibitor, DTT, ExpandTMLong Template PCR system.

Schleicher & Schuell (Dassel, Germany): Protran™ nitrocellulose transfer membrane, nitrocellulose acetate membrane filter.

Seikagaku (Tokyo, Japan): Zymolyase-20T

Serva (Heidelberg, Germany): Coomassie, Serva BlueR, PEG, PMSF, Acrylamide-Bis solution 30% (37:5:1), Citifluor.

Stratagene (La Jolla, USA): PfuTurbo™ DNA Polymerase II, Yeast Carrier DNA.

3.1.3 Buffers and growth media

3.1.3.1 Buffers

1 x TAE	1 mM EDTA 40 mM Tris/AcOH pH 8.0
1 x SDS-PAGE running buffer	25 mM Tris 192 mM Glycine 1% SDS (Sodium-Dodecylsulfate)
6 x SDS-PAGE sample buffer	348 mM Tris-HCl, pH 6.8 30% v/v glycerol 10% w/v SDS 60 mM DTT 0.0012% w/v Bromophenol blue
SDS-Gel staining solution	1.2 g/l Coomassie-Brilliant-BlueR-250 50% Ethanol 10% acetic acid
SDS-Gel destaining solution	10% Ethanol 10% acetic acid
Western blotting buffer	25 mM Tris 192 mM Glycine 15% Methanol 0.08% SDS

Stripping buffer	63 mM Tris/HCl pH 6.7 2% SDS 100 mM β -Mercaptoethanol
1 x TBS	10 mM Tris/HCl pH 7.5 154 mM NaCl
1 x TBSt	1 x TBS 0.1% Tween20
Blocking buffer	1 x TBS 5% skimmed milk powder
Antibody buffer	1 x TBSt 0.5% skimmed milk powder
ECL solution 1	2.5 mM Luminol 400 μ M Coomarcic acid 100 mM Tris/HCl pH 8.5
ECL solution 2	0.018% H ₂ O ₂ 100 mM Tris/HCl pH 8.5

3.1.3.2 Buffers and growth media for bacterial work

Luria-Bertani (LB) medium	1% tryptone (Difco) 0.5% yeast extract (Difco) 1% NaCl (Merck) (+ 1.5% agar for solid medium)
TYM medium	2% tryptone (Difco) 0.5% yeast extract (Difco) 0.1 M NaCl (Merck) 10 mM MgSO ₄

Ampicillin (antibiotic additive) was prepared as 1000 x stock solution (100 g/l) and filter sterilized before usage.

3.1.3.3 Buffers and growth media for yeast

YPD medium 2% peptone (Difco)
 1% yeast extract (Difco)
 2% glucose
 (+ 3% agar for solid medium)

SD-Drop-out-medium 0.67% yeast nitrogen base w/o amino acids (Difco)
 4% 25 x Drop-out-mix stock solution
 2% glucose
 (+ 3% agar for solid medium)

25 x Drop-out-mix	Adenine hemisulfate salt	400 mg
	L-arginine (HCl)	200 mg
	L-aspartic acid	1 g
	L-glutamic acid (monosodium salt)	1 g
	L-histidine	200 mg
	L-leucine	600 mg
	L-lysine	300 mg
	L-methionine	200 mg
	L-phenylalanine	500 mg
	L-serine	3.75 g
	L-threonine	2 g
	L-tryptophan	400 mg
	L-tyrosine	300 mg
	L-valine	1.5 g
	Uracil	200 mg
	in 400 ml H ₂ O	

To guarantee selective growth of certain yeast strains amino acids with regard to the respective selective marker were omitted.

SR-Drop-out-medium 0.67% yeast nitrogen base w/o amino acids (Difco)

4% 25 x Drop-out-mix stock solution

2% raffinose

(+ 3% agar for solid medium)

(+ 2% galactose for induction)

3.1.3.4 Buffers and growth media for cell culture

Growth Medium Dulbecco's Modified Eagle's Medium (Biochrom AG)

10% foetal calf serum

2 mM glutamine (Gibco)

100 U/ml Penicillin (Gibco)

100 µg/ml Streptomycin (Gibco)

Growth Medium Dulbecco's Modified Eagle's Medium/F-12 (Gibco)

w/o steroids

10% Charcoal/Dextran treated fetal bovine serum (HyClone)

2 mM glutamine (Gibco)

100 U/ml Penicillin (Gibco)

100 µg/ml Streptomycin (Gibco)

1 x PBS (Gibco)

OptiMEM (Invitrogen)

Trypsin-EDTA (Gibco)

Trypsin-EDTA w/o phenol red (Gibco)

3.1.3.5 Buffers and growth media for zebrafish

E3 embryo medium 5 mM NaCl

0.17 mM KCl

0.33 mM CaCl₂

0.33 mM MgSO₄

0.1% Methylene Blue (fungicide)

3.1.4 Bacterial and yeast strains, cell and zebrafish lines

3.1.4.1 *Escherichia coli* strains

Strain	Genotype	Reference
DH5 α F'	<i>F'</i> /endA1 hsdR17(<i>r_K-m_K</i> +) supE44 thi-1 recA1 gyrA (<i>Nal</i> ' ^r) relA1 D(<i>lacZYA-argF</i>) _{U169} (m80lacZDM15)	Novagene
SURE	<i>e14-</i> (<i>McrA-</i>) D(<i>mcrCB-hsdSMR-mrr</i>)171 endA1 supE44 thi-1 gyrA96 relA1 lac recB	Novagene

3.1.4.2 *Saccharomyces cerevisiae* strains

Strain	Genotype	Reference
YPH499	<i>MATa ura3-52 lys2-801 ade2-101 trp1Δ63</i> <i>his3Δ200 leu2Δ1</i>	(Sikorski and Hieter, 1989)
EJ250	<i>MATa ade2-101 lys2-801 trp1Δ1 his3Δ200</i> <i>leu2Δ1 ura3-52 URA3::ARE-ADE2</i>	(Ceraline <i>et al.</i> , 2003)
<i>hsp104Δ::LEU2</i>	<i>MATa ura3-52 lys2-801 ade2-101 trp1Δ63</i> <i>his3Δ200 leu2Δ1 hsp104Δ::LEU2</i>	Sarah Broadley

3.1.4.3 Cell lines

Strain	Description	Reference
Neuro-2a (N2a)	Murine neuroblastoma cells	ATCC CCL-131
SH-SY5Y	Human neuroblastoma cells	ATCC CCL-2

3.1.4.4 *Danio rerio*

The wild type line AB was used for all experiments.

3.1.5 Plasmids and Oligonucleotides

3.1.5.1 Plasmids

Plasmid	Description	Reference
pCS2+	Expression vector for mammalian cells and <i>in vitro</i> transcription. It is also functional as RNA or DNA in zebrafish embryos.	http://sitemaker.umich.edu/dlturner.vectors
pCDNA 3.1/Myc-His/ lacZ	Eukaryotic expression vector containing the gene for β -Galactosidase.	Invitrogen
pCDNA3.1hygro+ Hdj1	Expression vector for mammalian cells containing the gene for human Hdj1.	Annette Haacke
pCDNA3.1-myc Htt20Q	Expression vector for mammalian cells, containing the gene for huntingtin exon 1 with 20 glutamines and a myc-tag.	(Schaffar <i>et al.</i> , 2004)
pCDNA3.1-myc Htt96Q	Expression vector for mammalian cells, containing the gene for huntingtin exon 1 with 96 glutamines and a myc-tag.	(Schaffar <i>et al.</i> , 2004)
p423Gal	Yeast expression vector (2μ , <i>HIS3</i>), <i>GAL1</i> promoter.	(Mumberg <i>et al.</i> , 1994)
pCMV-AR65	Eukaryotic expression vector containing a human AR cDNA with 65 CAG repeats.	(Brooks <i>et al.</i> , 1997)
pAR _{WT}	Yeast expression vector (2μ , <i>TRP1</i>), <i>GPD</i> promoter, containing a human AR cDNA with 27 CAG repeats fused to EYFP.	(Ceraline <i>et al.</i> , 2003)
p423tet	Yeast expression vector (<i>CEN6</i> , <i>HIS3</i>), <i>tetO</i> promoter.	Katja Siegers
pCM184	Yeast expression vector (<i>CEN6</i> , <i>TRP1</i>), <i>tetO</i> promoter.	(Gari <i>et al.</i> , 1997)
p415Gal	Yeast expression vector (<i>CEN6</i> , <i>Leu2</i>), <i>GAL1</i> promoter.	(Mumberg <i>et al.</i> , 1994)
pRS/ARE-Ade2	Yeast integrative plasmid with <i>URA3</i> as the selection marker and <i>ADE2</i> linked to three copies of the androgen responsive element (ARE).	(Ceraline <i>et al.</i> , 2003)

Plasmid	Description	Reference
pSI421	Yeast cytosolic stress reporter plasmid (2 μ , <i>URA3</i>) containing the gene for β -Galactosidase linked to <i>SSA3</i> promoter element.	Katja Siegers
pGEM- <i>luc</i>	Cassette vector being a source of <i>luc</i> gene encoding firefly luciferase.	Promega
p425ADH	Yeast expression vector (2 μ , <i>LEU2</i>), <i>ADH1</i> promoter.	(Mumberg <i>et al.</i> , 1994)
YEp105	Yeast expression vector (2 μ , <i>TRP2</i>), <i>CUP1</i> promoter.	(Ecker <i>et al.</i> , 1987)

3.1.5.2 Oligonucleotides

Name	Nucleotide sequence
AR5M	5'-GGC GCG CAA TTG ATG GAA GTG CAG TTA GGG CTG GGA AGG G-3'
AR3S	5'-GGC CGT GTC GAC CTG GGT GTG GAA ATA GAT GGG CTT GAC-3'
AR2QN	5'- Pho-CAG CAG CAG CAA ACT GGC GC -3'
AR2QC	5'- Pho-CAG CAA GAG ACT AGC CCC AG -3'
p423TetA-5'AR	5'-CGC GGA TCC CAA ATG TGT GAA CAA AAG CTT ATT TCT GAA GAA GAC TTG GGT ATG CAG ATC CGC ATG GAA GTG CAG TTA GGG C-3'
p423TetA-3'155	5'-ATA GTT TAG CGG CCG CTC AGT CAT CCT CGT CCG GAG-3'
YEp105-5'AR	5'-CGC GGA TCC GCC CAA AAA AGA AGA GAA AGG TAG AAT TAG GAA CAG CAA TGG AAG TGC AGT TAG GGC-3'
YEp105-3'155	5'-CCG CTC GAG TCA GTC ATC CTC GTC CGG AG-3'
p423TetA-MYC	5'-CGC GGA TCC CAA ATG TGT GAA CAA AAG CTT ATT TCT GAA GAA GAC TTG GGT ATG CAG ATC TGC ATG GAA GTG CAG TTA GGG C-3'
YEp105-5'ARb	5'-CGC GGA TCC GCA TGG AAG TGC AGT TAG GGC-3'

p423TetA-5'ARb	5'-CGC GGA TCC CAA ATG GAA GTG CAG TTA GGG C-3'
p423TetA-3'WT	5'-ATA GTT TAG CGG CCG CTC ACT GGG TGT GGA AAT AG-3'
p423TetA-5'-FLAG	5'-CGC GGA TCC CAA ATG GAC TAC AAA GAC GAT GAC GAT AAA GCT GGA GAA TTC ATG GAA GTG CAG TTA GGG C-3'
5'BamHI-myc	5'-CGC GGA TCC CAA ATG TGT GAA CAA AAG C-3'
3'httBstAPI	5'-TCC TAA GCA GTT GTT GCT GTT GGA AGC TTT TGA GG-3'
5'httNdeI	5'-TTT CCT ATT GAC GTC ATA TGG G-3'

3.1.6 Antibodies

3.1.6.1 Primary antibodies

Antibody	Species	Reference
anti-myc (9E10)	mouse, monoclonal	Santa Cruz, sc-40
anti-FLAG (M2)	mouse, monoclonal	Sigma F3165
anti-FLAG (M2)	rabbit, polyclonal	Sigma F7425
anti-GFP	mouse, monoclonal	Roche 1814460
anti-polyglutamine (1C2)	mouse, monoclonal	Chemikon MAB1574
anti-luc	goat, polyclonal	Promega G7451
anti-AR (Ab-3)	rabbit, polyclonal	Oncogene PC167
anti-AR (N-20)	rabbit, monoclonal	Santa Cruz sc-816
anti-hsp40	rat, polyclonal	Stressgen SPA400
anti- β -Gal	mouse, polyclonal	Sigma G4644

3.1.6.2 Secondary antibodies

Antibody	Species	Reference
anti-mouse-IgG-HRP	goat	Sigma A4416
anti-mouse-CY3	goat	Dianova
anti-mouse-FITC	goat	Dianova

Antibody	Species	Reference
anti-rabbit-IgG-HRP	goat	Sigma A9169
anti-rabbit-CY3	goat	Dianova
anti-rabbit-FITC	goat	Dianova
anti-goat-IgG-HRP	rabbit	Sigma A5420

3.2 Methods

3.2.1 DNA subjected methods

3.2.1.1 Plasmid preparation

Overnight bacterial cultures carrying the plasmid of interest were grown at 37 °C at 240 rpm. Plasmid preparations were performed with Qiagen's *Mini-, Midi- and EndoFree-Plasmid-Maxi-Kit* according to supplier's instructions. The concentration was determined by a photometer at 260 nm (Beckman DU640 Spectrophotometer). Constructs were verified by DNA sequencing (Sequiserve, Germany).

3.2.1.2 Restriction digestion of DNA

The restriction enzymes used for this study were purchased from New England Biolabs (NEB). Plasmids and PCR products were digested according to supplier's instructions.

3.2.1.3 Dephosphorylation of 5'-protruding DNA ends

To prevent religation of vector backbone the digested plasmids were treated with calf intestine alkaline phosphatase (*CIP*, NEB) according to the supplier's instructions.

3.2.1.4 Agarose gelelectrophoresis of DNA

6 x *Loading Dye Solution* (Fermentas) was added to the DNA samples that subsequently, were separated by agarose gelelectrophoresis in 1 x TAE buffer at 90-120 V. The gelelectrophoresis chamber was purchased from BioRad. The gels contained 0.7-1% agarose (in 1 x TAE buffer) and 1 µg/ml ethidium bromide (BioRad). The *Gene Ruler 1 kb-DNA-Ladder* (Fermentas) was used as size marker. The DNA was visualized using UV light (MWG Biotech) and where required, extracted with *QIAquick* (Qiagen) according to the supplier's instructions.

3.2.1.5 Polymerase chain reaction (PCR)

PCR mediated amplification of DNA was performed in a *T3 Thermocycler* (Biometra) according to a standard protocol with minor modifications, when necessary. PCR running conditions also followed a standard protocol, annealing temperature and extension time varied according to primer composition and template length. *Taq*-polymerase (Promega), *Pfu*-Polymerase (Promega) or the *Expand Long Template* system (Roche) was used. A typical PCR reaction with corresponding cycling conditions is shown below.

DNA template	25 ng – 250 ng
Primer	20 pmol each
dNTPs	1 mM
Polymerase buffer	1 x
Polymerase	2.5 U
Final volume	25µl, 50 µl or 100 µl
Cycle count	30
Initial strand separation	95 °C, 5 min
Annealing	52 – 58 °C, 60 seconds
Cycle strand separation	95 °C, 60 seconds
Extension	72 °C, 1 min per kbp of DNA
Final extension	72 °C, 10 min
Storage	4 °C or -20 °C

The PCR product was purified with the *PCR Purification Kit* (Qiagen) according to supplier's instructions.

3.2.1.6 DNA ligation

For ligation, vector DNA and DNA insert, at a ratio of 1:7, and 1 μ l (100 U) *T4-DNA-Ligase* (NEB) were incubated in ligase buffer at 25 °C for 2 h or, for increased efficiency, at 16 °C overnight and transformed into chemically competent *E. coli* SURE or DH5 α F' cells.

3.2.1.7 In vitro transcription

Vectors containing the gene of interest were linearized and *in vitro* transcription was performed with the *MessageMachine Kit* (Ambion, TX) according to supplier's instruction. The concentration was determined by a photometer (NanoDrop-1000 Spectrophotometer, NanoDrop).

3.2.2 Biochemical methods

3.2.2.1 Determination of protein concentration

The protein concentration of protein extracts was determined photometrically (DU640 Spectrophotometer, Beckman) at a wavelength of 595 nm using the *Protein Assay Kit* (BioRad). This assay is based on the method of Bradford (Bradford, 1976). Before, a standard curve was made with known protein amounts of BSA.

3.2.2.2 SDS-PAGE

SDS - PAGE (sodiumdodecylsulfate polyacrylamide gel electrophoresis) was performed using a discontinuous buffer system (Laemmli, 1970) in *Mini-Protean 3 System* electrophoresis chambers (BioRad). Polyacrylamide gels were prepared with a BioRad system.

Chemicals	Separating gel				Stacking gel
	8%	10%	12.5%	15%	5%
30% Acrylamide/ 0.8% Bisacrylamide	2.25 ml	2.85 ml	3.4 ml	4.25 ml	640 μ l
1.875 M Tris-HCl pH8.8	1.75 ml	1.75 ml	1.75 ml	1.75 ml	-
0.6 M Tris-HCl pH6.8	-	-	-	-	1 ml
10% SDS	83.5 μ l	83.5 μ l	83.5 μ l	83.5 μ l	35 μ l
TEMED	5 μ l	5 μ l	5 μ l	5 μ l	5 μ l
10% APS	50 μ l	50 μ l	50 μ l	50 μ l	20 μ l
H ₂ O	4.35 ml	3.75 ml	3.2 ml	2.37 ml	2.5 ml

SDS loading buffer was added to protein samples to 1 x concentration. Samples were heated at 96 °C for three minutes and briefly centrifuged prior to loading. Gelelectrophoresis was carried out at a voltage of 90-160 V. *Prestained Protein Marker* (Fermentas) was used as size marker.

3.2.2.3 Coomassie staining of SDS-PAGE gels

SDS-PAGE gels were treated with staining solution for 1 h at room temperature and subsequently, the gels were treated with destaining solution to remove the unbound stain. Where required, gels were dried overnight between two cellophane foils (*GelAirDryer*, BioRad).

3.2.2.4 Western Blotting of SDS-PAGE gels and immunodetection

Proteins were separated by SDS-PAGE and transferred to nitrocellulose membranes (*Protran*, Schleicher&Schuell) in a semi-dry western blotting unit (SemiPhore) at a constant current of 100 mA/gel (Towbin *et al.*, 1979) for 2 h. Nitrocellulose membranes were blocked in 5% skimmed milk powder in TBSt for 30 min or overnight. The membranes were then incubated with primary antibody in TBSt for at least 2 h and extensively washed in TBSt before incubation with the secondary antibody in TBSt (at least 1 h). After

extensive washing, protein bands were detected by incubating the membranes with ECL chemiluminescence solution or *ECL+* (Amersham) and exposure on the *Image Reader LAS 3000* (Fujifilm). Where required, the bound antibodies were removed upon incubation at 50 °C for 1 h in stripping buffer followed by intensive washes in TBSt.

3.2.2.5 Dot blot assay

Dot blot assay was used to estimate the total amount of protein without earlier separation. 5 µg of total cell extract (yeast) was spotted directly onto nitrocellulose membrane. The membrane was then air-dried and processed as described above.

3.2.2.6 *In vitro* aggregation

In vitro aggregation reactions were performed essentially as described (Schaffar *et al.*, 2004). Briefly, purified GST-Htt exon 1 fusions (3 µM) were mixed with 3 or 30 µM Congo red, 313B02 (3), 293G02 (4), 306H03 (5), or DMSO. To initiate the aggregation reaction, 2.5 U *PreScission* Protease in buffer A (50 mM Tris-HCl, pH 7.4; 150 mM KCl) was added. Reactions were incubated at 30 °C for 8 hours and then stopped by adding an equal volume of 4% SDS / 100 mM DTT.

3.2.2.7 Filter retardation assay

For the detection and quantification of aggregates the filter retardation assay (Scherzinger *et al.*, 1997) was used. When analysing SDS-insoluble aggregates, an equal volume of 4% SDS / 100 mM DTT was added to benzonase (40 U, Merck) treated yeast, cell or zebrafish embryo extracts. The mixture was heated for 5 min at 96°C and dilutions of between 25 and 1000 µg were filtered through a cellulose acetate membrane (pore size = 0.2 µm, Schleicher&Schuell) equilibrated in 0.1% SDS. The slots of the apparatus (Hoefer) were washed several times with 0.1% SDS. The membrane was blocked in 5% skimmed milk

powder in TBSt for 30 min or overnight and the subsequent immunodetection was carried out as described in 3.2.2.4.

3.2.2.8 Subcellular fractionation and formic acid treatment

For subcellular fractionation, extracts were centrifuged at 100,000 × g for 30 min to obtain the supernate and pellet fractions. The pellet was washed once with the appropriate lysis buffer, centrifuged at 100,000 × g for 15 min and either dissolved in SDS sample buffer or 100% formic acid. The latter was incubated for 3 h at 37 °C with agitation (600 rpm), vacuum-dried, resuspended in SDS-sample buffer, as previously reported (Hazeki *et al.*, 2000) and analyzed by SDS-PAGE.

3.2.2.9 Size exclusion chromatography

Total cell extracts were centrifuged at 20,000 × g at 4 °C for 30 min and ~2 mg of the supernate was subjected to size exclusion chromatography on FPLC system with Superdex200 column at 4 °C. The appropriate lysis buffer was used as running buffer. Fractions were analyzed by immunoblotting. The chromatographic resolution was between 25 kDa and 2,500 kDa determined by protein standards.

3.2.2.10 Co-Immunoprecipitation

Total cell extracts were centrifuged at 20,000 × g at 4 °C for 30 min and 400 µg of the supernate was incubated with 2 µg of anti-myc antibody (Santa Cruz) overnight at 4 °C with agitation. 100 µl of protein G-Sepharose beads slurry was washed four times for 3 min at 660 × g at 4 °C with 1 ml of lysis buffer. The beads were resuspended in 100 µl of lysis buffer with 15% BSA and incubated overnight at 4 °C. After a washing step, the lysate was transferred to a minicolumn and 100 µl of protein G-Sepharose beads slurry was added. The resulting protein G-Sepharose mix was incubated for 4 hours at 4 °C with agitation and subsequently washed extensively with cell lysis buffer. Finally, the

bound antibody and antigen complex was incubated in SDS loading buffer at 95 °C for 10 min and eluted by centrifugation.

3.2.2.11 Trichloroacetic acid (TCA)-precipitation

TCA precipitation was performed to concentrate protein samples prior to SDS-PAGE analysis. Protein samples were mixed at 1:2 ratio with a 20% TCA solution and incubated for 15 min at 4 °C. After centrifugation at 20,000 x g for 15 min at 4 °C, pellets were washed three times with 900 µl of cold acetone and the resulting pellets were dried at room temperature after the last wash. Pellets were then resuspended in SDS loading buffer and boiled for 10 min at 95 °C.

3.2.3 *Escherichia coli* work

3.2.3.1 Chemically competent *E. coli* cells and transformation

E. coli SURE or DH5αF' cells were grown in 800 ml TYM until midlog phase (OD₆₀₀ ~0.6), chilled, centrifuged (4,000 x g) and carefully resuspended in 100 ml cold, filter sterilized Tfb I. Cells were pelleted (4,000 x g) again and resuspended in 20 ml cold, filter sterilized Tfb II. 200 µl aliquots were frozen in liquid nitrogen and stored at -80 °C.

For transformation, competent cells were thawed on ice. 50-200 µl cells were mixed with 1 µl plasmid DNA or 10-20 µl ligation reaction and incubated on ice for another 20 min. Cells were heat-shocked at 42 °C for 90 s and subsequently placed on ice for 2 min. 800 µl of LB medium was added and incubated for 60 min at 37 °C. The transformation reaction was plated on selective agar plates and incubated at 37 °C, until colonies have developed.

Tfb I	30 mM KOAc
	50 mM MnCl ₂
	100 mM KCl
	10 mM CaCl ₂
	15% (v/v) glycerol

TfB II	10 mM Na-MOPS pH 7.0
	75 mM CaCl ₂
	10 mM KCl
	15% (v/v) glycerol

3.2.4 Yeast work

3.2.4.1 Transformation

For yeast transformation, 1 ml of an overnight culture was spun down in a centrifuge for 30 sec at 10,000 x g. The supernate was discarded, 10 µl of carrier DNA plus 0.5-1 µg transforming DNA was added and vortexed. After the addition of 500 µl PLATE solution with subsequent vortexing, and addition of 57 µl DMSO the mixture was vortexed briefly and incubated for 15 min at room temperature. Heat shock was carried out at 42 °C for 15 min and the cells were pelleted at 10,000 x g for 30 sec. Most of the supernate was removed and the residual was used to resuspend the cells that were finally spread onto selective plates.

PLATE solution	40% PEG 3350
	0.1 M Lithium acetate
	10 mM Tris/HCl pH 7.5
	1 mM EDTA

3.2.4.2 Yeast lysis

Depending on the amount of yeast cells, yeast cultures were centrifuged at 1,000 x g for 20 min and the pellet was resuspended in 200-500 µl cold lysis buffer. An equal amount of glass beads was added and the preparations were vortexed for 4 x 1 min. On occasion, they were put on ice to allow cooling down. Benzonase was added (75 U), and the extracts were incubated at 4 °C for 1 h with gentle agitation. Extracts were centrifuged at 2,000

x g for 3 min at 4 °C. The supernate was collected and protein concentration was determined with a protein assay kit (Bio-Rad).

Lysis buffer	25 mM Tris/HCl pH7.5
	50 mM KCl
	10 mM MgCl ₂
	1 mM EDTA
	5% Glycerol
	1 mM PMSF
	1 x protease inhibitor cocktail (Roche)

3.2.4.3 Immunofluorescence microscopy

For the fixing, 1 ml of 1 M potassium phosphate (pH 6.5) and 1.2 ml formaldehyde were added to 10 ml of yeast culture and incubated for 1 h at room temperature. After addition of 1 ml cold SP the cells were centrifuged at 600 x g at 4 °C for 5 min. Cells were resuspended in 1 ml cold SP and transferred into a 1.5 ml Eppendorf tube. They were washed five times by centrifugation at 600 x g at 4 °C for 5 min with subsequent resuspension in 1 ml of cold SP. Following the last washing the cells were resuspended in 900 µl of SP β and 100 µl of zymolyase solution was added. The cells were incubated for 2-3 h at 30 °C with agitation (650 rpm) followed by an incubation for 5 min on ice. The generated spheroblasts were washed again five times (see above) before they were finally resuspended in 100-200 µl of cold SP. For the staining, multi-well slides for microscopy were prepared by adding 20 µl of polylysine solution (0.5 mg/ml) to each well, followed by an incubation for 2 min at room temperature. The wells were washed five times with water and 20 µl spheroblasts were applied per well followed by an incubation for 10 min at room temperature. The spheroblasts were washed with 20 µl PBS-B. The slides were immersed in ice cold methanol for 5 min and afterwards, in ice cold acetone for 30 sec. After the slides got air-dried, 20 µl PBS-B was applied to each well for 60 min at room temperature. The

wells were washed twice with PBS-B and 20 μ l of primary antibody solution was added to each well. The slides were incubated in a wet chamber for 60 min at room temperature. Afterwards, the wells were washed six times with PBS-B before application of the second antibody solution. Again, the slides were incubated in a dark, wet chamber for 60 min. After six additional washes with PBS-B the slides were air-dried. 4 μ l of DAPI mounting medium was added to each well and the slides were covered by coverslips and sealed with nail polish. For long term storage they were put at -20 °C.

SP	0.1 M KPO ₄ pH 6.5 1.2 M Sorbitol
SP β	14 μ l Mercaptoethanol 10 ml SP
Zymolyase solution	2.5 mg Zymolyase (20T) in 1 ml SP β
PBS	50 mM NaPO ₄ pH 7.5 300 mM NaCl
PBS-B	50 mM NaPO ₄ pH 7.5 150 mM NaCl 1% BSA
DAPI mounting medium	75% <i>Citifluor</i> 25% PBS
0.25 μ g/ml DAPI (4',6-diamidino-2-phenylindole, dihydrochloride, Molecular Probes)	

3.2.4.4 Drop test

4 μ l of subsequent dilutions of 1:5, starting with an OD₆₀₀ of 0.1, were spotted on (selective) plates and incubated at the indicated temperature. Growth was documented in regular time intervals with a gel documentation setup (MWG Biotech).

3.2.4.5 Luciferase assay

To determine firefly luciferase activity in intact cells (Greer and Szalay, 2002), yeast cultures were grown in presence or absence of galactose (2%) until exponential phase and DHT was added to a concentration of 5 μ M for 2 h. An aliquot was taken to determine firefly luciferase activity in intact cells by mixing with 5 volumes of 100 mM potassium-luciferin (Promega, Madison, USA) and measuring light emission for 10 sec using a Lumat LB 9507 luminometer (EG&G Berthold, Bad Wildbach, Germany). Values for luciferase activity were normalized to OD₆₀₀ of the yeast culture, and the results of the galactose induced cultures were normalized to the uninduced ones.

3.2.4.6 β -Galactosidase assay

β -Galactosidase assays were performed essentially as described (Guarente, 1983). Equal amounts of protein extract were added to Z β , ONPG-Z in Z buffer was added to a concentration of 615 μ g/ml, and reactions were incubated at 30 °C for 50 min. The reaction was stopped by the addition of Na₂CO₃ to 278 mM, and the A420 was measured relative to the blank, which contained yeast lysis buffer. Yeast extracts were prepared and protein concentration was determined as described above. Equal amounts of protein in 100 μ l yeast lysis buffer were transferred to an Eppendorf tube. A blank tube with 100 μ l yeast lysis buffer served as a control. 600 μ l of Z β buffer and 100 μ l of 2 x Z β was added to the reaction and the blank tubes.

Z buffer	60 mM Na ₂ HPO ₄ (pH 7.0)
	40 mM NaH ₂ PO ₄
	10 mM KCl
	1 mM MgSO ₄

Z β buffer	60 mM Na ₂ HPO ₄ (pH 7.0)
	40 mM NaH ₂ PO ₄
	10 mM KCl
	1 mM MgSO ₄

	50 mM β -mercaptoethanol
2 x Z β buffer	60 mM Na ₂ HPO ₄ (pH 7.0) 40 mM NaH ₂ PO ₄ 10 mM KCl 1 mM MgSO ₄ 100 mM β -mercaptoethanol
ONPG-Z	4 mg/ml in Z buffer (pH 7.0)

3.2.5 Cell culture work

3.2.5.1 Culturing

The adherent cell lines used in this study were cultured in culture plates (Costar) of variable well size or in *Cellstar* tissue culture flasks (Greiner) in water vapour saturated 5% CO₂ atmosphere at 37 °C. Frequently, upon reaching confluency, the cells were split as follows. The cells were washed twice with PBS and incubated with Trypsin/EDTA for 5 min at 37 °C. Trypsin was inactivated by the addition of fresh medium. Subsequently, the cells were resuspended by pipetting and 1:5 or 1:10 dilutions were cultured continuously.

3.2.5.2 Determination of cell number and transient transfection

One day before transfection, the cells were Trypsin/EDTA treated as described above and resuspended in supplemented medium. 20 μ l of cells were mixed with 20 μ l 0.4% Trypan Blue Solution (Sigma) and the number of living cells was determined using a counting chamber (Neubauer) and the inverted microscope Diavert (Leitz) according to supplier's instructions. Cells were plated in supplemented medium so that they reached 50-90% confluency the next day. The cells were transfected by a liposome-mediated method using LipofectAMINE Plus™ (Life Technologies, Inc.) according to supplier's instructions. After

incubation of cells at 37 °C for 3 h, the transfection mixture was removed, and cells were incubated with supplemented medium up to 48 h.

3.2.5.3 Preparation of cell extracts

The cells were washed twice with cold phosphate-buffered saline (PBS). 1 ml of cold lysis buffer was added, incubated for 10 min on ice, scraped from the plate and pelleted by centrifugation at 2,000 x g for 3 min at 4 °C. The supernate was collected, and protein concentration was determined with a protein assay kit (Bio-Rad).

PBS	8 mM Na ₂ HPO ₄ x 7 H ₂ O (pH 7.0) 2 mM NaH ₂ PO ₄ x H ₂ O 70 mM NaCl
Lysis buffer	0.5% TritonX-100 0.5% sodium deoxycholate 1 x protease inhibitor cocktail (Roche) in PBS

3.2.5.4 Immunofluorescence microscopy

The cells were seeded on coverslips in a 12-well plate one day before transfection. Transfection was carried out as described above. Thereafter, the coverslips containing the cells were washed three times with PBS and incubated in cold methanol on ice for 5 min. After three additional washes with PBS, the cells were incubated in a 1:200 dilution of primary antibody (in PBS-B) for 1 h. The cells were washed three times in PBS for 10 min and incubated in a 1:350 dilution of secondary antibody and 1:4000 dilution of DAPI (4',6-diamidino-2-phenylindole, dihydrochloride, Molecular Probes) in PBS for 1h. After three additional washes, the coverslips were mounted onto slides with ProLong® (Antifade Kit, Molecular Probes). Fluorescence was visualized with an

Axiovert200M inverted fluorescence microscope (Zeiss, Jena, Germany). Images were captured digitally with a Zeiss AxioCam HRm camera and assembled in PhotosHop 8.0 (Adobe Systems, Mountain View, CA).

PBS-B 1% BSA in PBS

3.2.5.5 Drug treatment

3 h after transfection the transfection medium was removed and supplemented medium containing 50 µM PGL-135, 10 µM 313B02, 10 µM 293G02, 10µM 306H03, 5 µM DHT or DMSO as control, was added for up to 48 h.

3.2.5.6 MTT assay

One day before transfection, cells were plated in 24-well plates. Transfection was carried out as described above. After total incubation of cells at 37 °C for 48 h the medium was removed and 500 µl of a MTT solution (0.42 mg/ml in serum-free DMEM) was added and incubation was continued for further 2h. 500 µl cell lysis buffer was added, and the MTT crystals were dissolved by repeated pipetting. Absorbance values at 570 nm were determined with the Synergy HT Fluorescence Microplate Reader (BioTek Instruments, Inc.).

Lysis buffer 20% (v/v) sodium dodecyl sulphate (SDS)
 50% (v/v) *N,N*-dimethylformamide

3.2.6 Zebrafish work

3.2.6.1 Animal husbandry

Zebrafish were maintained, mated, and raised as described (Mullins *et al.*, 1994). Embryos were kept at 28°C and staged as described (Kimmel *et al.*, 1995).

3.2.6.2 Agarose plates for holding embryos

Liquefied 1.5% agarose was poured into a 100 mm plastic Petri dish to a depth of about 5 mm. A plastic mould was floated into the agarose. After solidification the mould was removed and the agarose was covered with E3 to inhibit over drying.

3.2.6.3 Embryo injection

Eggs were collected approximately 30 min after mating and placed in the slots of an agarose plate (preparation described above). mRNA was injected with the use of a microinjector (FemtoJet, Eppendorf) at a concentration of 1 $\mu\text{g}/\mu\text{l}$ into the yolk of embryos at the 1–2 cell stage. Co-injections were performed with 1 $\mu\text{g}/\mu\text{l}$ polyglutamine-GFP mRNA and either 1 $\mu\text{g}/\mu\text{l}$ β -Gal mRNA as a control or 0.5 $\mu\text{g}/\mu\text{l}$ Hdj1 and 0.5 $\mu\text{g}/\mu\text{l}$ Hsp70-YFP mRNA. Embryos were cultured at 28.5 °C in E3, unfertilized eggs were removed, and if required, embryos were scored 24 h post-fertilization according to their appearance.

3.2.6.4 Acridine Orange staining

Zebrafish embryos were dechorionated and anesthetized with Tricaine (0.016% w/v). To assess apoptotic cell death, the embryos were immersed in 3 $\mu\text{g}/\text{ml}$ Acridine Orange (acridinium chloride hemi[zinc chloride]; AO; Molecular Probes) for 15 min and washed three times with E3.

3.2.6.5 TOPRO-3 staining

Zebrafish embryos were dechorionated and anesthetized with Tricaine (0.016% w/v). For nuclear staining, embryos were immersed in 1:1000 dilution of TOPRO-3 stain (monomeric cyanine nucleic acid stain; Molecular Probes) for 30 min at room temperature and washed three times with E3.

3.2.6.6 Microscopy and time-lapse analysis

Zebrafish embryos were dechorionated, anesthetized with Tricaine (0.016% w/v), and orientated in 3% methyl cellulose on coverslips. Fluorescence was visualized with an LSM510 META inverted confocal microscope (Zeiss, Oberkochen, Germany). An emission spectrum of 488 nm – 560 nm was chosen to detect GFP, YFP and Acridine Orange, for the detection of TOPRO-3 an emission spectrum of 633 nm – 670 nm was used. For 3D imaging, a stack of 10 frames was collected at an interval of 10-24 μm between adjacent slices, and the images were assembled to obtain a 3D projection. To dissociate the GFP/AO or GFP/YFP fluorescence signals, analysis was performed by emission fingerprinting in confocal lambda mode. Reference spectra of the single fluorochromes were taken and subsequently used to separate the overlapping emission spectra of the samples (linear unmixing, Dickinson *et al.* 2001). A stack of 2-3 frames of the embryonic tail region 24 h post-fertilization was collected at an interval of 20 μm , and the number of AO stained cells was counted to estimate the amount of apoptotic cells. For the time-lapse analysis of the living cells, zebrafish embryos 24 h post-fertilization were orientated in 1.2% low melting agarose (1.2% in E3 with Tricaine 0.09% w/v) and covered with E3. Images were taken 24, 28, and 32 hours post-fertilization.

3.2.6.7 Fish lysis

Injected embryos were resuspended in cold lysis buffer and lysed by passing through a 0.6 mm needle. After freezing and thawing the extracts, benzonase was added (75 U), and the extracts were incubated at 4 °C for 1 h with gentle agitation. Extracts were centrifuged at 2,000 \times g for 3 min at 4 °C in the presence of glass beads to facilitate separation of the chorion debris. The supernate was collected and protein concentration was determined with a protein assay kit (Bio-Rad). For the detection of Hsp70-YFP (and Q102-GFP in Figure 18 B), embryos were first dechorionated and yolk dissected, as previously described (Evans *et al.*, 2005).

Lysis buffer 0.5% Triton X-100
 0.5% sodium deoxycholate
 1 x protease inhibitor cocktail (Roche)
 in PBS

4 Results

A common feature of neurodegenerative diseases, such as Alzheimer's disease, prion diseases, and polyglutamine diseases, including Huntington's disease (HD) and SBMA, is the accumulation and deposition of characteristic amyloid or amyloid-like fibrils of the respective disease proteins in the brain (Aguzzi and Haass, 2003; Ross and Poirier, 2005). In HD and SBMA, the degeneration of neurons is associated with the intracellular deposition of inclusion bodies (IBs) that contain fibrillar aggregates of polyglutamine-expanded huntingtin (htt) or androgen receptor (AR), respectively, and likely represent the final manifestation of a multi-step aggregation pathway involving several intermediate species (Poirier *et al.*, 2002). The latter are suspected of causing cytotoxicity through various mechanisms including aberrant interactions, *e.g.* inactivation of essential transcription factors, and inhibition of the ubiquitin proteasome system (Bennett *et al.*, 2005; Schaffar *et al.*, 2004). A critical step in both fibril formation and toxicity is thought to be the generation of N-terminal fragments containing the pathogenic polyglutamine stretch (Davies *et al.*, 1997; Lunkes *et al.*, 2002).

This study describes the development of a novel zebrafish model of HD to identify chemical compounds that suppress aggregation of amyloidogenic proteins. As a result, anti-prion compounds were identified as novel inhibitors of polyglutamine aggregation, suggesting that polyglutamine aggregates and prions may share common structural epitopes. In addition, this study presents a novel yeast model of SBMA revealing that N-terminal polyglutamine-containing fragments cause toxicity and inhibit androgen receptor transactivation capacity.

4.1 Development of a zebrafish model for polyglutamine disease suitable for whole organism validation of candidate compounds

In the field of neurodegenerative disorders, there has been considerable debate about the role of aggregates. Although neither the structure of a polyglutamine fibril nor the mechanisms mediating toxicity are yet fully understood, much attention has been focused on identifying means to disrupt or alter the polyglutamine aggregation pathway (Di Prospero and Fischbeck, 2005). Many promising compounds with anti-aggregation activity have been identified *in vitro* and in cell based assays but further investigations with respect to their effect in a vertebrate organism are restricted to the expensive and time consuming rodent models (Heiser *et al.*, 2002; Hockly *et al.*, 2006). This study describes the establishment of an alternative vertebrate HD model in zebrafish suitable for whole organism validation of candidate compounds.

4.1.1 The establishment and characterization of a zebrafish model of HD

For the development of a zebrafish model of polyglutamine disease mRNA of various polyglutamine containing huntingtin constructs were injected in varying concentrations into the yolk of zebrafish embryos at the 1-2 cell stage. Unfertilized eggs were removed and the embryos were examined up to a week with regard to phenotypical abnormalities. Injection of the huntingtin constructs gave rise to a whole set of phenotypical abnormalities which were however, inconsistent and varying between the clutches, independent of the sequences flanking the polyglutamine stretch. Due to the lack of a clear phenotype, the research was limited to the GFP-tagged huntingtin fragments since the transparency of the zebrafish embryo permitted straightforward *in vivo* analysis of these constructs (Figure 9). The constructs used for this study consist of an N-terminal fragment of htt containing 4, 25, or 102 Q fused to green fluorescent protein (Q4-GFP; Q25-GFP; Q102-GFP, respectively; Figure 9). Two constructs,

namely Q4-GFP and Q25-GFP, were used as a control since the polyglutamine stretch does not exceed the pathogenic threshold of about 38 Q. The third construct, Q102-GFP, exceeds this threshold and was therefore considered as the pathogenic species.

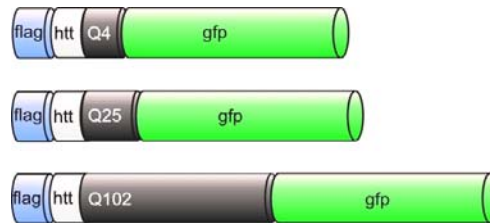


Figure 9: Polyglutamine-fusions used in this study.

Depicted are the constructs used in this study which consist of an N-terminal FLAG tag upstream of the first 16 amino acids of the huntingtin protein followed by a polyglutamine stretch with either 4, 25 or 102 Q fused to green fluorescent protein.

4.1.1.1 Polyglutamine-expanded htt is deposited into inclusions of SDS-insoluble aggregates in *D. rerio*

An essential step towards a zebrafish model of HD was to reproduce key features of HD. Embryos at the 1-2 cell stage were injected with mRNA of the constructs (Figure 9). Q4-GFP and Q25-GFP fusion proteins were diffusely distributed, whereas the mutant polyglutamine-expanded htt fusion protein, Q102-GFP, accumulated in inclusion body-like aggregates throughout most embryos after 24 h (Figure 10).

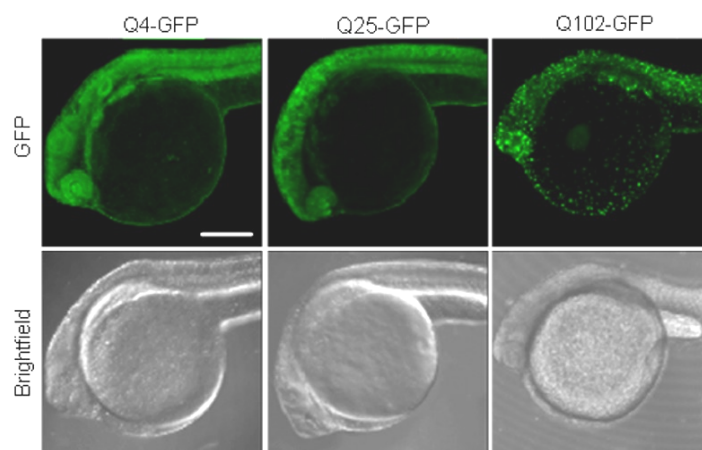


Figure 10: Q102-GFP forms inclusions in *D. rerio*.

Flourescent (*top panels*) and brightfield (*bottom panels*) images of zebrafish embryos expressing Q4-GFP, Q25-GFP, or Q102-GFP, 24 h post-fertilization. *Scale bar*, 200 μ m.

To gain more insights into the cellular distribution of the constructs, the analysis was focused on the hatching gland, a monolayer of cells that is located on the pericardium (on the yolk sac ventral to the head). Hence, artificial signals from neighbored layers were avoided. Expression of Q102-GFP resulted in a massive appearance of inclusions in the hatching gland, unlike Q4-GFP (data not shown) and Q25-GFP (Figure 11).

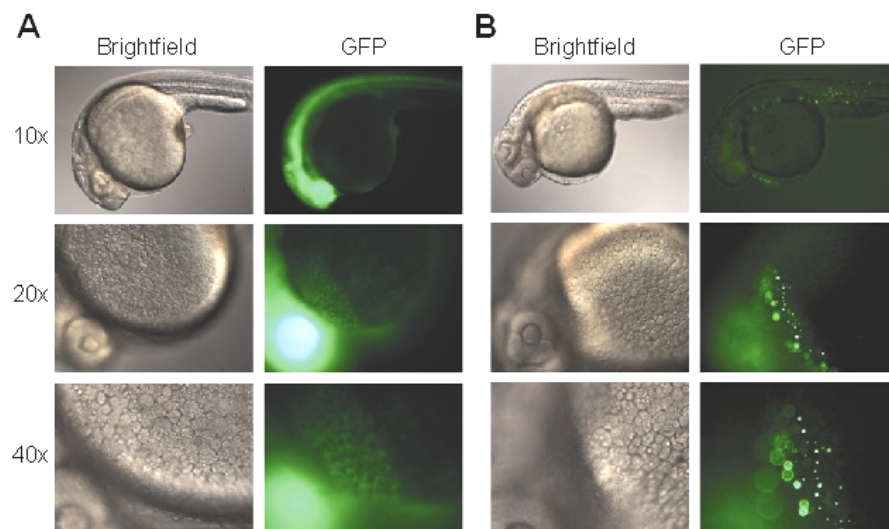
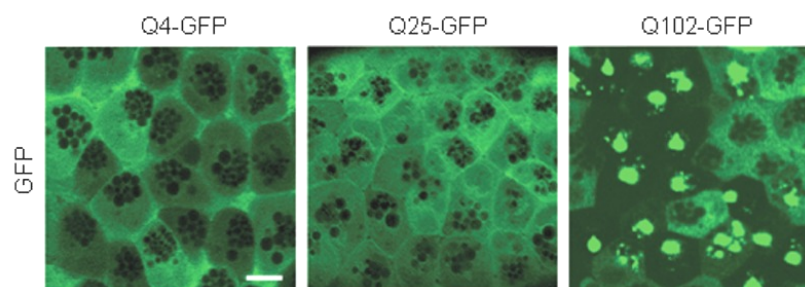


Figure 11: Aggregate formation in the hatching gland upon expression of Q102-GFP.

Brightfield and fluorescent images of zebrafish embryos expressing Q25-GFP (A) or Q102-GFP (B), 24 h post-fertilization at different magnifications.

Higher magnification images of the hatching gland indicated that Q102-GFP, but not the shorter polyglutamine variants, accumulated in large, cytoplasmic inclusions adjacent to the nuclei (Figure 12).

A



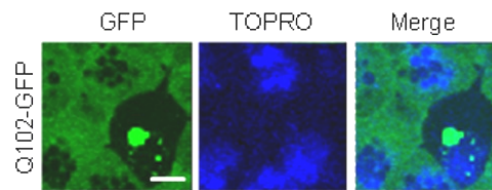
B

Figure 12: The inclusions formed by Q102-GFP are relatively large in size and perinuclearly localized.

(A) High magnification images of polyglutamine-GFP expression patterns in the embryonic hatching gland. *Scale bar*, 10 μm . (B) Embryos expressing Q102-GFP stained with TOPRO (shown in blue) to visualize nuclei in the hatching gland. *Scale bar*, 10 μm .

Analysis of embryos at later time points using time-lapse microscopy showed that Q102-GFP inclusions grew in size by efficient incorporation of soluble Q102-GFP, resulting in its depletion from the cytoplasm (Figure 13).

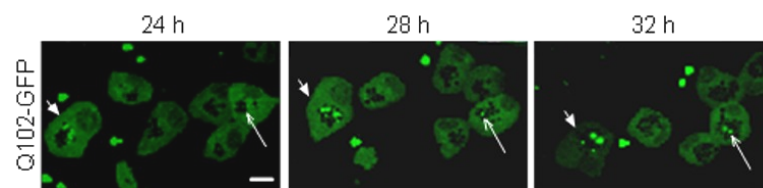


Figure 13: The Q102-GFP inclusions grow in size by incorporation of soluble Q102-GFP.

The dynamics of Q102-GFP aggregation, as monitored by time-lapse microscopy 24, 28, and 32 h post-fertilization. The formation of an aggregate structure (*long arrow*) and the incorporation of soluble Q102-GFP into pre-existing aggregates (*short arrow*) are indicated. These images have been corrected for photobleaching effects. *Scale bar*, 10 μm .

To get insights into the biochemical properties of the inclusions, total cellular extracts of injected embryos 24 h post-fertilization were subjected to high speed centrifugation. Both Q4- and Q25-GFP remained exclusively in the soluble supernate fraction, whereas a significant portion of Q102-GFP was found in the SDS-insoluble pellet fraction and could only be dissolved by formic acid treatment (Figure 14 A; Hazeki *et al.*, 2000). Analysis of total embryo extracts by an established filter trap assay (Scherzinger *et al.*, 1997) confirmed that Q102-GFP, but not Q4-GFP or Q25-GFP, formed large SDS-insoluble aggregates that were retained by the 200 nm pore sized membrane (Figure 14 B).

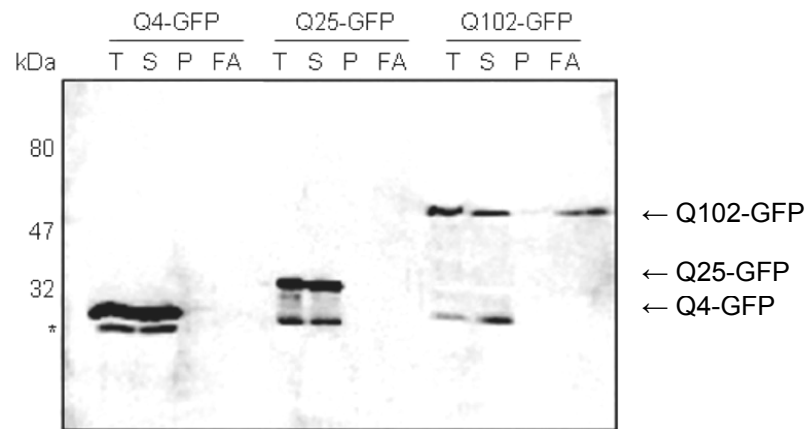
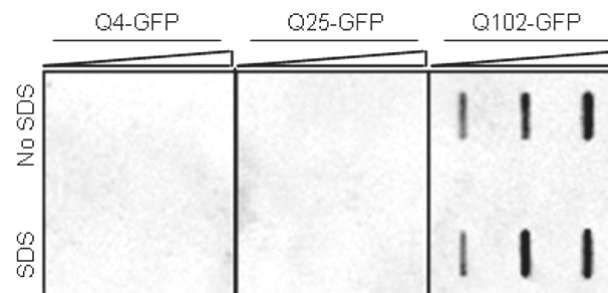
A**B**

Figure 14: Q102-GFP forms SDS-insoluble aggregates in *D. rerio*.

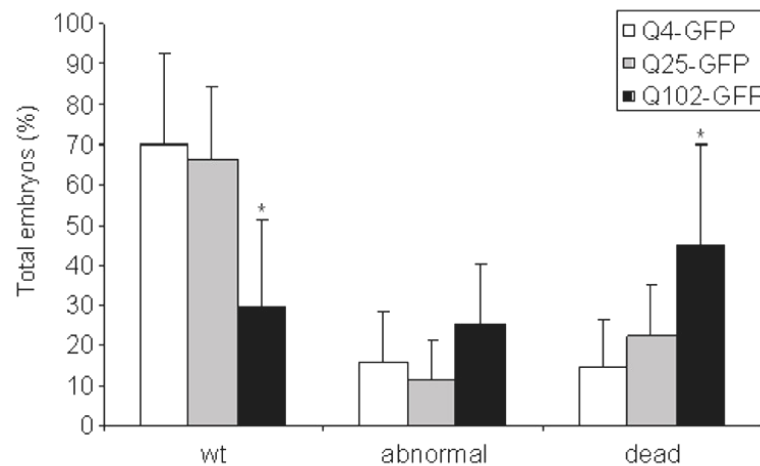
(A) Analysis of the solubility of the polyglutamine-GFP fusions. Extracts from embryos (24 h post-fertilization) expressing Q4-GFP, Q25-GFP, or Q102-GFP were subjected to high speed centrifugation, and the resulting fractions were analyzed by SDS-PAGE and western blotting with anti-GFP antibody. *T*, total cell lysate; *S*, supernate; *P*, pellet fraction dissolved in SDS; *FA*, pellet fraction dissolved in formic acid. *Asterisk*, free GFP cleaved from the fusion protein. (B), Filter trap analysis of polyglutamine-GFP fusions. Increasing amounts (25 µg, 50 µg and 100 µg) of total cell extracts from (A) were analyzed by filter trap assay in the presence (*bottom row*) and absence (*top row*) of SDS/DTT at 95°C.

4.1.1.2 Polyglutamine length dependent toxicity is independent of detectable inclusions

To determine whether the polyglutamine-GFP fusion proteins caused toxicity, the phenotypes of embryos expressing Q4-, Q25-, or Q102-GFP, were evaluated 24 h post-fertilization. Due to the aforementioned diversity of different phenotypes, the embryos were scored as visibly normal, abnormal, or dead. Q102-GFP expression was associated with increased numbers of dead or

morphologically abnormal embryos when compared to Q4- or Q25-GFP expression (Figure 15 A). Noteworthy among the abnormal embryos, a characteristic ‘cyclopic’ phenotype was increasingly observed in embryos expressing Q102-GFP (Figure 15 B).

A



B

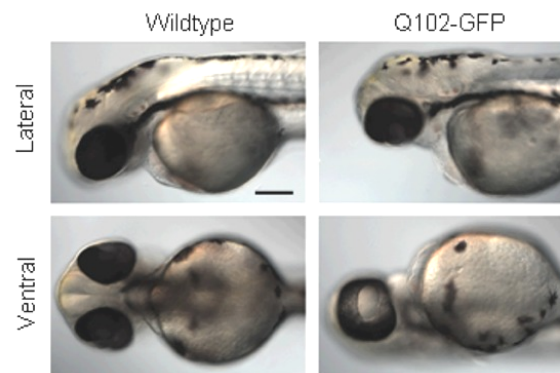
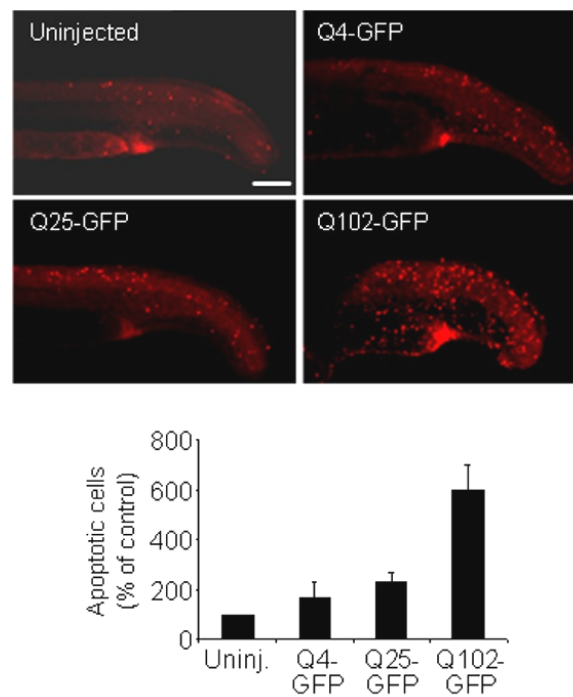
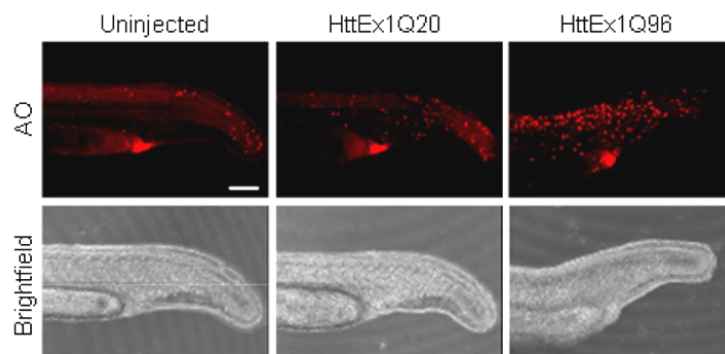


Figure 15: Expression of Q102-GFP causes toxicity in zebrafish embryos.

Embryos were injected at the 1-2 cell stage with mRNA encoding the indicated GFP fusions. (A) Normal (wt), abnormal, and dead embryos were counted 24 h post-fertilization. Data are mean values of $n=12-20$ experiments \pm S.D. *, $p < 0.01$ versus Q4-GFP or Q25-GFP injected embryos (Bonferroni's post hoc test). (B) Brightfield images of a wildtype embryo and an embryo expressing Q102-GFP, 48 h post-fertilization. Scale bar, 100 μ m.

This mutant phenotype is characterized by fusion of the eyefields yielding a single eye in the midline (Blader and Strahle, 1998). Since only a subset of embryos showed this phenotype, it was not suitable for any kind of screening.

Acridine Orange staining of embryos indicated that Q102-GFP expression caused increased apoptosis. Low levels of apoptosis and abnormal phenotypes in embryos expressing Q4-GFP and Q25-GFP were also observed, which was likely due to background toxicity caused by these fusion proteins (Figure 16 A). Injection of a similar construct, huntingtin exon 1 containing 96 glutamines (HttEx1Q96), confirmed the elevated apoptotic activity upon expression of polyglutamine-expanded fragments (Figure 16 B).

A**B**

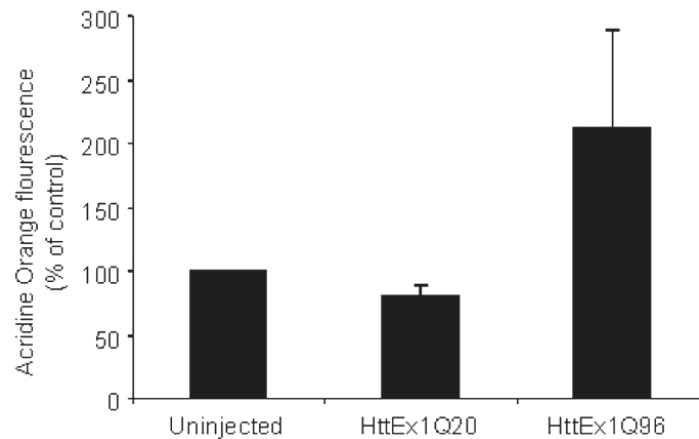


Figure 16: Expression of polyglutamine-expanded protein is associated with increased apoptosis.

(A) Fluorescent images of Acridine Orange stained embryos expressing the indicated polyglutamine-GFP fusions 24 h post-fertilization and subsequent quantification of apoptotic cells. As a negative control, uninjected embryos expressing no polyglutamine-GFP fusion were also analyzed (*Uninj.*). *Scale bar*, 100 μm . Data are mean values of $n=3-4$ experiments \pm S.D. (C) Fluorescence images of Acridine Orange stained embryos expressing the indicated htt constructs 24 h post-fertilization and subsequent quantification. As a negative control, uninjected embryos were also analyzed (Uninjected). *Scale bar*, 100 μm . The values are the means \pm S.D.

Interestingly, further analyses showed that nearly all (~95%) of the apoptotic cells were devoid of visible inclusions, which must be $> \sim 0.5 \mu\text{m}$ in diameter for detection in the experimental setup used in this study. On the other hand, almost all cells containing detectable inclusions were non-apoptotic (~99%), suggesting that pre-fibrillar Q102-GFP may instead be the toxic agent (Figure 17 A). Indeed, apoptotic cells containing diffusely distributed Q102-GFP were detected (Figure 17 B). Thus, these results indicate that expression of polyglutamine-expanded htt is toxic to the zebrafish embryo, but toxicity is not associated with the presence of visible inclusions.

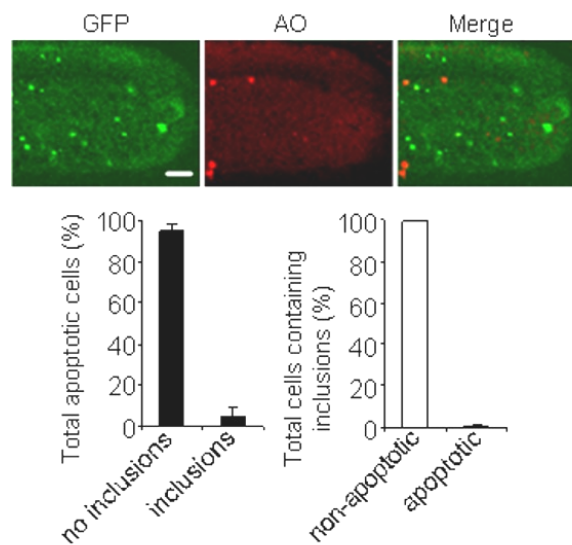
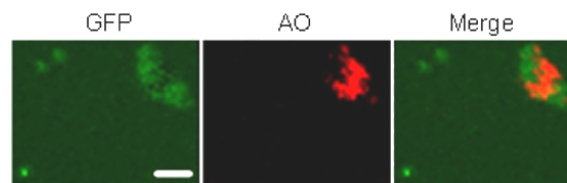
A**B**

Figure 17: Apoptotic cells are largely devoid of visible inclusions.

(A), Confocal images of Acridine Orange stained embryos expressing the indicated polyglutamine-GFP fusions 24 h post-fertilization that demonstrate that aggregate structures containing Q102-GFP are in the majority of cases not detectable in apoptotic cells. *Scale bar*, 20 μm . Quantitation of apoptotic cells with and without inclusions, as well as quantitation of cells containing inclusions that are apoptotic versus non-apoptotic is also shown. Data are mean values of $n=3$ experiments \pm S.D. (B), Higher magnification images of the embryonic hatching gland showing an apoptotic cell with diffusely distributed Q102-GFP. Neighboring cells containing aggregates are not apoptotic. *Scale bar*, 10 μm .

4.1.1.3 Hsp70 and Hsp40 suppress both polyglutamine aggregation and toxicity

Molecular chaperones are known to modulate both polyglutamine aggregation and toxicity (Barral *et al.*, 2004). To evaluate whether this important feature can be reproduced in the zebrafish embryo, the effect of the human chaperones Hsp70 and Hsp40 on Q102-GFP aggregation and toxicity were tested. 1-2 cell staged embryos were injected with mRNA of Q102-GFP and β -

Galactosidase as a control, or Q102-GFP and both Hsp40 and Hsp70 fused to YFP (Hsp70-YFP). Co-expression of Hsp40 and Hsp70-YFP reduced the amount of SDS-insoluble aggregates of Q102-GFP, as judged by the filter trap assay, while total protein levels of Q102-GFP were not detectably altered (Figure 18 A and B). Fluorescence microscopy revealed that Hsp70-YFP associated with inclusions of Q102-GFP (Figure 18 C), suggesting that the chaperone machinery recognized Q102-GFP as an aberrantly folded species.

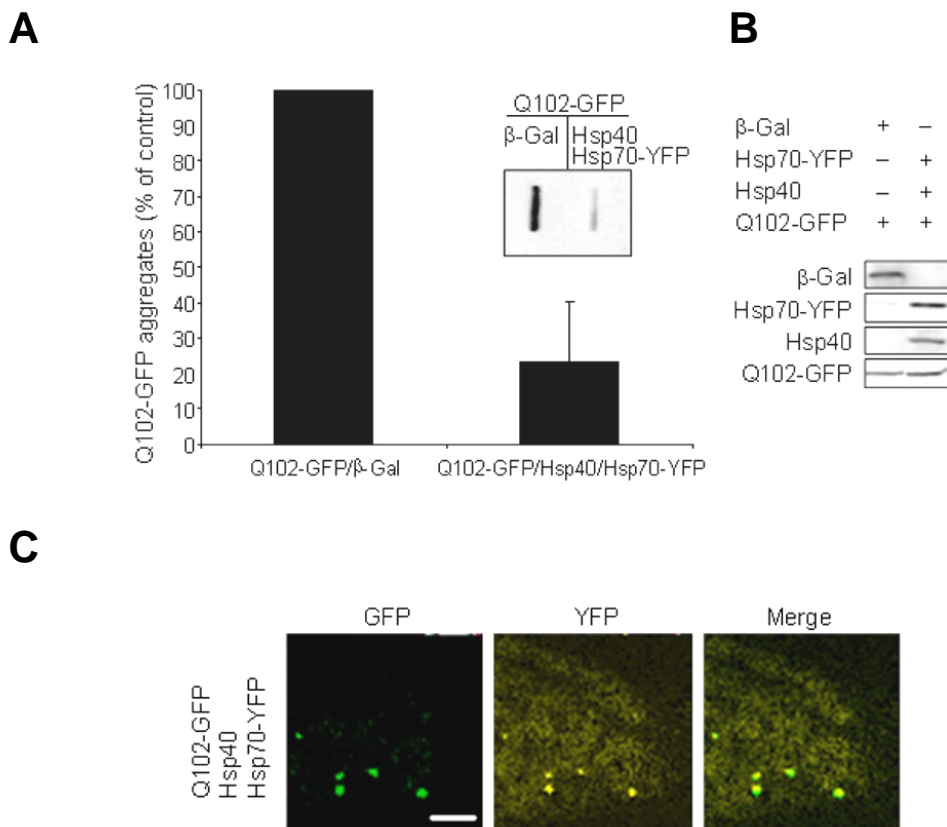


Figure 18: Hsp40 and Hsp70-YFP suppress polyglutamine aggregation.

(A), Filter trap analysis of total extracts derived from embryos injected with Q102-GFP mRNA together with β -Galactosidase mRNA (control) or Hsp40 and Hsp70-YFP mRNA at the 1-2 cell stage. Total SDS-insoluble aggregates trapped on the membrane were detected with anti-GFP and quantified. Signal intensity resulting from the co-injection of Q102-GFP mRNA with β -Galactosidase mRNA was defined as 100%. (B), Western blot analysis of total extracts from (A) to detect β -Galactosidase, Hsp40, Hsp70-YFP, and SDS-soluble Q102-GFP. (C) Confocal images showing that Hsp70-YFP colocalizes with Q102-GFP inclusions, as assessed by emission fingerprinting. Scale bar, 20 μ m.

Among the reduction of SDS-insoluble aggregates, expression of Hsp40 and Hsp70-YFP reduced the number of detectable inclusions (~41.8% of control, data

not shown), apoptotic cells (~80% of control, data not shown), and dead embryos (Figure 19), while increasing the number of phenotypically normal embryos expressing Q102-GFP. Aggregation and toxicity associated with Q102-GFP expression in zebrafish is partially suppressed by Hsp40 and Hsp70.

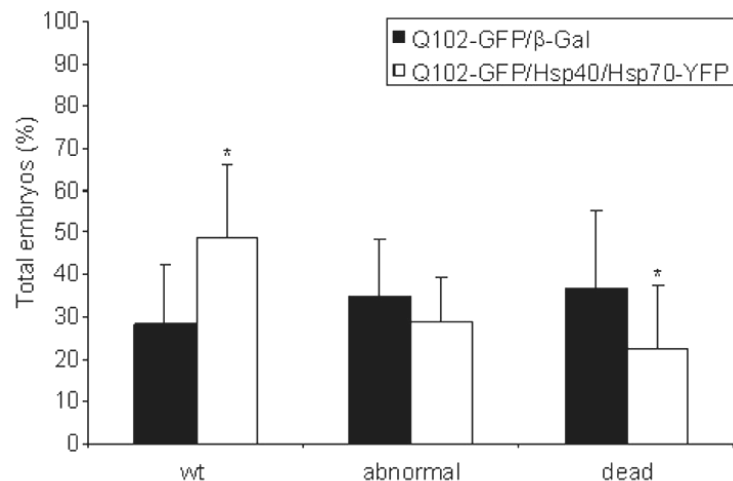


Figure 19: Hsp40 and Hsp70-YFP suppress polyglutamine mediated toxicity.

Quantitation of normal (wt), abnormal, and dead embryos 24 h post-fertilization, after injection at the 1-2 cell stage with Q102-GFP and β -Galactosidase or Hsp40/Hsp70-YFP mRNA. Data are mean values of $n=20$ experiments \pm S.D. *, $p < 0.01$ versus Q102-GFP/ β -Galactosidase injected embryos (ANOVA).

4.1.2 Identification of compounds that inhibit polyglutamine aggregation

Expression of polyglutamine-expanded htt gave rise to the formation of large, SDS-insoluble inclusions and was associated with enhanced apoptosis, as well as pronounced morphological defects and reduced viability of zebrafish embryos, reproducing a key feature of HD pathology. Chaperones are able to suppress polyglutamine mediated aggregation and toxicity in zebrafish. Hence, the newly established zebrafish model proved useful in evaluating the effectiveness of compounds in inhibiting polyglutamine aggregation and toxicity in the context of a whole vertebrate organism.

Drug absorption into the zebrafish embryo is likely facilitated by its aqueous environment and lack of blood brain barrier at early stages in

development; therefore, compounds could be tested for their effect on polyglutamine aggregation while minimizing complicating factors that impede absorption. Importantly, the zebrafish model system allows for the evaluation of drug effectiveness in a whole organism, taking into account the stability and cellular targeting of the tested compound, as well as the assessment of potential side effects of the drug at active concentrations. The unique feature that drug testing can be performed within two days made this model a cost and time efficient alternative to existing rodent models of HD.

4.1.2.1 Evaluation of known inhibitors of the polyglutamine aggregation process in *D. rerio*

The effect of known inhibitors on Q102-GFP aggregation was tested in this vertebrate system (Figure 20). PGL-135 and Congo red (Hockly *et al.*, 2006; Sanchez *et al.*, 2003) reduced Q102-GFP aggregation in zebrafish, as judged by the filter trap assay (Figure 22). In contrast, Isoproterenol HCl did not alter Q102-GFP aggregation in the zebrafish embryo, consistent with a recent study in a cell culture model (Wang *et al.*, 2005). Surprisingly, Mycophenolic acid, a compound known to suppress htt inclusion formation in cell culture (Wang *et al.*, 2005), had no effect on Q102-GFP aggregation in zebrafish at the maximum tolerated dose. Thus, in the case of PGL-135, Congo red, and Isoproterenol HCl, the results substantiate observations in other HD models. However, in contrast to data obtained in cell culture (Wang *et al.*, 2005), these findings suggest that Mycophenolic acid is not an effective inhibitor of polyglutamine aggregation in the vertebrate system.

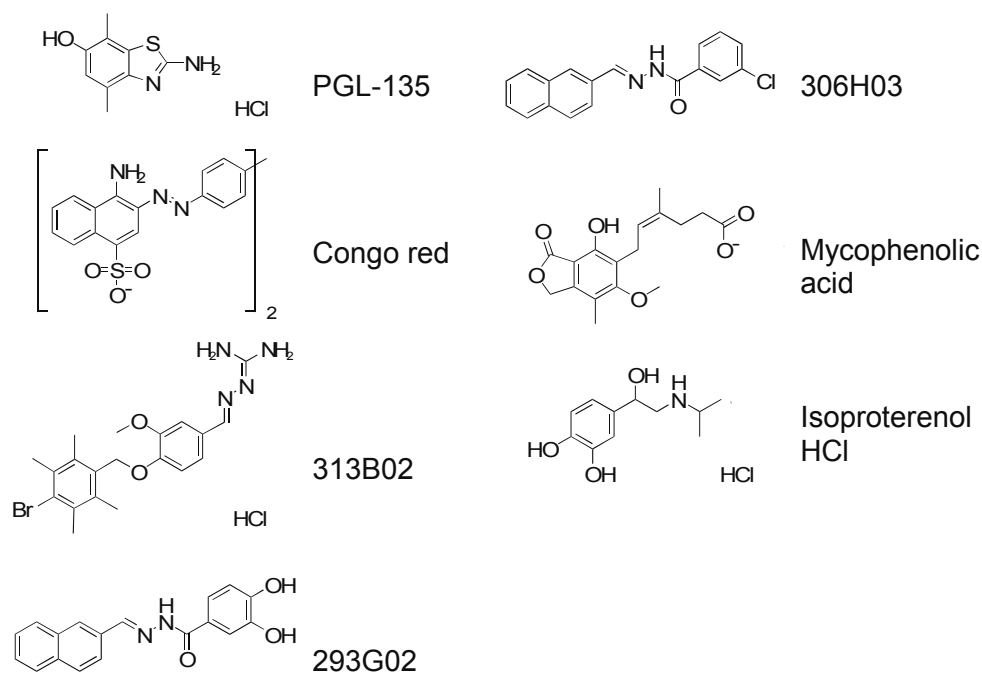


Figure 20: Molecular structures of the compounds tested.

4.1.2.2 Identification of new compounds that inhibit polyglutamine aggregation

Considering the hypothesis that polyglutamine and PrP^{Sc} aggregates have similar amyloid core structures (Govaerts *et al.*, 2004; Stork *et al.*, 2005), three compounds (313B02, 293G02, and 306H03) that were previously identified in *in vitro* screens for inhibitors of prion propagation (Bertsch *et al.*, 2005; pers. comm. A. Giese) were evaluated. All three of these compounds inhibited the aggregation of polyglutamine-expanded htt *in vitro* (Figure 21), indicating these compounds interact directly with mutant htt to reduce its aggregation.

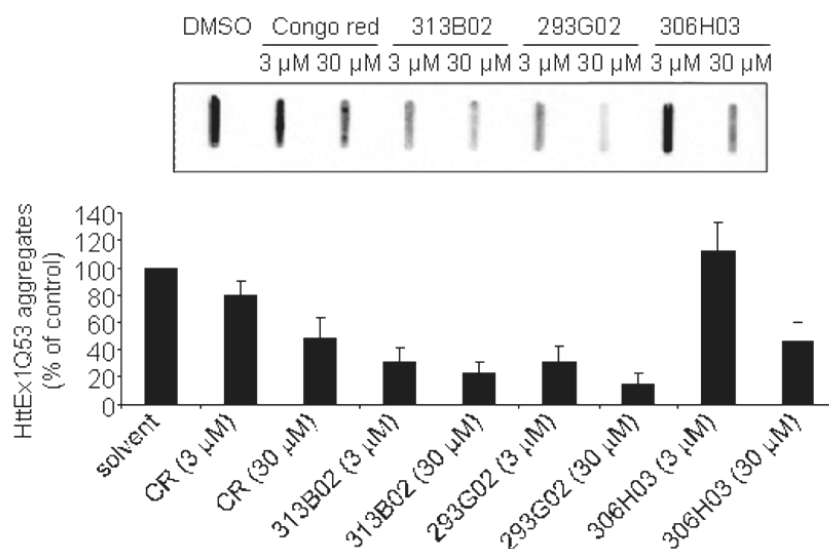


Figure 21: *N'*-benzylidene-benzohydrazides inhibit Q102-GFP aggregation *in vitro*.

Effect of the indicated chemical compounds on HA-HttEx1Q53 aggregation *in vitro*, as assessed by the filter trap assay (anti-HA) with quantitation. The signal intensity from the control sample containing solvent alone was set to 100%. Data are mean values of $n=3$ experiments \pm S.D.

However, only 293G02 and 306H03, both derivatives of *N'*-benzylidene-benzohydrazide (NBB), also inhibited the formation of detergent insoluble aggregates of Q102-GFP *in vivo* (Figure 22). Interestingly, 306H03 was a more effective inhibitor of polyglutamine aggregation than 293G02 *in vivo*, but not *in vitro* (Figure 22 and Figure 21). Notably, none of the studied compounds suppressed the abnormal morphology and death associated with Q102-GFP expression in zebrafish embryos (data not shown). Thus, the NBBs may interfere with the formation of large SDS-resistant polyglutamine aggregates downstream of the accumulation of toxic polyglutamine species.

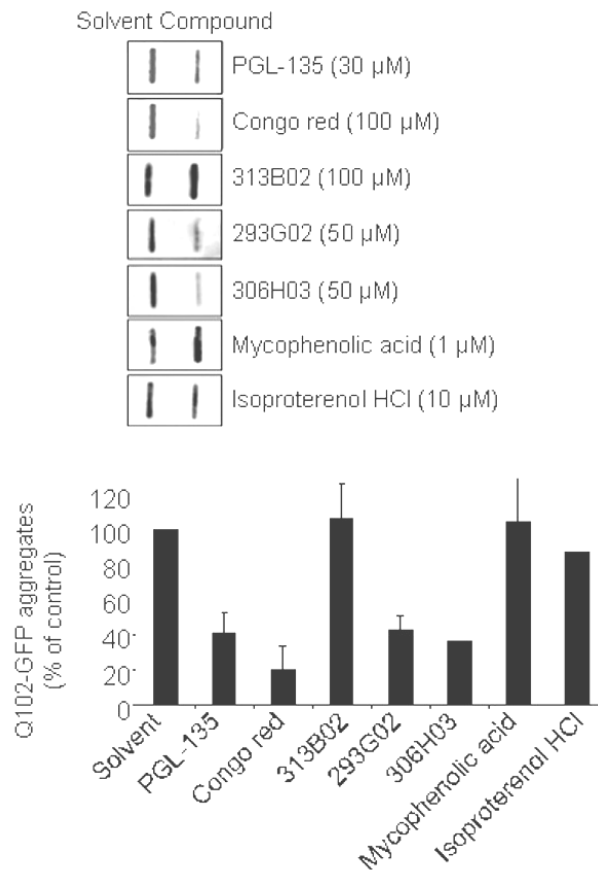


Figure 22: *N'*-benzylidene-benzohydrazides inhibit Q102-GFP aggregation *D. rerio*.

Filter trap analysis of extracts derived from embryos expressing Q102-GFP in the presence and absence of the indicated compounds. Embryos expressing Q102-GFP were treated for 24 h with DMSO or H₂O (solvent), 30 μM PGL-135, 100 μM Congo red, 100 μM 313B02, 50 μM 293G02, 50 μM 306H03, 1 μM Mycophenolic acid, or 10 μM Isoproterenol HCl. Extracts of embryos were analyzed using the filter trap assay (anti-GFP), followed by densitometric quantitation. The signal intensity from controls subjected to solvent alone was set to 100%. The data are mean values of n=3-5 independent injections ± S.D.

4.1.2.3 Confirmation of the effect of NBBs on polyglutamine aggregation in a mammalian neuroblastoma cell line

To substantiate the effect of NBBs on polyglutamine aggregation, a similar model of HD in mammalian neuroblastoma cells (N2a) was set up. N2a cells were transiently transfected with the same constructs that were also used in the zebrafish studies. In N2a cells, expression of Q102-GFP, but not Q4-GFP or Q25-GFP, resulted in the formation of large, perinuclear inclusions containing

SDS-insoluble aggregates; however, Q102-GFP was not overtly toxic to these cells under the tested conditions (Figure 23).

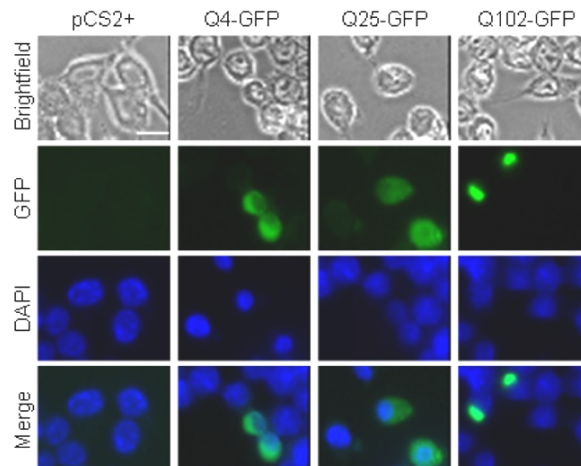
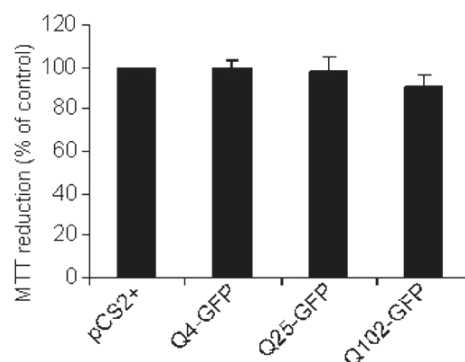
A**B****C**

Figure 23: Q102-GFP forms SDS-insoluble aggregates in N2a mouse neuroblastoma cells but does not cause significant toxicity.

(A), Brightfield and fluorescent images of N2a mouse neuroblastoma cells expressing empty vector (pCS2+), Q4-GFP, Q25-GFP, or Q102-GFP, 48 h post-transfection. To visualize nuclei, the cells were stained with DAPI. *Scale bar*, 20 μ m. (B), Extracts from N2a cells expressing the indicated constructs 48 h post transfection were analyzed by filter trap assay (anti-GFP; lower panel). (C), Cell viability assessment of N2a cells expressing the indicated constructs 48 h post-transfection. Cell viability was assessed via the MTT reduction assay. MTT reduction of N2a cells transfected with empty vector (pCS2+) was set to 100%. Data are mean values of n=4 experiments \pm S.D.

In accordance with the results from the zebrafish system, NBBs proved efficient in suppressing Q102-GFP aggregation in N2a cells (Figure 24). Taken together, these data suggest that NBBs represent a new class of compounds that effectively inhibit polyglutamine aggregation.

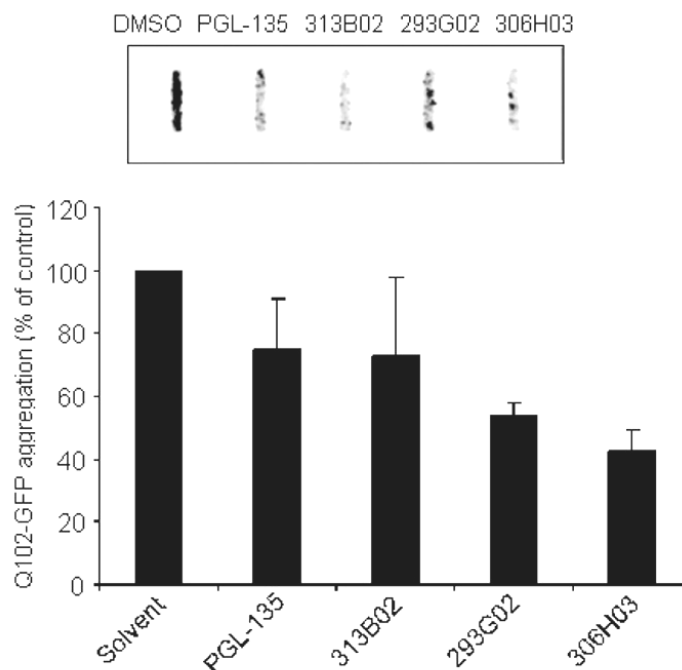


Figure 24: *N*-benzylidene-benzohydrazides inhibit Q102-GFP aggregation in N2a mouse neuroblastoma cells.

Effect of the indicated chemical compounds on Q102-GFP aggregation in N2a mouse neuroblastoma cells, as assessed by the filter trap assay (anti-GFP) with quantitation. The signal intensity from the control sample containing solvent alone was set to 100%. Data are mean values of $n=3$ experiments \pm S.D.

4.2 N-terminal polyglutamine-containing fragments inhibit androgen receptor transactivation function in a yeast model of SBMA

It is widely accepted that neuronal dysfunction and death in polyglutamine diseases is caused by the expanded polyglutamine repeat in the respective protein. Several non-exclusive hypotheses were proposed to explain polyglutamine mediated cytotoxicity which include among others, the inhibition of the ubiquitin proteasome system, formation of ion channels, impairment of

axonal trafficking but also the inactivation of essential transcription factors. For the latter, it was proposed that polyglutamine-expanded species, monomers but also oligomers, interact with glutamine-rich regions of transcriptional regulators and as a consequence, inactivate them (Cha, 2000; Sakahira *et al.*, 2002b; Schaffar *et al.*, 2004). In addition to this toxic gain-of-function mechanism shared by all polyglutamine diseases, a loss of function mechanism could contribute to polyglutamine disease pathogenesis, *e.g.* by rendering particular neurons exquisitely sensitive to the toxic gain-of-function effects that a polyglutamine expansion imparts to the disease protein (Thomas *et al.*, 2006).

This study presents the establishment of a yeast model for SBMA, which in addition to the possibility of investigating the toxic gain-of-function effects of polyglutamine containing AR fragments, also enables monitoring potential loss-of-function of the AR protein itself.

4.2.1 Development and characterization of a yeast model for SBMA

For the development of a yeast model of SBMA full-length constructs of the AR protein containing 2, 27, 65, or 102 Q (ARQ2; ARQ27; ARQ65; ARQ102, respectively) were expressed in *S. cerevisiae* YPH499 (Figure 25). Former studies proposed that proteolytic cleavage of polyglutamine-expanded AR at the potential caspase-3 cleavage site ¹⁵²DEDD¹⁵⁵ is a crucial event in SBMA pathogenesis unmasking the cytotoxicity of AR (Butler *et al.*, 1998; Cowan and Raymond, 2006; Ellerby *et al.*, 1999; Kobayashi *et al.*, 1998; Li *et al.*, 2007; Wellington *et al.*, 1998). For this reason N-terminal fragments of AR (amino acid 1-155) containing polyglutamine stretches in the non-pathogenic range (2 Q or 27 Q) or pathogenic range (65 Q or 102 Q), with or without a nuclear localization signal (NLS) were also expressed in *S. cerevisiae* YPH499 (Figure 26).

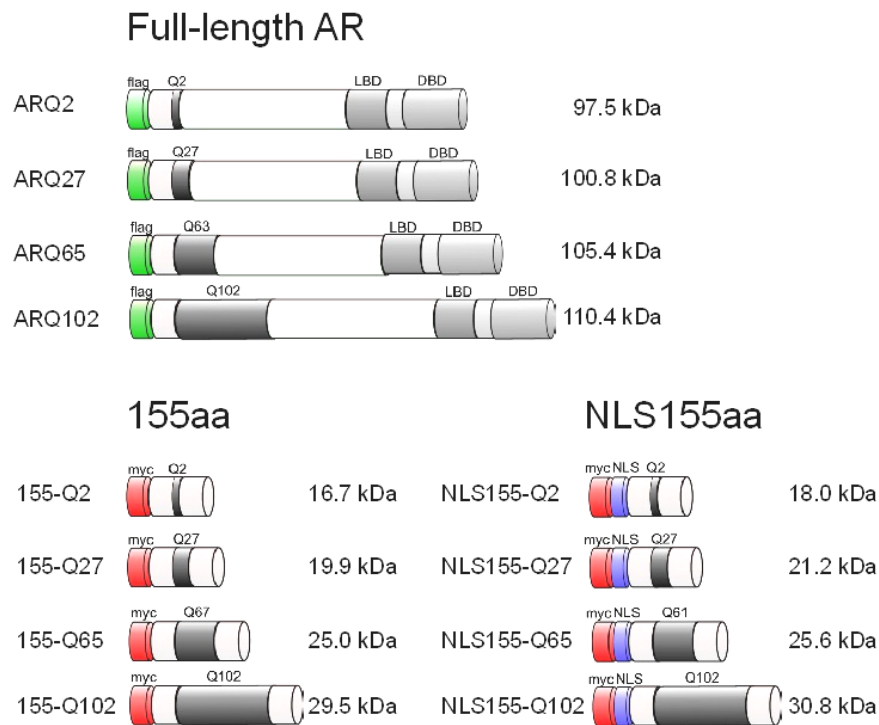


Figure 25: Schematic diagram of the constructs used in this study.

The full-length AR constructs and N-terminal fragments are shown. The ligand-binding domain (LBD) and DNA-binding domain (DBD) are highlighted as well as the polyglutamine tract with the number of glutamines (Q) as indicated. The polyglutamine stretch of the ~65 Q constructs is coded by an unstable CAG repeat, which lead to slightly different amount of glutamines in the respective constructs. For a better understanding, these constructs are named as Q65. The fragments which are meant to be targeted to the nucleus have an N-terminal nuclear localization signal (NLS). The full-length constructs contain an N-terminal FLAG tag whereas the fragments contain an N-terminal myc tag. The calculated molecular weights are shown on the right.

4.2.1.1 Polyglutamine-expanded N-terminal AR fragments cause toxicity in *S. cerevisiae*

The expression of full-length AR proteins containing polyglutamine stretches in the pathogenic range (ARQ65 or ARQ102) neither caused toxicity nor did they form detectable aggregates in yeast cells (Figure 26).

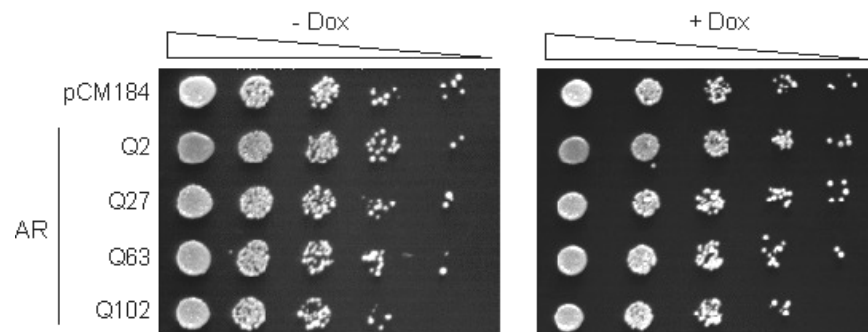
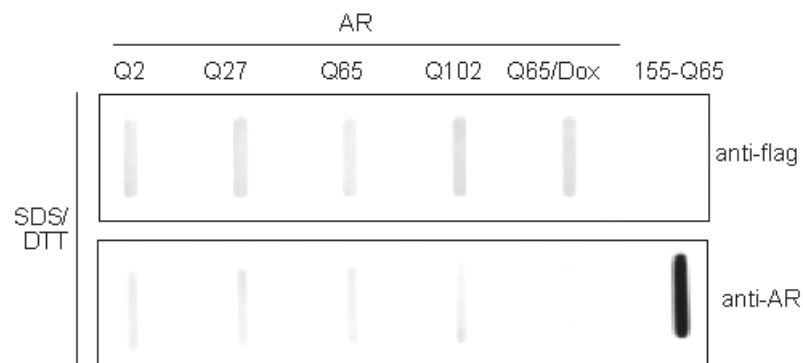
A**B**

Figure 26: Expression of polyglutamine-expanded full-length AR neither cause toxicity nor forms SDS-insoluble aggregates in yeast.

(A), Growth analysis of wild-type yeast cells upon expression of full-length AR proteins varying in the size of the polyglutamine stretch. Growth of wild-type yeast cells in the presence or absence of FLAG-tagged AR constructs was examined by 5-fold serial dilutions after 3 days at 30 °C on plates lacking (induction) or containing (no induction) Doxycycline, respectively. (B), Filter trap analysis (anti-FLAG and anti-AR, respectively) of full-length ARs with 2, 27, 65 and 102 glutamines, full-length ARQ65 in the presence of Doxycycline and of the aggregating N-terminal fragment 155-Q65. 750 µg of total cell extracts were analyzed in the presence of SDS/DTT at 95 °C. Expression of the constructs was checked by SDS-PAGE and western blotting (data not shown).

In contrast, expression of the fragments caused polyglutamine length-dependent toxicity in yeast, which was enhanced when the fragments were targeted to the nucleus, with NLS155-Q102 conferring the most severe toxicity (Figure 27). The observed inhibition of cell growth was not dependent on the presence of androgens, such as DHT (data not shown). Thus, it seems that the mutant polyglutamine stretch is no longer toxic in the protective context of the full-length protein, which is consistent with results from other model systems (Cowan *et al.*, 2003; Ellerby *et al.*, 1999).

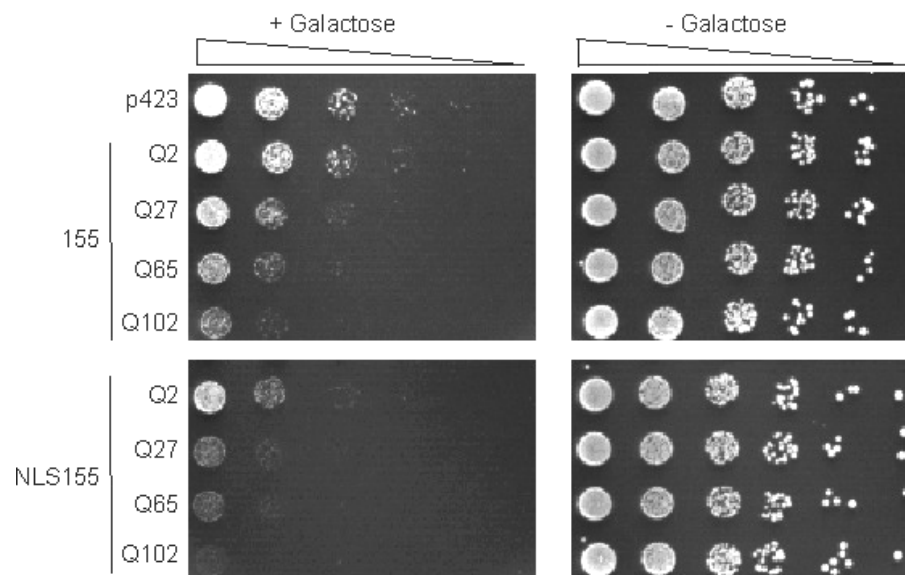
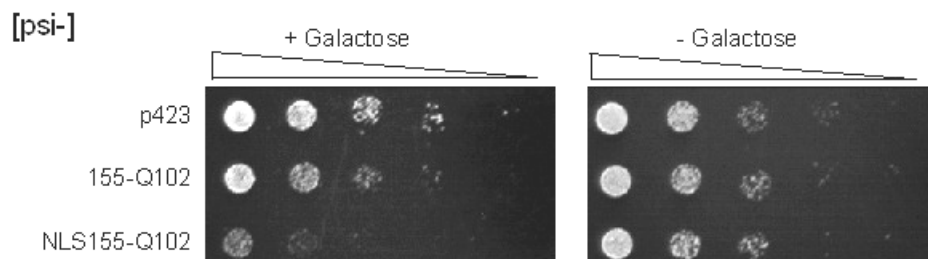


Figure 27: Expression of polyglutamine-expanded N-terminal AR fragments cause toxicity in yeast.

The expression of myc-tagged N-terminal AR fragments (\pm NLS) with 2, 27, 65 and 102 glutamines was induced on plates containing Galactose. Growth was examined after 3 days at 30 °C.

As yeast prions are thought to influence polyglutamine toxicity (Meriin *et al.*, 2002), yeast strains were also evaluated after being cured of prions by guanidinium hydrochloride (GuHCl). Toxicity caused by expression of either 155-Q102 or NLS155-Q102 persisted after GuHCl treatment (Figure 28 A). In the absence of Hsp104p, which is known to be required for prion propagation (Chernoff *et al.*, 1995), both 155-Q102 and NLS155-Q102 likewise remained toxic (Figure 28 B). These results indicate that toxicity caused by N-terminal fragments of polyglutamine-expanded AR is not reliant on yeast prions.

A



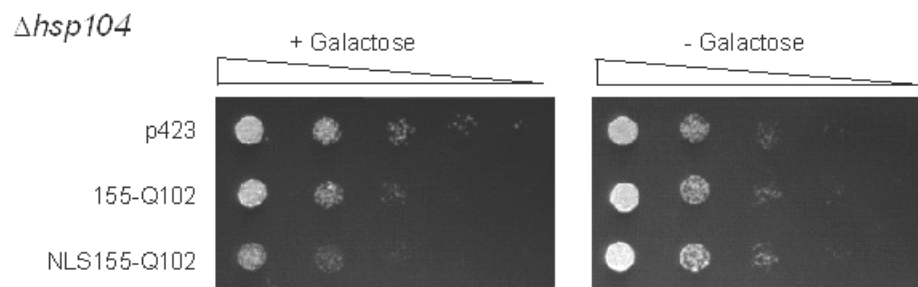
B

Figure 28: Toxicity caused by N-terminal fragments of polyglutamine-expanded AR is not reliant on yeast prions.

(A), Growth defect of prion-cured yeast cells upon expression of 102 Q containing N-terminal AR fragments. Cells were raised in GuHCl and growth was examined after 3 days at 30 °C. (B), Growth defect of *hsp104* Δ ::*LEU2* strain upon expression of 102Q containing N-terminal AR fragments. Growth was examined as in (A).

4.2.1.2 Enhanced toxicity is associated with soluble polyglutamine oligomers, and not insoluble aggregates

To determine whether polyglutamine-dependent toxicity correlates with the presence of large insoluble aggregates, the intracellular distribution of the AR fragments in yeast cells was initially analyzed by immunofluorescence microscopy using an antibody against the N-terminal myc epitope of the AR fragments. As expected, fragments containing non-pathogenic polyglutamine stretches, 155-Q2 and 155-Q27, were mainly diffusely distributed; while 155-Q65 accumulated in large, round foci or inclusion bodies (IBs, Figure 29). Unexpectedly, 155-Q102 did not efficiently accumulate in IBs, but instead formed dispersed, irregularly shaped foci. Nuclear targeting did not substantially alter the localization of the fragments containing 2 or 27 Q (NLS155-Q2, NLS155-Q27, respectively), but did promote a more diffuse distribution of fragments containing a pathogenic polyglutamine stretch, and in the case of NLS155-Q102, efficient targeting to the nucleus.

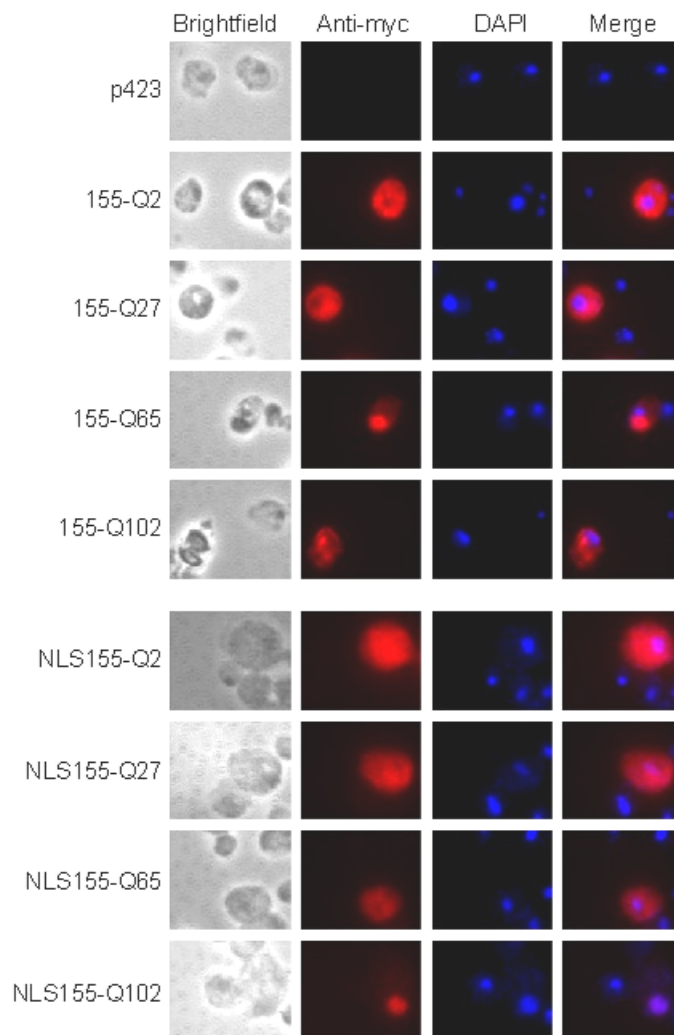


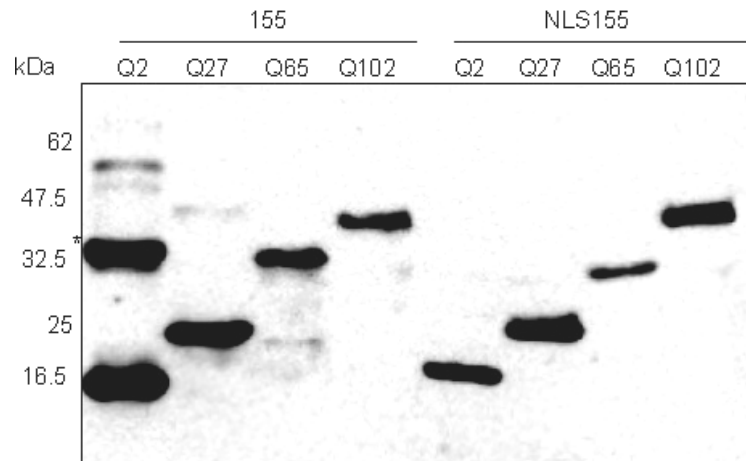
Figure 29: The expression of polyglutamine-expanded N-terminal AR fragments cause the formation of visible inclusions.

Wild-type yeast cells expressing myc-tagged N-terminal AR fragments (\pm NLS) with 2, 27, 65 and 102 Q were analyzed by indirect immunofluorescence. The myc-tagged fragments were immunolabeled with anti-myc antibody coupled to Cy3-conjugated secondary antibody, and nuclei were counterstained with DAPI.

Analysis of whole cell extracts using SDS-PAGE and western blotting revealed stable fragments of the expected size, taking into consideration that the effect of polyglutamine tract length on protein migration is greater than might be predicted by protein length alone (Merry *et al.*, 1998; Figure 29). Additional SDS-insoluble material containing 155-Q27 and 155-Q65 was detected in the stacking gel (data not shown). The filter trap assay was used to assess the accumulation of AR fragments in large SDS-insoluble aggregates, which are retained by the 0.2 μ m pore-sized filter (Scherzinger *et al.*, 1997). Surprisingly, only 155-Q65 formed

substantial amounts of aggregates that were detergent resistant, a characteristic of polyglutamine amyloid fibrils (Figure 30 B).

A



B

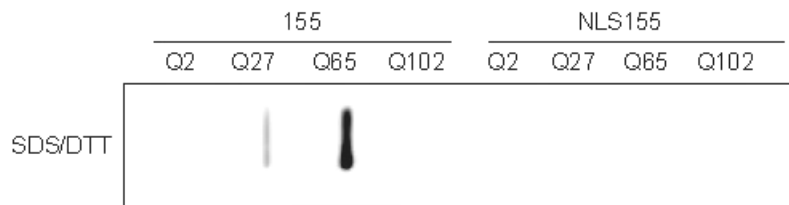


Figure 30: 155-Q65 forms SDS-insoluble aggregates in yeast.

(A), Analysis of the solubility of the AR fragments. Extracts from yeast cells expressing myc-tagged N-terminal AR fragments (\pm NLS) with 2, 27, 65 and 102 Q were analyzed by SDS-PAGE and western blotting with anti-myc antibody. The effect of polyglutamine tract length on protein migration is greater than might be predicted by protein length alone, consistent with what has been noted by others (Merry *et al.*, 1998). Asterisk, not specified additional product. (B), Filter trap analysis of N-terminal AR fragments. 750 μ g of total cell extracts from (A) were analyzed by filter trap assay in the presence of SDS/DTT at 95°C.

The polyglutamine-expanded AR fragments with the greatest toxicity (155-Q102 and NLS155-Q102; Figure 27), had the least propensity to form large SDS-insoluble fibrillar aggregates. To confirm this result and to exclude artifacts due to unequal expression rates, 155-Q65 was expressed under control of a titratable yeast promoter. The dot blot assay was used to assess the total amount of AR fragments in the cell extracts (Figure 31 lower panel) and the filter trap assay was done in parallel to monitor the amount of aggregates (Figure 31 upper panel). Even reducing the expression of 155-Q65 (Dox) to 2% of total 155-Q102

(Gal) and 155-Q65 (Gal), respectively, still resulted in aggregate formation. Thus, the discrepancy in accumulation of 155-Q65 versus 155-Q102 in SDS-insoluble aggregates was not caused by dissimilar expression levels.

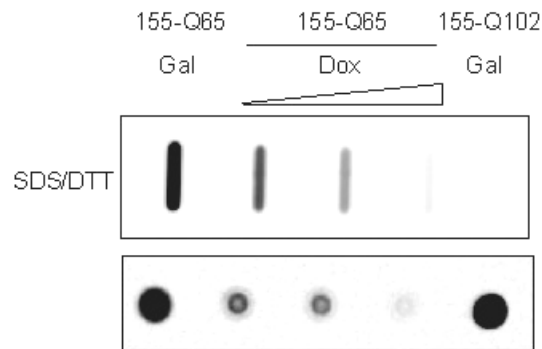


Figure 31: 155-Q65 but not 155-Q102 forms SDS-insoluble aggregates in yeast.

Filter trap analysis of N-terminal AR fragments (upper panel). 750 μg of total cell extracts from yeast cells expressing 155-Q65 or 155-Q102 under the control of a galactose inducible promoter or, expressing 155-Q65 under the control of a doxycycline regulatable promoter (in the presence of 0.02, 0.04, or 0.08 $\mu\text{g}/\text{ml}$ doxycycline) were analyzed by filter trap assay with anti-myc antibody in the presence of SDS/DTT at 95°C. 4 μg of each lysate was spotted on a nitrocellulose membrane to compare the total amount of protein with anti-myc antibody (lower panel).

Consistent with the filter trap results, high speed centrifugation revealed that both 155-Q102 and NLS155-Q102 in contrast to 155-Q65 fractionated almost exclusively in the soluble supernatant fraction (Figure 32 and data not shown). These data suggest that pronounced toxicity is associated with soluble forms of 155-Q102 and NLS155-Q102.

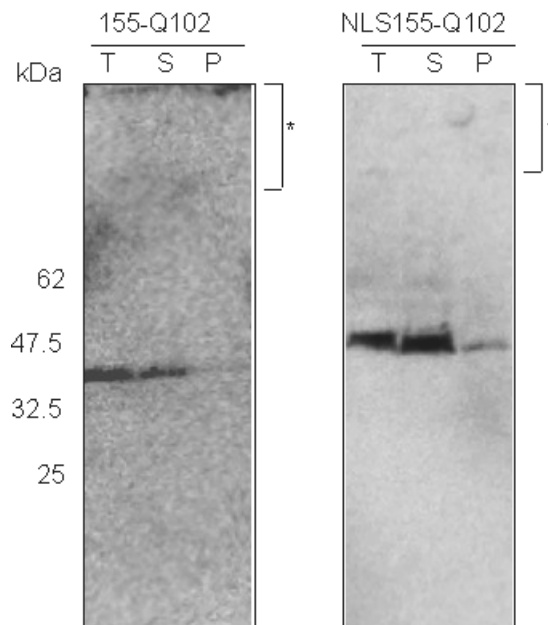


Figure 32: Polyglutamine-expanded N-terminal AR fragments, 155-Q102 and NLS155-Q102, fractionate almost exclusively in the supernatant fraction.

Extracts from yeast cells expressing myc-tagged N-terminal AR fragments (\pm NLS) with 102Q were subjected to high speed centrifugation, and the resulting fractions were analyzed by SDS-PAGE and western blotting with anti-myc. T, total cell lysate; S, supernate; and P, pellet fraction. *, stacking gel.

In recent studies about HD but also SBMA it was hypothesized that soluble oligomers of polyglutamine containing fragments are the main toxic species causing neurodegeneration (Behrends *et al.*, 2006; Li *et al.*, 2007). The results revealed that the most toxic fragment, namely NLS155-Q102, is largely soluble in yeast (Figure 30). Further characterization of these toxic soluble forms was accomplished using a gel filtration approach. Supernatant fractions of yeast cell extracts of NLS155-Q102 or NLS155-Q2 as a control were subjected to size-exclusion chromatography after centrifugation at 20,000 \times g. In comparison to NLS155-Q2 that showed a single, dominant fraction at \sim 50-100 kDa, NLS155-Q102 fractionated as 200-500 kDa species (Figure 33). Thus, toxicity caused by NLS155-Q102 is associated with soluble oligomers in the 200-500 kDa size range.

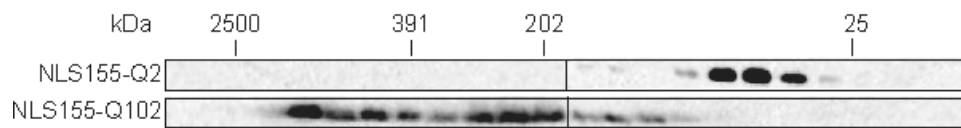


Figure 33: Oligomer formation of NLS155-Q102.

Size-exclusion chromatography on a Superdex 200 column of soluble fractions from yeast cells expressing NLS155-Q2 and NLS155-Q102 which were detected with anti-myc antibody.

4.2.1.3 Expression of polyglutamine-expanded N-terminal AR fragments activates a cytosolic stress reporter in *S. cerevisiae*

Next, a stress reporter was applied to determine if expression of the polyglutamine constructs causes cellular stress in yeast cells. This stress reporter consists of a heat shock response element of the *SSA3* promoter which is fused to *lacZ* (HSE-*lacZ*) (Boorstein and Craig, 1990). To test the responsiveness of the stress reporter, a control strain expressing a non-stress related protein, Gim3p, was subjected to heat shock (37 °C). This caused a ~2.5 fold increase in β -galactosidase activity compared to untreated control (Figure 34). When expressing either 155-Q102 or NLS155-Q102, a ~2 fold increase in β -galactosidase activity relative to strains expressing their 2 Q counterparts was detected (Figure 34). These data indicate that the toxic accumulation of 155-Q102 and NLS155-Q102 as soluble misfolded species elicits a substantial heat shock response in yeast.

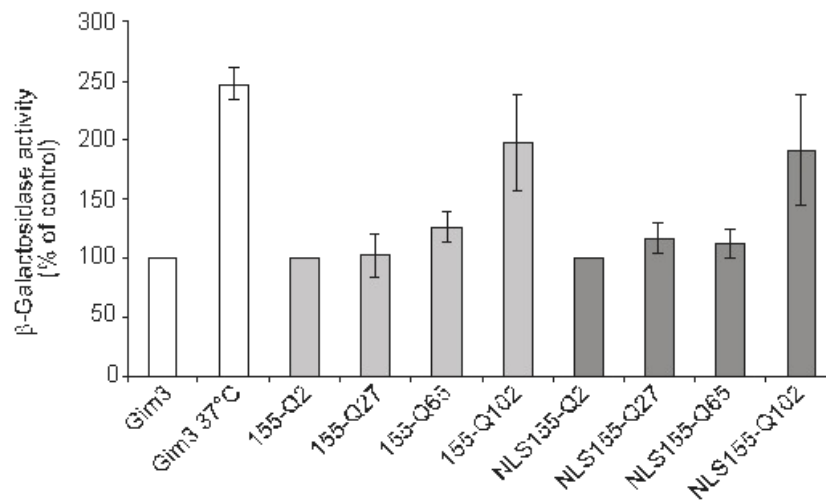


Figure 34: The expression of polyglutamine expanded N-terminal AR fragments cause cellular stress in yeast.

The β -Galactosidase activity of extracts from a stress reporter yeast strain expressing Gim3 at 30 °C and 37 °C as a control and from yeast cells expressing myc-tagged N-terminal AR fragments (\pm NLS) with 2, 27, 65 and 102 Q was determined. The Galactosidase activity from Gim3 at 30 °C, 155-Q2 and NLS155-Q2 was set to 100%. The data are mean values of n=3 independent experiments \pm S.D.

4.2.2 A newly established reporter system to evaluate the effect of the polyglutamine stretch on AR transactivation capacity

Increasing evidence suggests an impairment of AR function in SBMA, but the underlying mechanism is not understood. As a possible explanation, it has been hypothesized that AR containing expanded polyglutamine is inherently deficient in activity (Buchanan *et al.*, 2004).

4.2.2.1 Setup of a reporter system to analyze AR transactivation capacity

To monitor AR transactivation capacity and elucidate the mechanism of its inactivation, a yeast reporter system was established, in which the luciferase gene is under control of androgen response elements (ARE-*luc*). As has been shown for similar reporter systems (Ceraline *et al.*, 2003), the production of active luciferase, which can be detected in live yeast cells using fluorimetry, depends on both the addition of androgen to yeast media and the presence of functional AR (Figure 35).

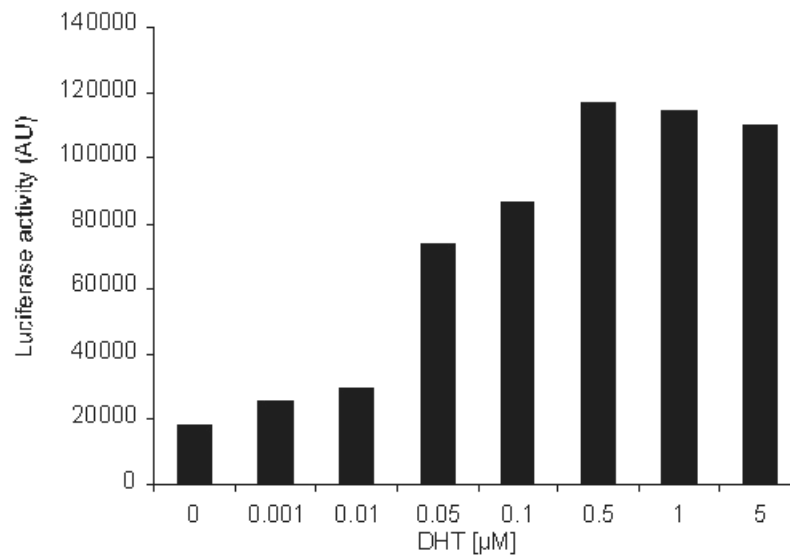
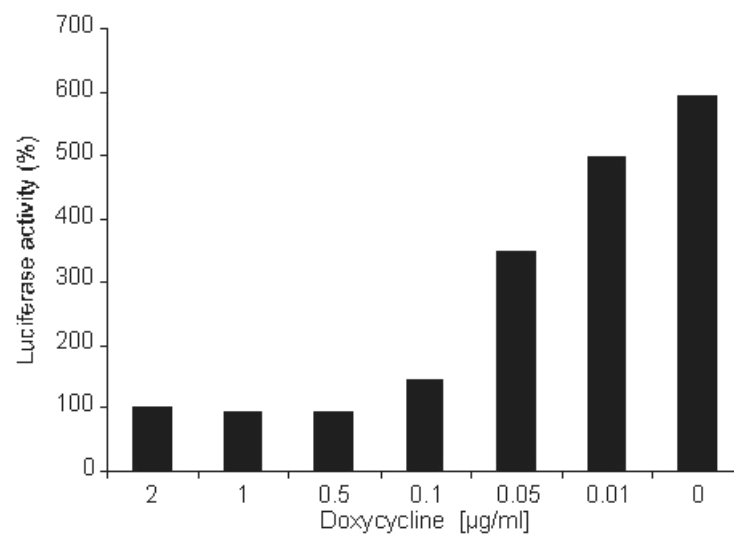
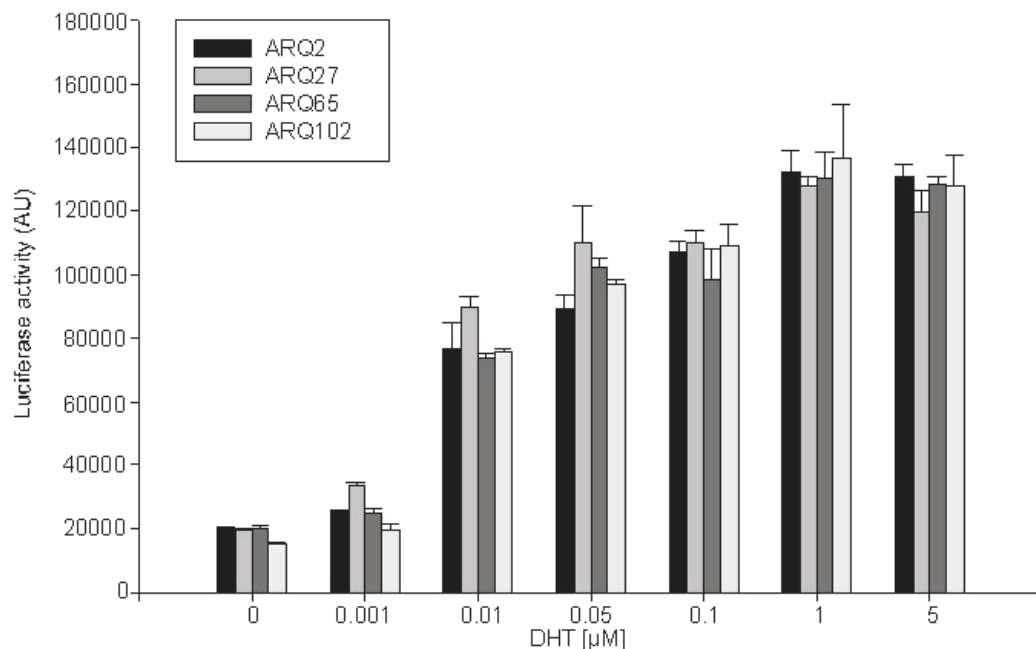
A**B**

Figure 35: The AR-mediated production of active luciferase requires the ligand (DHT) and the expression of functional AR.

(A), Yeast cells expressing full-length AR with 27 Q were grown until mid-log phase. DHT was added at the indicated concentrations for two hours and luciferase activity was determined. (B), Yeast cells expressing full-length AR with 2 Q were grown until mid-log phase in the presence of doxycycline (represses the expression) at the indicated concentrations. DHT (5 µM) was added for three hours and luciferase activity was determined.

4.2.2.2 Transactivation function of AR is polyglutamine-independent

Since the reporter system proved useful, the transactivation function of full-length AR with increasing polyglutamine lengths (ARQ2, ARQ27, ARQ65, ARQ102) was assayed in yeast cells containing *ARE-luc*. For all strains, a dose response curve was taken by the addition of several amounts of DHT (0 – 5 μM final concentration) to the media for 2 h. In all conditions, active luciferase was similarly produced in a manner dependent on the concentration of the DHT androgen (Figure 36 A and B). The half-maximal response (EC_{50}) of DHT was calculated to be 14.3×10^{-3} μM for ARQ2, 5.2×10^{-3} μM for ARQ27, 6.7×10^{-3} μM for ARQ65, and 11.9×10^{-3} μM for ARQ102, respectively. Equal expression levels of AR constructs in the analyzed strain subjected to 5 μM DHT was confirmed using SDS-PAGE and western blotting (Figure 36 C). These data indicate that the transactivation function of AR in yeast is polyglutamine-independent. Therefore, polyglutamine-expanded AR is intrinsically functional, but is likely inactivated during disease progression.

A

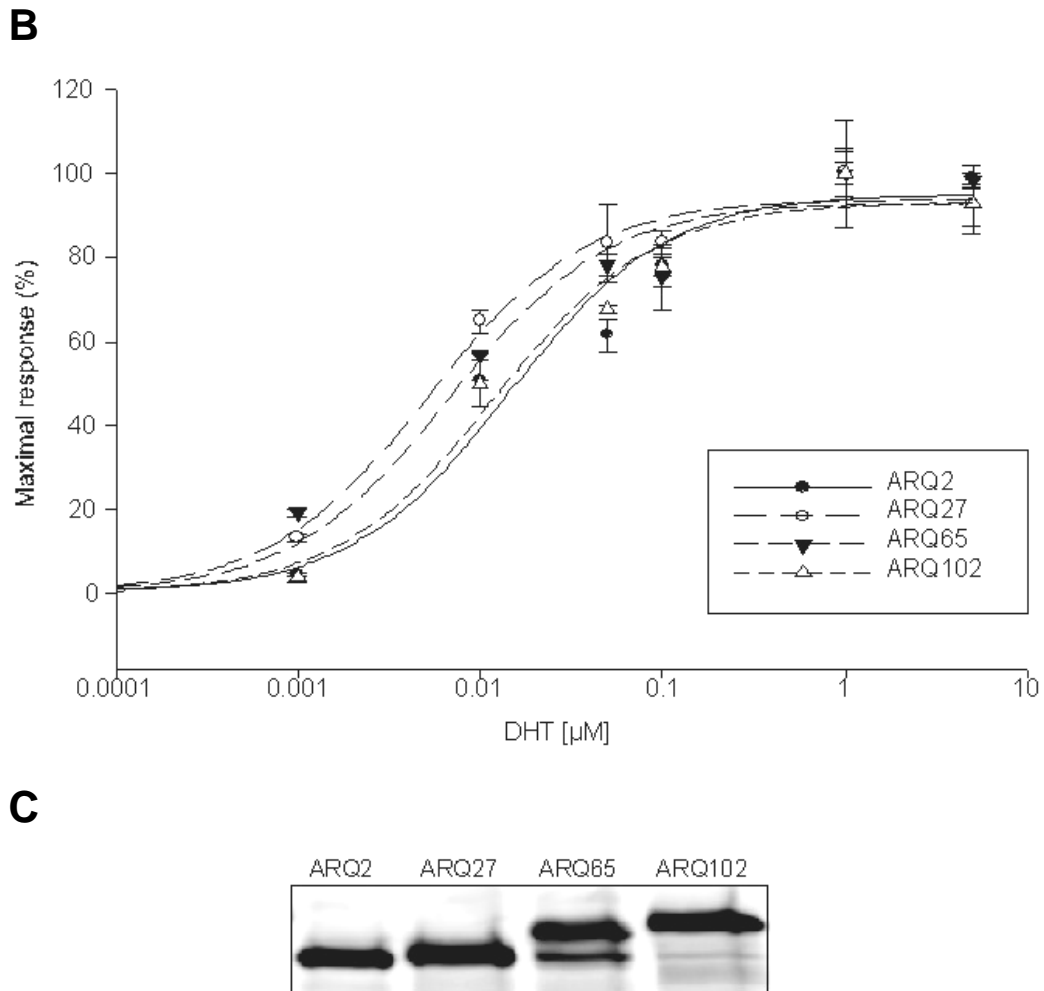


Figure 36: The size of the polyglutamine stretch has no impact on AR transactivation capacity.

(A), Yeast cells expressing full-length AR with 2, 27, 65 and 102 Q were grown in duplicate until mid-log phase. DHT was added to one set of cells for two hours and luciferase activity of all constructs was determined. The data are mean values of $n=3$ independent experiments \pm S.D. (B), Dose response curves of the full-length ARs with the respective data taken from (A). (C), cell extracts from (A) were analyzed by SDS-PAGE and western blotting with anti-myc antibody to check expression levels.

4.2.3 Analysis of the effect of N-terminal polyglutamine-containing AR fragments on AR transactivation capacity

Since these results do not support a linear decrease of intrinsic AR activity with progressive expansion of the polyglutamine stretch probably factors *in trans* significantly alter the transactivation capacity of polyglutamine-expanded AR during SBMA progression such that signs of mild-to-moderate AIS appear. The fact that the course of AIS, namely slowly progressive, resembles

neurological symptoms suggests a common origin. Interestingly, it was shown that neurodegeneration in SBMA originates from oligomers comprised of N-terminal polyglutamine-containing AR fragments in a mouse model of SBMA (Li *et al.*, 2007). On the other hand, polyglutamine-expanded species aggregate and sequester polyglutamine containing proteins and were also shown to interact with glutamine-rich regions of transcriptional regulators disturbing the activity of the latter (Cha, 2000; Sakahira *et al.*, 2002b; Schaffar *et al.*, 2004; Stenoien *et al.*, 1999). This proposes N-terminal polyglutamine-expanded AR fragments to be the origin of both neurodegeneration and partial AIS in SBMA.

4.2.3.1 Full-length AR is recruited into SDS-insoluble aggregates composed of the polyglutamine-expanded N-terminal AR fragments

In yeast, full-length polyglutamine-expanded AR is not toxic and does not efficiently form insoluble aggregates either (Figure 26). Most likely, the sequences surrounding the polyglutamine stretch protect intact AR from initiating the aggregation process, as predicted from other findings (Adachi *et al.*, 2007; Butler *et al.*, 1998; Cowan *et al.*, 2003; Davies *et al.*, 1997; Ellerby *et al.*, 1999). To determine whether full-length polyglutamine-expanded AR is also protected from co-aggregation or recruitment processes, full-length ARQ65 were co-expressed with the aggregating 155-Q65 fragment in yeast grown in the presence or absence of DHT. Analysis of yeast extracts using the filter assay, followed by immunodetection with an antibody against the N-terminal FLAG tag of full-length AR proteins, revealed that full-length ARQ65 was partially recruited into SDS-insoluble aggregates of 155-Q65 in a hormone-independent manner (Figure 37). As expected, full-length ARQ2 was not retained with the 155-Q65 aggregates demonstrating that the recruitment phenomenon is polyglutamine-dependent. Consistently, fluorescence microscopy of yeast strains revealed ARQ65, but not ARQ2, colocalized with aggregates of 155-Q65 in yeast cells in the presence and absence of DHT (Figure 37).

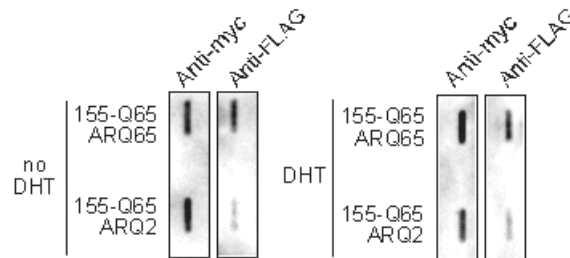
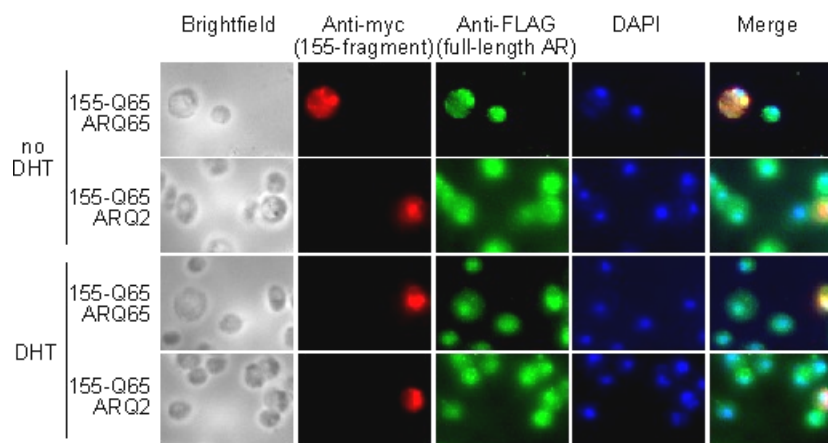
A**B**

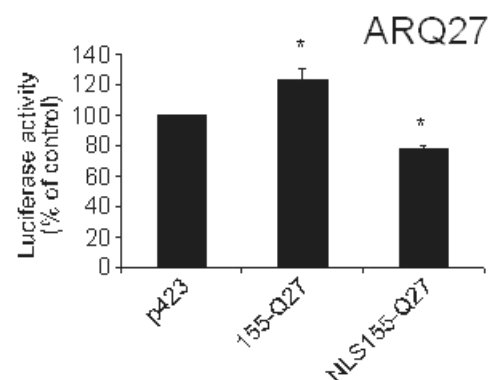
Figure 37: Recruitment of full-length ARQ65 into SDS-insoluble aggregates of 155-Q65.

(A), Filter trap analysis of N-terminal AR fragments. 500 μ g of total cell extracts of wild-type yeast cells co-expressing myc-tagged 155-Q65 and FLAG-tagged AR65Q or AR2Q as a control, were analyzed by filter trap assay in the absence (right) and presence (left) of DHT (5 μ M). (B), Wild-type yeast cells from (A) were analyzed by indirect immunofluorescence. The myc-tagged fragments were immunolabeled with anti-myc antibody coupled to Cy3-conjugated secondary antibody, the FLAG-tagged full-length AR constructs were immunolabeled with anti-FLAG antibody coupled to FitC and nuclei were counterstained with DAPI.

4.2.3.2 Polyglutamine-expanded N-terminal fragments impair activity of the corresponding full-length AR

As a next step, the toxic polyglutamine fragments were analyzed on their ability to inactivate full-length AR. Clinical evidence points to an impairment of AR function in SBMA (Dejager *et al.*, 2002), but the mechanism is not yet understood. To monitor AR function in a simulated disease state, the

activity of full-length AR was analyzed in the presence of its aggregating fragment derivatives. AR activity was therefore monitored in *ARE-luc* yeast co-expressing either full-length ARQ27, ARQ65, or ARQ102 with its corresponding N-terminal fragment using the luciferase assay. To eliminate growth rate dependent artifacts, luciferase measurements were normalized to those obtained from co-expression of the fragments with full-length ARQ2, which would not be susceptible to polyglutamine-mediated effects. Luciferase activity mediated by ARQ65 was slightly reduced by the aggregating fragments, 155-Q65 and NLS155-Q65 (Figure 38 B). However, more pronounced reduction in luciferase activity mediated by ARQ102 was observed in the presence of its soluble, aggregating derivatives, especially NLS155-Q102, which primarily forms soluble oligomers (Figure 38 C). In control reactions, luciferase activity mediated by full-length AR containing a non-pathogenic polyglutamine stretch, ARQ27, was not reduced in the presence of its respective fragment 155-Q27, and was slightly reduced in the presence of NLS155-Q27 (Figure 38 A). The latter result might come from a general impairment of transcription when these fragments are targeted to the nucleus. In summary, these results indicate that the transactivation function of full-length ARQ102 is compromised by its N-terminal fragments in a polyglutamine-dependent manner.

A

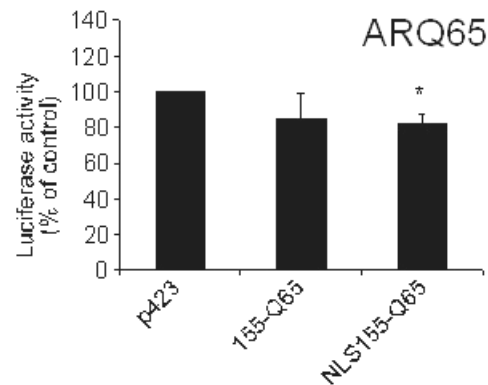
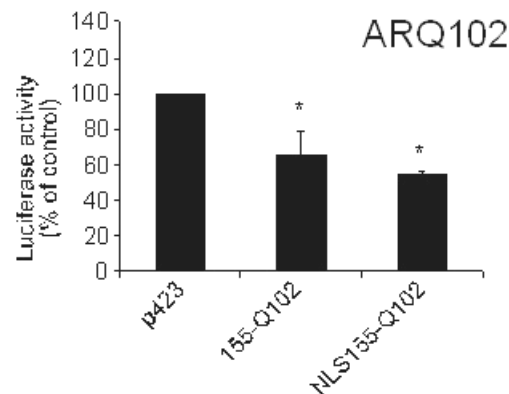
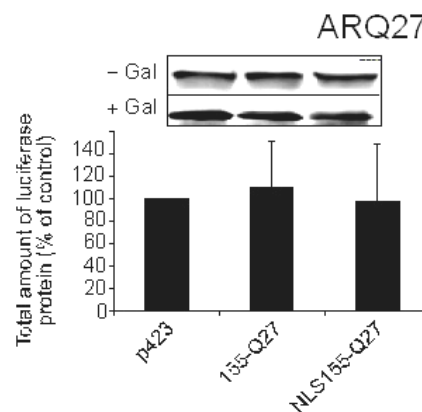
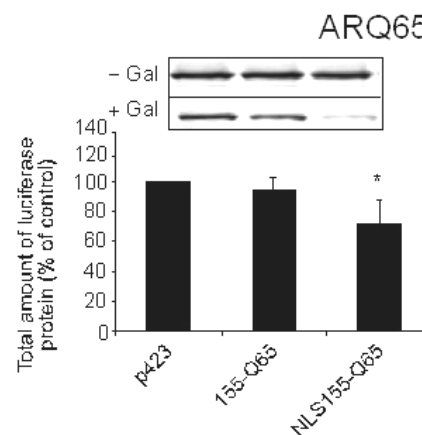
B**C**

Figure 38: Luciferase activity mediated by polyglutamine-expanded AR is decreased by its N-terminal polyglutamine-expanded fragments.

Yeast cells expressing full-length AR with 27, 65 or 102 Q with their respective fragments (155-Q27/Q65/Q102 and NLS155-Q27/Q65/Q102) or empty vector (p423) were grown in duplicate until mid-log phase. DHT was added to one set of cells for two hours and luciferase activity of all samples was determined. In parallel, all fragments were co-expressed with ARQ2 as a control. Luciferase activity upon co-expression of empty vector p423 was set to 100%. Means \pm SD of 3 independent experiments are shown. *, $p < 0.05$ versus empty vector control (unpaired t-test).

To substantiate these results, and to eliminate potential interference with luciferase folding caused by polyglutamine fragments, steady-state levels of luciferase protein present in extracts derived *ARE-luc* yeast co-expressing full-length AR with its corresponding fragment were analyzed. As controls, extracts from yeast co-expressing ARQ2 with the polyglutamine fragments were again determined in parallel to assess artifactual changes in luciferase levels (Figure 39). In cells expressing full length ARQ102, luciferase accumulated to

significantly lower levels in the presence of its corresponding mutant polyglutamine fragments, 155-Q102 and NLS155-Q102, relative to analogous ARQ2 conditions (Figure 39 C). A similar tendency was observed for conditions with full-length ARQ65 (Figure 39 B). In contrast, in cells expressing full-length ARQ27 with its corresponding fragments (155-Q27 or NLS155-Q27), the level of luciferase did not significantly change (Figure 39 A). These results mirror those obtained in Figure 38, and suggest that fragments of polyglutamine-expanded AR have the capacity to inactivate their full-length counterparts during pathogenesis. Furthermore, the most substantial reduction in luciferase activity was associated with the 155-Q102 and NLS155-Q102 fragments, which accumulate as toxic, soluble species, rather than detergent-insoluble aggregates.

A**B**

C

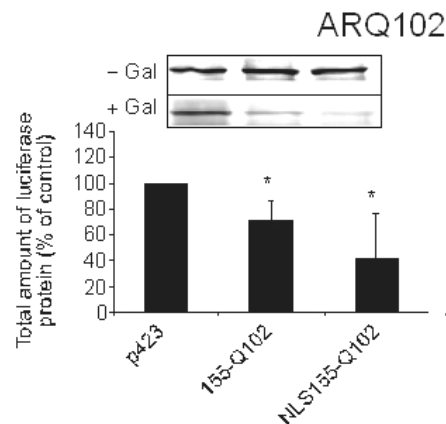


Figure 39: Luciferase protein levels produced by polyglutamine-expanded AR are decreased by its N-terminal polyglutamine-expanded fragments.

Yeast cells expressing full-length AR with 27 (A), 65 (B) and 102 Q (C) were grown with the respective fragments (155-Q27/Q65/Q102 and NLS155-Q27/Q65/Q102) or empty vector (p423) in duplicate until mid-log phase. In parallel, all fragments were co-expressed with ARQ2 as a control. DHT was added to one set of cells for two hours and cell extracts were analyzed by SDS-PAGE and Western blotting using anti-luciferase with subsequent quantitation. The total amount of luciferase protein upon co-expression of empty vector p423 was set to 100%. Means \pm SD of 3-4 independent experiments are shown. *, $p < 0.05$ versus empty vector control (unpaired t-test).

4.2.3.3 Soluble forms of 155-Q102 and NLS155-Q102 interact with full-length AR in a polyglutamine-dependent manner

To address the mechanism of inactivation of full-length AR by the 155-Q102 and NLS155-Q102 fragments, immunoprecipitation experiments were conducted. Extracts of yeast cells co-expressing 155-Q102 or NLS155-Q102 with full-length ARQ102 or ARQ2 were subjected to high-speed centrifugation. Fragments were precipitated from the supernatant fraction using an anti-myc antibody, and the amount of co-precipitated full-length protein was assessed by SDS-PAGE and western blotting. Significant amounts of ARQ102, but not ARQ2, were bound specifically to soluble 155-Q102 and NLS155-Q102 (Figure 40). Thus, the data suggest that soluble forms of 155-Q102 and NLS155-Q102 interact with full-length AR in a polyglutamine-dependent manner. Since NLS155-Q102 primarily accumulates as toxic oligomers in the 200-500 kDa range (Figure 33), it seems that these species are the primary toxic agents that bind to and inactivate full-length AR.

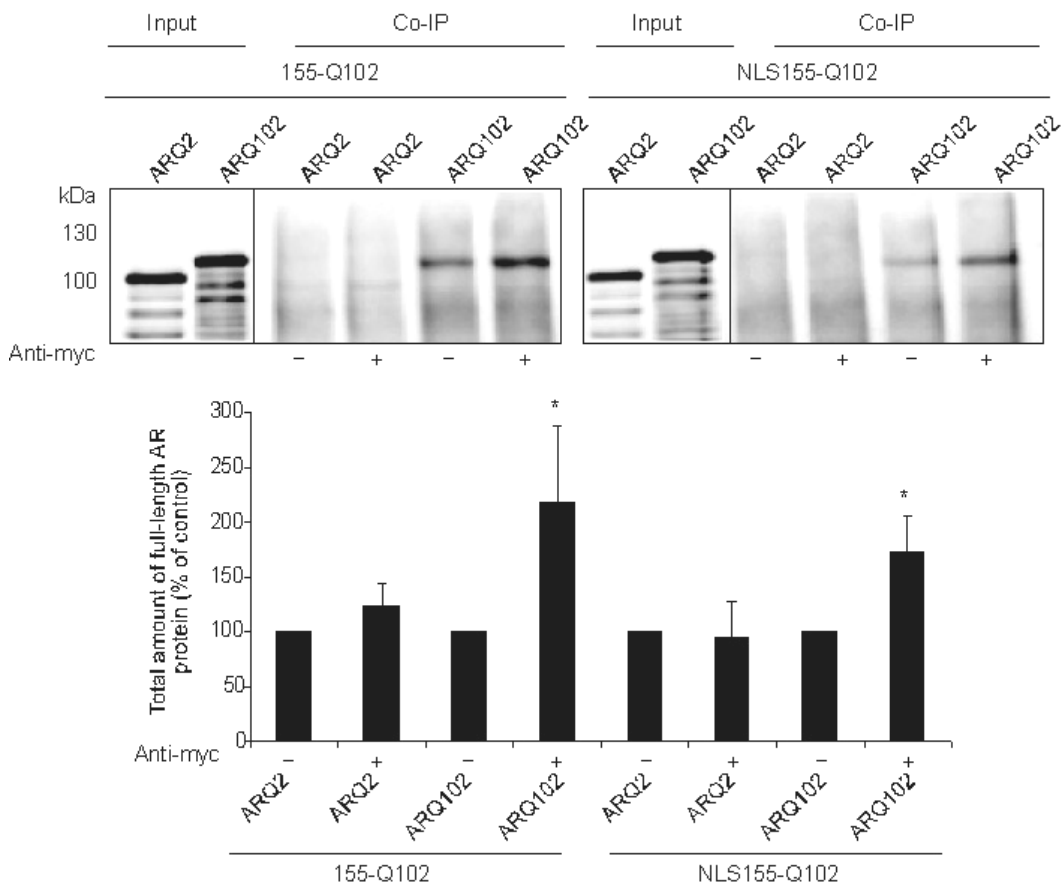


Figure 40: Full-length AR co-immunoprecipitates with soluble forms of its N-terminal fragments in a polyglutamine-dependent manner.

Whole extracts of yeast cells co-expressing myc-tagged 155-Q102 (\pm NLS) and FLAG-tagged AR102Q or AR2Q (as a control) grown until mid-log phase were subjected to high-speed centrifugation. The resulting supernatant fraction was incubated with anti-myc and Sepharose G beads, and immunoprecipitated complexes were isolated. Soluble fractions of cell extracts (Input) and the immunoprecipitated complexes (Co-IP) were analyzed by SDS-PAGE and western blotting with anti-AR. The amount of co-immunoprecipitated full-length AR was quantified (bottom panel). Means \pm SD of 3-4 independent experiments are shown. *, $p < 0.05$ versus absence of anti-myc antibody (unpaired t-test).

4.2.4 Analysis of the effect of polyglutamine-expanded huntingtin exon 1 on AR transactivation capacity

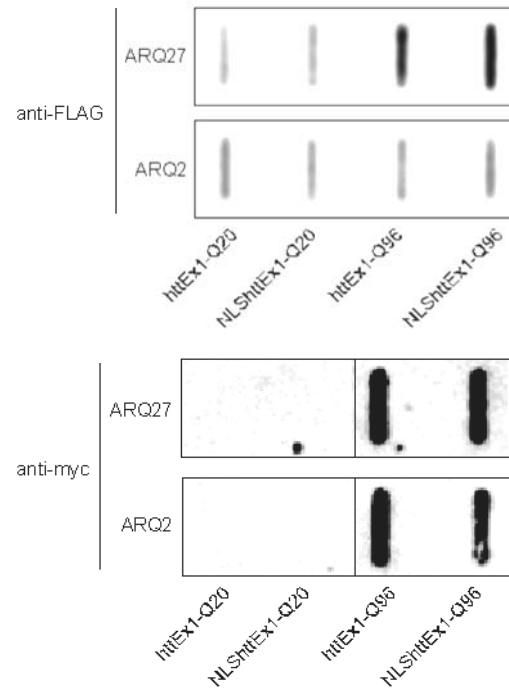
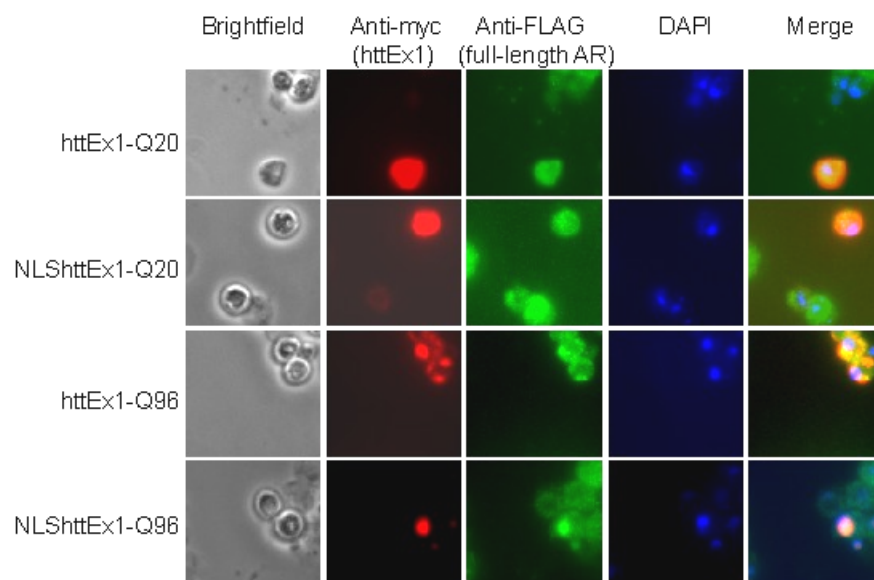
It is hypothesized that the protein context of the expanded polyglutamine stretch bias disease-specific processes, as flanking regions were shown to affect the toxicity of the polyglutamine stretch (Dehay and Bertolotti, 2006; Duennwald *et al.*, 2006a).

Recent work has demonstrated testicular degeneration in mouse models of HD and specific testicular pathology, *e.g.* a significant decrease in spermatogenesis, in HD patients (Papalexi *et al.*, 2005; Van Raamsdonk *et al.*, 2007). Interestingly, the authors suggest the onset of the testicular phenotype occurs later in life due to a direct toxic effect of polyglutamine-expanded huntingtin in the testis (Van Raamsdonk *et al.*, 2007). This is supported by the fact that huntingtin and the AR protein are highly expressed in the testis (Guo *et al.*, 2003). It might be possible that polyglutamine-expanded huntingtin fragments, analogous to polyglutamine-expanded N-terminal AR fragments, impair the transactivation capacity of full-length AR resulting in testicular pathology in HD patients. Hence, the polyglutamine stretch, despite different flanking regions, mediates toxicity that leads to testicular pathology in both, HD and SBMA patients.

4.2.4.1 Polyglutamine-expanded huntingtin exon 1 fragments recruit full-length AR into SDS-insoluble aggregates

To determine whether full-length AR is recruited into aggregates composed of polyglutamine-expanded huntingtin fragments as observed for N-terminal polyglutamine containing AR fragments, full-length AR_{Q2}, AR_{Q27}, or AR_{Q65} were co-expressed with the aggregating httEx1-Q96 ± NLS or httEx1-Q20 ± NLS as a control in yeast. Analysis of yeast extracts using the filter assay, followed by immunodetection with an antibody against the N-terminal FLAG tag of full-length AR proteins, revealed that full-length AR with 27 Q and 65 Q (AR_{65Q}) was partially recruited into SDS-insoluble aggregates of httEx1-Q96 and NLShttEx1-Q96, respectively (Figure 41 A and data not shown). Full-length AR with 2 Q (AR_{2Q}) was not retained with the aggregates demonstrating that the recruitment phenomenon is polyglutamine-dependent. Consistently, fluorescence microscopy of yeast strains revealed AR_{Q65} and AR_{Q27} but not AR_{Q2}, colocalized with aggregates of httEx1-Q96 and NLShttEx1-Q96 in yeast cells (Figure 41 B, C and data not shown). These results indicate that full-length AR is recruited via its polyglutamine stretch into SDS-insoluble aggregates of

httEx1-Q96 (and NLShttEx1-Q96) in analogy to the recruitment into SDS-insoluble aggregates of N-terminal polyglutamine-expanded AR fragments.

A**B**

C

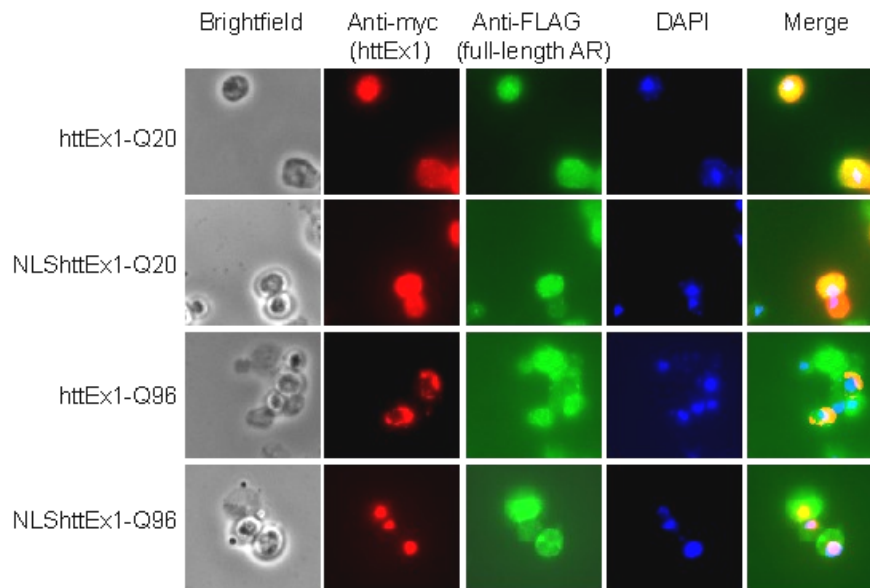


Figure 41: Recruitment of full-length ARQ27 into SDS-insoluble aggregates of httEx1-Q96 \pm NLS.

(A), Filter trap analysis of httEx1 fragments. 50 μ g of total cell extracts of wild-type yeast cells co-expressing FLAG-tagged ARQ27 (upper panel) or ARQ2 (lower panel) as a control and myc-tagged httEx1 fragments (httEx1-Q20 \pm NLS and httEx1-Q96 \pm NLS) were analyzed by filter trap assay with anti-FLAG antibody. (B, C), Wild-type yeast cells from (A) were analyzed by indirect immunofluorescence. The myc-tagged fragments were immunolabeled with anti-myc antibody coupled to Cy3-conjugated secondary antibody, the FLAG-tagged full-length ARQ27 (B) and ARQ2 (C) constructs were immunolabeled with anti-FLAG antibody coupled to FitC and nuclei were counterstained with DAPI.

4.2.4.2 The transactivation capacity of full-length polyglutamine containing ARs is impaired by polyglutamine-expanded huntingtin exon 1 fragments

To analyze the impact of the regions flanking the polyglutamine stretch on AR transactivation capacity full-length ARQ102 was co-expressed with either httEx1-Q96 \pm NLS or httEx1-Q20 \pm NLS as a control. To eliminate growth rate dependent artifacts, luciferase measurements were normalized to those obtained from co-expression of the fragments with full-length ARQ2. The analysis revealed that luciferase activity mediated by full-length ARQ102 was substantially reduced in the presence of httEx1-Q96 and NLShttEx1-Q96, to \sim 66% and 58% of its normal activity whereas the presence of httEx1-Q20 and

NLShttEx1-Q20 did not (~90% and 99%, respectively; Figure 42). This result indicates that the transactivation function of full-length AR102 is also compromised by polyglutamine-expanded huntingtin fragments and suggests that the transactivation function of polyglutamine-expanded AR is compromised in the presence of polyglutamine-containing fragments.

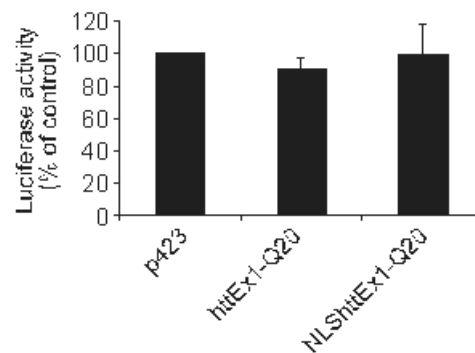
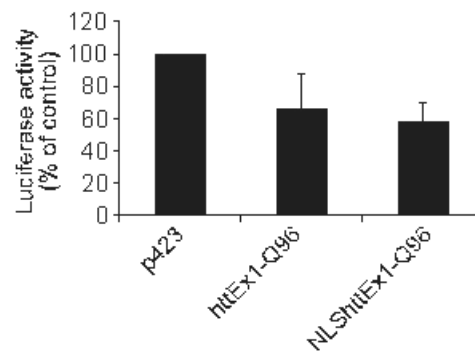
A**B**

Figure 42: Polyglutamine-expanded huntingtin fragments decrease AR mediated luciferase activity.

Yeast cells expressing full-length AR with 102 Q were grown with huntingtin fragments containing a non-pathogenic polyglutamine stretch (A, httEx1-Q20 and NLShttEx1-Q20) or a pathogenic polyglutamine stretch (B, httEx1-Q96 and NLShttEx1-Q96) or empty vector (p423) in duplicate until mid-log phase. DHT was added to one set of cells for two hours and luciferase activity of all constructs was determined. In parallel, all fragments were co-expressed with ARQ2 as a control. The luciferase activity upon co-expression of empty vector p423 was set to 100%. The data are mean values of n=3 independent experiments \pm S.D.

To verify these results, the amount of luciferase present in extracts derived from ARE-*luc* yeast co-expressing full-length AR with httEx1 fragments was analyzed. As controls, extracts from yeast co-expressing ARQ2 with the

httEx1 fragments were determined in parallel to assess artifactual changes in luciferase levels (Figure 43). In cells expressing full length ARQ102, luciferase accumulated to significantly lower levels (~80% and 59%) in the presence of polyglutamine-expanded httEx1, httEx1-96Q and NLShttEx1-96Q, whereas the presence of httEx1 with a non-pathogenic polyglutamine stretch, httEx1-Q20 and NLShttEx1-Q20, had no significant impact (~90% and 99%, respectively; Figure 43). Taken together, these results indicate that the expanded polyglutamine stretch and not the sequences flanking the polyglutamine stretch, of aggregating fragments mediate inactivation of full-length AR.

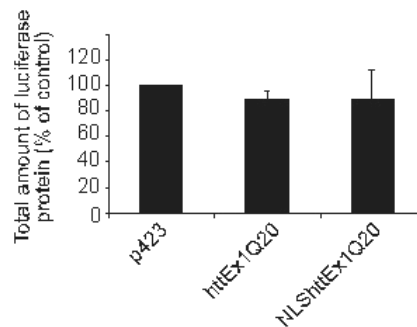
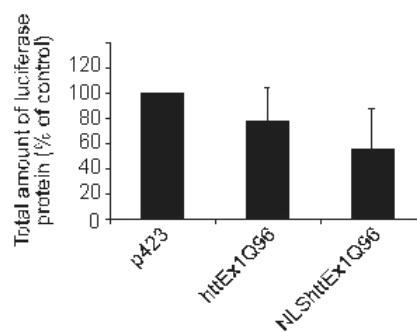
A**B**

Figure 43: Polyglutamine-expanded huntingtin fragments decrease AR mediated total amount of luciferase protein.

Yeast cells expressing full-length AR with 102 Q were grown with huntingtin fragments containing a non-pathogenic polyglutamine stretch (A, httEx1-Q20 and NLShttEx1-Q20) or a pathogenic polyglutamine stretch (B, httEx1-Q96 and NLShttEx1-Q96) or empty vector (p423) in duplicate until mid-log phase. In parallel, all fragments were co-expressed with ARQ2 as a control. DHT was added to one set of cells for two hours and cell extracts were analyzed by SDS-PAGE and western blotting with anti-luciferase antibody with subsequent quantitation. The total amount of luciferase protein upon co-expression of empty vector p423 was set to 100%. The data are mean values of n=3 independent experiments \pm S.D.

5 Discussion

Studies worldwide revealed that currently at least 15 percent of the population over 65 in western countries suffer from neurodegeneration. In the U.S. alone, the total cost of Alzheimer's disease, the most common neurodegenerative disease, in 2002 has been estimated at \$100 billion per year (http://focus.hms.harvard.edu/2002/June21_2002/forum.html), and as the human life span increases, the number of people over 65 will double over the next 30 years. These are worrisome facts that force research to focus on neurodegeneration and thus, the aberrant folding of proteins.

When research started in that field decades ago, the proteinaceous deposits in patients composed of amyloidogenic aggregates were soon declared the toxic species responsible for the degeneration of neuronal cells, since they are a common hallmark of all the amyloidoses. In Alzheimer's disease, for example, the A β peptide misfolds and forms highly ordered fibrillar aggregates. Similar aggregates are also formed by proteins with an expanded polyglutamine stretch, *e.g.* huntingtin in Huntington's disease or AR in SBMA. This 'aggregate hypothesis' persisted for a long time, and it is only recently that this view has begun to change. The poor overlap between neurons with visible inclusions and neurons actually undergoing degeneration on the one hand and studies showing aggregate formation being benign on the other started a process of rethinking. Currently, soluble oligomeric folding intermediates of the disease proteins are suspected to exert neurotoxicity, which was shown for A β oligomers and polyglutamine-expanded proteins (Arrasate *et al.*, 2004; Behrends *et al.*, 2006; Cleary *et al.*, 2005; Ross and Poirier, 2005; Walsh *et al.*, 2002). But it might well be that neurodegeneration is the result of an interplay of numerous non-exclusive mechanisms mediated by different species formed in the pathway towards mature fibrils, including monomers and the mature fibrils themselves (Michalik and Van Broeckhoven, 2003). These species seem to have features which are independent of the protein context and lead to similar toxic phenotypes for intrinsically unrelated proteins such as A β peptide, prion protein, or the polyglutamine-expanded huntingtin and AR protein (Kayed *et al.*, 2003).

The molecular mechanisms underlying neurodegeneration are also far from being fully understood. In the case of polyglutamine diseases, it is most probably a gain-of-function mechanism of the aggregation prone proteins that causes cytotoxicity, as supported by the dominant inheritance pattern, together with extensive studies on cell culture and animal models of these diseases (Piccioni *et al.*, 2001; Zoghbi and Orr, 2000). This is most evident in patients of complete androgen insensitivity syndrome (CAIS), who lack functional AR protein due to a mutation in the gene coding for AR. Although they suffer from disturbances in various androgen-mediated mechanisms, they do not develop neurodegenerative symptoms. Thus, it is likely that it is the expanded polyglutamine repeat that confers toxicity at the neuronal level in SBMA (Brooks and Fischbeck, 1995; Piccioni *et al.*, 2001). However, sequences flanking the polyglutamine repeat might also influence pathogenesis (Duennwald *et al.*, 2006a). So far, several non-exclusive hypotheses were proposed to explain polyglutamine mediated neurodegeneration, which include transcriptional dysregulation (Cha, 2000; Sakahira *et al.*, 2002b; Schaffar *et al.*, 2004), inhibition of the ubiquitin proteasome system (Bennett *et al.*, 2007; Pandey *et al.*, 2007), sequestration of cytoplasmic and nuclear proteins (Harjes and Wanker, 2003; Li and Li, 2004), plasma membrane damages (Hirakura *et al.*, 2000; Monoi *et al.*, 2000; Trushina and McMurray, 2007), and impairment of axonal and dendritic trafficking (Lee *et al.*, 2004; Piccioni *et al.*, 2002). Various species of polyglutamine-expanded protein, including monomers, oligomers or large aggregates, were shown to be involved in at least one of these processes.

Regardless of the specific oligomeric state, the overall activity of the disease causing protein is altered either due to intrinsic properties of the elongated polyglutamine stretch or a reduction in the total amount of the respective protein due to aggregation. The resulting loss-of-function effect of the disease protein might contribute to disease pathogenesis and explain differences in pathology among polyglutamine diseases (Dragatsis *et al.*, 2000; Leavitt *et al.*, 2001; Leavitt *et al.*, 2006b; Thomas *et al.*, 2006).

5.1 *Danio rerio*, a new model organism to identify inhibitors of polyglutamine aggregation

In polyglutamine diseases, major effort has been put into identifying means to disrupt or alter the polyglutamine aggregation pathway with the overall goal to suppress polyglutamine mediated toxicity (Di Prospero and Fischbeck, 2005). As the aggregation pathway accounts for the generation of toxic species, several screens were carried out, most of them *in vitro* or in cell based assays, to identify inhibitors of the aggregation process. Since it is unclear which step of the aggregation pathway the compound has to inhibit in order to prevent cytotoxicity, these compounds have to be reevaluated in terms of their capacity to suppress toxicity. Ideally this should be done in a whole organism to allow the simultaneous analysis of potential adverse effects. So far, further investigations with respect to the effect of drug candidates in a vertebrate organism are restricted to rodent models (Heiser *et al.*, 2002; Hockly *et al.*, 2006). As these experiments are expensive and time consuming, the reevaluation of all promising drug candidates is not feasible and effective compounds may remain undiscovered.

5.1.1 Zebrafish model for HD

This study describes the establishment of a zebrafish HD model system suitable for the whole organism validation of candidate compounds. The zebrafish has several key advantages over other *in vivo* models of HD. In comparison to *Drosophila melanogaster* or *Caenorhabditis elegans*, it is a vertebrate organism and contains homologues to many human genes, including the htt gene (Figure 8), making it a valuable tool to model human diseases such as HD (Karlovič *et al.*, 1998). Unlike the established rodent HD models, *in vivo* drug tests can be performed in a time and cost efficient way. Additional advantages include the robustness of the embryos that facilitates experimental manipulation, the transparency of zebrafish embryos allowing for the visualization of morphological and physiological features in the live embryo, and the aqueous

environment of the zebrafish, which facilitates drug administration (Zon and Peterson, 2005). In contrast to cell culture, the zebrafish model system allows for the evaluation of drug effectiveness in a whole organism, taking into account the stability and cellular targeting of the tested compound, as well as the assessment of potential side effects of the drug at effective concentrations.

The zebrafish model of HD described in this study is based on the expression of mRNA of N-terminal fragments of htt containing 4, 25 or 102 Q fused to green fluorescent protein (Figure 9). The mRNA was injected at the 1-2 cell stage. As the intensity of the GFP-signal decreased after 48 h most likely due to degradation and translation (data not shown), the analysis was restricted to zebrafish embryos up to 36 h. The advantage of mRNA injection over DNA injection in zebrafish is the homogenous distribution of the mRNA upon cell division. As a consequence thereof, the expression of the constructs is ubiquitous and mimics the overall expression of htt in humans (DiFiglia *et al.*, 1995; Gutekunst *et al.*, 1995; Trotter *et al.*, 1995).

As expected, the constructs were homogeneously expressed throughout the embryo with polyglutamine-expanded htt (Q102-GFP) giving rise to the formation of large inclusions (Figure 10, Figure 11 and Figure 12). These inclusions turned out to be composed of predominantly SDS-insoluble aggregates (Figure 14), a hallmark of HD that has also been observed in patients and in animal models of HD (Davies *et al.*, 1997; DiFiglia *et al.*, 1997; Jackson *et al.*, 1998; Satyal *et al.*, 2000). The inclusions, which are perinuclear and relatively large in size (Figure 12) grew by efficient incorporation of soluble Q102-GFP, resulting in its depletion from the cytoplasm (Figure 13).

Aggregation was not restricted to a specific region as aggregates were detected throughout the entire embryo. However, a certain threshold concentration of Q102-GFP is required to initiate aggregation, since only a subset of cells expressing Q102-GFP shows aggregate formation (Figure 12).

Expression of Q102-GFP was also associated with pronounced morphological defects and reduced viability of zebrafish embryos (Figure 15). Thus, another characteristic of HD, namely polyglutamine mediated toxicity, could be reproduced in the zebrafish model. Interestingly, among the visibly

abnormal embryos, a characteristic 'cyclopic' phenotype was increasingly observed in embryos expressing Q102-GFP (Figure 15). This mutant phenotype is characterized by fusion of the eyefields yielding a single eye in the midline (Blader and Strahle, 1998) and has recently been found to be associated with defects in Ca^{2+} homeostasis of the endoplasmic reticulum in zebrafish (Creton, 2004). The observed enhancement of the cyclopic phenotype may therefore reflect an adverse effect of Q102-GFP on Ca^{2+} homeostasis. Indeed, perturbed Ca^{2+} homeostasis is hypothesized to be involved in HD pathogenesis (Bezprozvanny and Hayden, 2004).

In concordance with the morphological defects, the expression of Q102-GFP was also associated with enhanced apoptosis (Figure 16). The increased apoptosis upon expression of Q4-GFP and Q25-GFP in comparison to the untreated embryos is most probably a result of the injection process itself (Figure 16). This might also explained the increased occurrence of dead and morphologically abnormal embryos (Figure 15).

Previous studies in cell culture suggested that polyglutamine toxicity is not primarily caused by detectable inclusions (Arrasate *et al.*, 2004; Schaffar *et al.*, 2004). In the zebrafish model the majority of apoptotic cells were devoid of visible inclusions. Hence, in line with the aforementioned studies, inclusions of polyglutamine-expanded htt do not contribute directly to toxicity in a vertebrate organism. Probably, smaller inclusions/aggregates with a diameter $< \sim 0.5 \mu\text{m}$, which would escape detection using the experimental setup in this study, are involved in causing toxicity in the zebrafish system.

An important observation was that both the aggregation and toxicity of mutant htt was suppressed by the molecular chaperones, Hsp40 and Hsp70, mimicking observations from other HD models (Barral *et al.*, 2004). Thus, key features of HD are reproduced in this zebrafish model, which make it a valid model organism for identifying factors that influence disease pathogenesis.

5.1.2 The anti-prion compounds inhibit the aggregation of polyglutamine-expanded fragments

Drug absorption into the zebrafish embryo is likely facilitated by its aqueous environment and lack of blood brain barrier at early stages in development; therefore, compounds can be tested for their effect while minimizing complicating factors that impede absorption. To evaluate the suitability of the zebrafish model to identify inhibitors of polyglutamine mediated aggregation and toxicity, known inhibitors of the polyglutamine aggregation process were analyzed for their effect in the zebrafish model. Subsequent to mRNA injection the clutches were divided in two groups, half of which was treated with the drug and the other half with the respective solvent as a control.

The effect of PGL-135, Congo red and Isoproterenol HCl in the zebrafish model is consistent with studies in other HD models (Hockly *et al.*, 2006; Sanchez *et al.*, 2003; Wang *et al.*, 2005). Surprisingly, Mycophenolic acid, a compound known to suppress htt inclusion formation in cell culture (Wang *et al.*, 2005), had no effect on Q102-GFP aggregation in zebrafish at the maximum tolerated dose (Figure 22). Since Mycophenolic acid caused pronounced apoptosis in the brain region of the zebrafish embryo at higher doses (data not shown), concentrations shown to have an effect on polyglutamine aggregation in cell culture (Wang *et al.*, 2005) could not be tested. Therefore, the zebrafish model also permits evaluation of whether a compound causes toxic side effects when present at effective concentrations in a whole organism. In summary, the obtained results for the known inhibitors of polyglutamine aggregation confirm the use of the zebrafish model to evaluate and identify inhibitors of polyglutamine mediated aggregation.

Two of the candidate compounds, 313B02 and 293G02, were previously identified as inhibitors of the recruitment of prion monomers into PrP^{Sc} aggregates (Bertsch *et al.*, 2005), while compound 306H03 has since been discovered in a similar screen (A. Giese, pers. comm.). PrP^{Sc} and mutant htt are neurodegenerative disease proteins that accumulate in structurally similar fibrillar aggregates that may have a common beta-helical amyloid core structure

(Govaerts *et al.*, 2004; Stork *et al.*, 2005). Taking such analogies into consideration, inhibitors of the aggregation of PrP^{Sc} may also be effective in preventing polyglutamine protein aggregation. As hypothesized, it turned out that anti-prion compounds are indeed potent inhibitors of polyglutamine aggregation not only *in vitro* but also in zebrafish (Figure 21 and Figure 22). This observation suggests that polyglutamine aggregates and prions share common structural epitopes. To substantiate the effect of the tested drugs, their ability to suppress polyglutamine aggregation was additionally evaluated in a N2a neuroblastoma cell culture model of HD (Figure 23). The obtained results confirmed those from zebrafish and propose NBBs as effective inhibitors of polyglutamine aggregation and further established the zebrafish system as a valid model to study human disease (Figure 24). Taken together, these findings reinforce the view that common mechanisms underlie the pathogenesis of diverse neurodegenerative diseases and suggests that common therapeutic targets may exist.

The newly established zebrafish model proved useful in evaluating the effectiveness of compounds in inhibiting polyglutamine aggregation and toxicity in the context of a whole vertebrate organism. The unique feature that drug testing can be performed within two days would make this model a cost and time efficient alternative to existing mouse models of HD. The ability to differentiate between effects on polyglutamine mediated aggregation versus toxicity is another advantage of the zebrafish system, which is lacking in several other HD models, such as the N2a cell culture model tested in this study (Figure 23). The zebrafish model also takes into account the stability and the cellular targeting of compounds in an organism. For example, one of the tested compounds, 313B02, was effective in inhibiting polyglutamine aggregation *in vitro*, but was not effective as an aggregation inhibitor *in vivo* (Figure 21 and Figure 22), suggesting that this compound is not stable and/or not targeted efficiently in the zebrafish. In addition, the zebrafish model also enables to analyze whether a compound caused side effects when present at active concentrations in a whole organism as observed for Mycophenolic acid.

Based on this study, NBBs may constitute a new class of compounds with “generic” anti-aggregation activity, perhaps preventing the misfolding and

aggregation of a wide variety of neurodegenerative disease proteins. NBBs provide a novel and promising lead structure for the development of new therapeutics in several regards. The NBBs used in this study satisfy Lipinski's 'rule of 5' for drug-likeness by having fewer than 5 H-bond donors, 10 H-bond acceptors, a molecular weight smaller than 500, and a calculated Log P (cLogP) smaller than 5, which would predict efficient absorption or permeation (Lipinski *et al.*, 2001). Importantly, the results indicate that in a vertebrate organism, NBBs can reach the cytoplasm in active concentrations without causing overt toxic side effects up to the limits of their solubility in water. Furthermore, the analyses indicate that the hydroxyl groups of the NBB compounds, which were shown to be crucial for anti-prion activity *in vitro* (Bertsch *et al.*, 2005), are not essential for inhibition of polyglutamine aggregation *in vivo*. In fact, 293G02, although exhibiting the highest potency *in vitro*, was a less effective inhibitor of polyglutamine aggregation than 306H03 *in vivo* (Figure 21, Figure 22 and Figure 24). Most likely, the presence of a chloride group, rather than hydroxyl groups, enhances cell permeability by decreasing the total polar surface area (tPSA) from 81.92 Å² (293G02) to 41.46 Å² (306H03) and increasing the hydrophobicity cLogP from 2.94 (293G02) to 4.67 (306H03). Thus, NBBs such as 306H03 may be developed that are more likely to cross the blood brain barrier efficiently. Presumably, the disease-modifying therapeutic effect of aggregation inhibitors in protein aggregation diseases also depends on the nature of the toxic species and whether toxicity occurs primarily through a loss-of-function or gain-of-function mechanism. New classes of drugs which interfere with aggregate formation at the molecular level such as the NBBs may provide valuable tools to further dissect the molecular steps involved in disease pathogenesis *in vivo*.

The nature of the toxic species may explain why NBBs could suppress the formation of SDS-insoluble aggregates without detectably suppressing polyglutamine toxicity (Figure 22). Presumably, NBBs effectively inhibit primarily later stages of Q102-GFP aggregation. Thus, early soluble intermediates in the htt aggregation pathway associated with toxicity may still accumulate. In line with this assumption, upon addition of NBBs a shift in the total amount of SDS-insoluble to SDS-soluble aggregates was observed (data not shown). Hence,

it seems likely, that the NBBs inhibit the conversion of SDS-soluble polyglutamine-oligomers into SDS-insoluble, amyloidogenic fibrils. In support of this possibility, results that were published after this study showed that Congo red inhibits the growth of oligomers, but not the initial formation of fibrils (Takahashi *et al.*, 2007). In concordance, in the zebrafish model of HD Congo red inhibited aggregate formation but not toxicity analogous to the NBBs (Figure 22 and data not shown). A computer-based simulation of NBB docking to a polyglutamine protofibril predicts that NBBs as well as Congo red specifically bind to the ends of the polyglutamine helices, a mechanism that would prevent fibril growth (Thomas Hirschberger, pers. comm.). Future studies aimed at assaying structural derivatives of NBBs may lead to the identification of more effective suppressors of polyglutamine toxicity.

Large scale screens will continue to identify promising compounds that inhibit aggregation processes *in vitro* or in cell culture. A systematic approach for validating such candidate compounds should include the judicious use of vertebrate model systems to evaluate efficacy against polyglutamine aggregation and toxicity before proceeding to clinical trials. Cost and time-efficient drug testing using the zebrafish model described here is likely to prove useful for this purpose.

The establishment of a transgenic zebrafish line expressing a pathogenic polyglutamine construct should also be taken into consideration. By taking advantage of the same genetic background in a transgenic line, direct screening for compounds that inhibit polyglutamine-mediated aggregation and toxicity could be performed using ideally only one fish per compound. Due to a constant expression of the pathogenic construct the analyses would not be restricted to the embryonic state and compounds might be identified that ameliorate symptoms at later stages. In this way such a transgenic zebrafish line could also deliver insights on age-related toxic effects caused by polyglutamine containing fragments.

5.2 *Saccharomyces cerevisiae*, a model organism to study mechanisms of polyglutamine mediated toxicity

The molecular mechanisms underlying polyglutamine mediated cytotoxicity are not yet fully understood. Based on studies in various models of polyglutamine disease, hypotheses were proposed to explain polyglutamine mediated cytotoxicity which include, among others, the inhibition of the ubiquitin proteasome system, formation of ion channels, impairment of axonal trafficking but also the inactivation of essential transcription factors. As a possible reason the polyglutamine-expanded proteins are thought to adopt new characteristics that trigger toxicity, a process that is known as a toxic gain-of-function mechanism. The impact that a partial loss of its intrinsic function could have on disease pathogenesis is unclear but studies on HD and also on SBMA revealed considerable evidence for a pathogenic role of diminished normal function of disease proteins containing polyglutamine repeat expansions (Dragatsis *et al.*, 2000; Leavitt *et al.*, 2001; Leavitt *et al.*, 2006b; Thomas *et al.*, 2006).

5.2.1 A yeast model for SBMA

S. cerevisiae has been frequently used to investigate aspects of polyglutamine toxicity because of its easy handling and maintenance, the short generation time and the ease of manipulating the genome, which allows biochemical studies from a single genetically defined cell (Drubin, 1989). Despite the low genomic complexity in comparison to higher eukaryotic organisms, it proved useful in reproducing and investigating key characteristics of polyglutamine disease, such as mechanisms of polyglutamine cytotoxicity and the formation and accumulation of polyglutamine aggregates (Dehay and Bertolotti, 2006; Duennwald *et al.*, 2006a; Krobitsch and Lindquist, 2000; Meriin *et al.*, 2002; Muchowski *et al.*, 2000). These studies which focused on Huntington's disease confirmed the correlation between the size of the polyglutamine stretch and aggregation propensity, analyzed the effect of

molecular chaperones on polyglutamine oligomerization, aggregation and toxicity, and also investigated polyglutamine mediated transcriptional dysregulation (Behrends *et al.*, 2006; Krobitch and Lindquist, 2000; Muchowski *et al.*, 2000; Schaffar *et al.*, 2004). Thus, investigations on polyglutamine diseases in yeast lead to important contributions to the understanding of molecular mechanisms underlying cytotoxicity.

This study established a yeast model of SBMA amenable to analysis of the toxic gain-of-function effects of polyglutamine containing AR fragments and potential loss-of-function of the AR protein itself. The yeast model of SBMA is based on the expression of either full-length AR containing 2Q, 27Q, 65Q or 102Q and/or the respective N-terminal fragments of AR in *S. cerevisiae*. Expression of full-length ARs with varying polyglutamine stretches were not toxic to yeast cells nor did they aggregate (Figure 26). This was probably because the N-terminus of full-length AR was not efficiently liberated by proteolysis (Figure 26), an event that is crucial to SBMA pathogenesis and was shown to be mediated by caspase-3 (Ellerby *et al.*, 1999; Kobayashi *et al.*, 1998; Wellington *et al.*, 1998). Since no yeast homologue of caspase-3 was identified (Madeo *et al.*, 2002), this could explain the lack of toxicity upon expression of polyglutamine-expanded full-length AR. In contrast, the N-terminal AR fragments caused polyglutamine length-dependent toxicity in yeast, which was enhanced when the constructs were targeted to the nucleus (Figure 27). The latter is concordant with observations in SBMA patients as well as in cellular and animal models (Adachi *et al.*, 2005; Gatchel and Zoghbi, 2005). The indispensable role cleavage plays in SBMA pathogenesis is also reflected in the missing effect upon addition of the ligand DHT, which neither resulted in toxicity nor in aggregation in yeast cells expressing full-length AR. Although it has been demonstrated that ligand-mediated targeting of the AR into the nucleus has a dramatic impact on SBMA pathogenesis (Katsuno *et al.*, 2006; Takeyama *et al.*, 2002), it seems that the crucial event which leads to toxicity is the proteolytic cleavage of AR that was shown to be both, polyglutamine- and ligand-dependent (LaFevre-Bernt and Ellerby, 2003).

Work on yeast prions proposed that in a yeast model of Huntington's disease, toxicity depends on polyglutamine aggregation mediated by a prion-like protein Rnq1 (Meriin *et al.*, 2002). Such a dependency on yeast prions was not observed in this yeast model of SBMA. The absence of both aggregated Rnq1 or Hsp104p had no obvious effect on toxicity, thus, suggesting a different mechanism of toxicity (Figure 28).

In recent studies in yeast, aggregation and toxicity of polyglutamine stretches within the pathological range was shown to be largely affected by its flanking sequences (Dehay and Bertolotti, 2006; Duennwald *et al.*, 2006b). Upon analyzing the aggregation characteristics of the N-terminal AR fragments, the most striking observation was the decreased propensity of the 102 glutamine AR fragment (155-Q102) to form SDS-insoluble aggregates comparing to the fragment containing 65 glutamines (155-Q65; Figure 30, Figure 31 and Figure 33). So far, this is the first study that contradicts the correlation between the size of the polyglutamine stretch and aggregation propensity. It remains unclear why the aggregation pathways of these constructs differ, but flanking sequences may sterically hinder the aggregation pathway of the Q102 constructs. In any event, these data suggest soluble oligomers, and not detergent insoluble fibrils, are the primary toxic agent, in line with other studies of polyglutamine proteins (Arrasate *et al.*, 2004; Li *et al.*, 2007; Schaffar *et al.*, 2004). That toxicity does not necessarily correlate with aggregation was also observed upon addition of an NLS to the N-terminal AR fragments. Aggregate-like structures were barely detected, nonetheless NLS constructs showed an increased toxicity compared to their respective untagged counterparts (Figure 27, Figure 29 and Figure 30). In line with these observations, another study showed that aggregate morphology alone does not determine polyglutamine toxicity (Duennwald *et al.*, 2006b). Nevertheless, a major toxic role of SDS-insoluble aggregates seen upon expression of 155-Q65 is highly unlikely, since expression of other constructs, for instance 155-Q102, was more toxic although no SDS-insoluble aggregates were detected (Figure 27 and Figure 30). This is in agreement with the currently postulated benign

and perhaps even protective role of aggregates in polyglutamine diseases (Arrasate *et al.*, 2004; Schaffar *et al.*, 2004).

Recent studies have shown that polyglutamine-expanded AR fragments elicit a cellular stress response in cell culture (Cowan *et al.*, 2003). To determine the capability of the polyglutamine fragments to cause cellular stress a previously identified reporter of cellular stress was used in yeast (Boorstein and Craig, 1990). Since the expression of 155-Q102 and NLS155-Q102 also activated a stress response in yeast cells, it seems likely that the underlying mechanism of polyglutamine fragment-mediated cellular stress response is not only restricted to mammalian cells (Figure 34). This observation confirmed the yeast system to be a valid model to study human disease.

5.2.2 N-terminal polyglutamine-expanded AR fragments decrease AR transactivation capacity

Due to its lack of endogenous AR and associated co-factors, the yeast system was an optimal choice for direct assessment of the function of human polyglutamine-expanded AR, both in isolation and in the presence of aggregating polyglutamine species as part of a simulated disease state.

The reporter system to monitor AR transactivation capacity in yeast is based on the luciferase gene being under control of androgen response elements (ARE-*luc*) and requires active AR as well as ligand (Figure 35). Although it was set up to analyze the effect of the polyglutamine-expanded AR fragments on the respective full-length constructs it also enabled to determine the intrinsic transactivation function of the full-length AR constructs used in this study. Strikingly, all full-length AR constructs were fully functional, suggesting that the polyglutamine-stretch in AR does not influence the intrinsic function of AR (Figure 36). This result contradicts numerous studies that report a linear decrease of transactivation function with progressive expansion of the polyglutamine repeat (Chamberlain *et al.*, 1994; Dejager *et al.*, 2002; Kazemi-Esfarjani *et al.*, 1995; Thomas *et al.*, 2006; Tut *et al.*, 1997). Unlike this work, the other studies were carried out in cell lines (Chamberlain *et al.*, 1994; Kazemi-Esfarjani *et al.*, 1995; Thomas *et al.*, 2006; Tut *et al.*, 1997) or are the result of a

study on SBMA patients (Dejager *et al.*, 2002), thus in cellular environments that are adapted to AR function. Since yeast has no homologue to AR, cofactors or miscellaneous interacting proteins are unlikely to exist. Therefore, AR transactivation capacity in this yeast system is most likely based on the intrinsic functionality of the AR protein and is not influenced by additional factors. These data suggest that AIS in SBMA is not a result of the intrinsic dysfunction of polyglutamine-expanded AR.

It is largely accepted that aggregates composed of polyglutamine-expanded fragments sequester, and as a consequence thereof, inactivate proteins containing polyglutamine stretches in the non pathogenic range (Chai *et al.*, 2002; Kim *et al.*, 2002; McCampbell *et al.*, 2000; Perez *et al.*, 1998; Rajan *et al.*, 2001). In an experimental setup that resembled an SBMA patient situation with an AR of ~65Q recruitment of full-length AR (ARQ65) into aggregates composed of the respective fragment (155-Q65) was detected (Figure 37). Artifacts can be ruled out since ARQ65 does not aggregate on its own and does not undergo cleavage (Figure 26 and data not shown). However, the recruitment does not seem to be very efficient, as co-localization was only detectable in some cells and the majority of full-length AR protein remained soluble. This is not surprising given that the AR exists in a complex with chaperones which, as a side-effect, probably shield AR from being recruited (Pratt and Toft, 1997; Freeman and Yamamoto, 2001; Pratt *et al.*, 2004). Even the presence of DHT did not significantly increase the susceptibility of AR to sequestration into the aggregates. This might again be a consequence of chaperones since after ligand binding, the AR remains in a complex with chaperones (Picard, 2006; Prescott and Coetzee, 2006).

As characteristics of AIS in SBMA develop progressively over a long period of time, similar to the neurodegeneration that appears later in life (Brinkmann, 2001; Dejager *et al.*, 2002), the aggregation prone, N-terminal polyglutamine-containing fragments that were recently proposed to be the cause of neurodegeneration in SBMA might play a major role in AIS (Li *et al.*, 2007). Indeed, a polyglutamine length-dependent effect of the fragments on full-length AR that increased with the number of glutamines could be observed in a scenario that mimics the SBMA disease state in yeast by expressing full-length

polyglutamine-expanded AR with its ~155 amino acid N-terminal fragment, which is thought to be generated after caspase-3 cleavage during SBMA pathogenesis (Figure 38 and Figure 39; Ellerby *et al.*, 1999; Kobayashi *et al.*, 1998; Wellington *et al.*, 1998). This reflects the situation in SBMA patients, who are mainly male, where expression of an X-linked mutant gene leads to accumulation of polyglutamine-expanded AR and its toxic N-terminal cleavage products (Adachi *et al.*, 2007; Ellerby *et al.*, 1999). The results indicate that full-length polyglutamine-expanded AR is substantially inactivated by its N-terminal fragments, especially the oligomer-forming NLS155-Q102 fragment (Figure 38). A minor effect on the activity of full-length ARQ27 caused by its fragments was also observed using luciferase activity as a read-out (Figure 38); however, direct measurement of steady-state luciferase protein levels revealed no indication of significant change in AR activity among conditions (Figure 39). This could mean that 155-Q27 and NLS155-Q27 affect luciferase folding/activity levels through an indirect mechanism unresolved by our studies. Taken together, our results provide the first evidence that polyglutamine-expanded N-terminal fragments, especially those that form soluble oligomers, substantially inactivate full-length polyglutamine-expanded AR, likely giving rise to AIS symptoms in SBMA.

It seems less likely that the observed decrease in transactivation capacity can be attributed to the possible recruitment of full-length AR into aggregates, as proposed (Butler *et al.*, 1998; Stenoien *et al.*, 1999) and observed in our study (Figure 37). As mentioned before, sequestration does not seem to be very efficient and 155-Q102 formed far less aggregates than for instance, 155-Q27 or 155-Q65, however it exerted the most prominent effect on AR transactivation capacity (Figure 38). The impact of the NLS tagged fragments on AR transactivation capacity was more prominent comparing to the untagged fragments (Figure 38).

Clinical data supports the proposed effect of polyglutamine-expanded N-terminal fragments on full-length AR in these studies. For instance, it was observed that impaired spermatogenesis becomes discernible late in adulthood in SBMA patients (Dejager *et al.*, 2002). AR is highly expressed in testis (Li *et al.*, 1998b) and was shown to be indispensable for spermatogenesis (De Gendt *et al.*,

2004; Eacker *et al.*, 2007). In SBMA patients, aggregates composed of N-terminal AR fragments were detected not only in neural tissue but also in testis (Adachi *et al.*, 2005; Li *et al.*, 1998b). Thus, aggregating polyglutamine-expanded fragments of AR are present in testis, where they would be ideally positioned to negatively affect AR activity required for spermatogenesis. This mechanism would explain why both SBMA and infertility are usually diagnosed late in life when aggregating N-terminal fragments of polyglutamine-expanded AR have accumulated to toxic levels, and often after the patients have fathered at least one child (Dejager *et al.*, 2002).

Recent studies suggest that aggregation and toxicity of polyglutamine stretches within the pathological range are largely affected by its flanking sequences (Dehay and Bertolotti, 2006; Duennwald *et al.*, 2006b). As polyglutamine-expanded huntingtin exon 1 (httEx1-Q96 and NLShttEx1-Q96) showed a comparable impact on full-length AR with 102 Q (ARQ102) as polyglutamine-expanded N-terminal AR fragments (155-Q102 and NLS155-Q102), the inhibitory effect on AR transactivation capacity appear to be mainly driven by the polyglutamine stretch (Figure 38, Figure 39, Figure 42 and Figure 43). The startling implication of this result is that AR inactivation and associated AIS symptoms could also be an inherent aspect of Huntington's disease (HD). Several intriguing lines of evidence support this notion. Human huntingtin for instance, is highly expressed not only in neural tissue, but also in testis (Strong *et al.*, 1993; Van Raamsdonk *et al.*, 2007). Strikingly, males affected with HD are frequently sexually dysfunctional as well as have testicular abnormalities and in analogy to the AIS in SBMA the testicular phenotype in HD occurs later in life (Fedoroff *et al.*, 1994; Van Raamsdonk *et al.*, 2007). Furthermore, testicular atrophy resulting in infertility, in parallel with cognitive and motor deficits was shown in mouse models of HD that express a polyglutamine expanded exon-1 encoded fragment of huntingtin or, full-length polyglutamine-expanded huntingtin, respectively (Mangiarini *et al.*, 1996; Sathasivam *et al.*, 1999; Van Raamsdonk *et al.*, 2006; Van Raamsdonk *et al.*, 2005). This effect was not rescued upon over-expression of wild-type huntingtin (Mangiarini *et al.*, 1996; Sathasivam *et al.*, 1999; Van Raamsdonk *et al.*, 2006; Van Raamsdonk *et al.*, 2005).

The earlier proposed assumptions of decreased testosterone levels or loss of GnRH neurons in the hypothalamus resulting in sexual dysfunction and testicular atrophy could not be maintained (Papalexi *et al.*, 2005; Van Raamsdonk *et al.*, 2007). A novel explanation of these observations suggested by this study is that polyglutamine-expanded fragments of huntingtin inactivate AR in HD mouse models and patients. This would give rise to the observed testicular abnormalities, which in comparison to the AIS in SBMA are however far less frequently reported in the literature. This might be due to the fact that in SBMA, inactivation of AR follows a two step mechanism. Primarily, the expanded polyglutamine stretch confers the AR to be more prone to aggregation and to cleavage which reduces the amount of functional AR available (Kobayashi *et al.*, 1998; LaFevre-Bernt and Ellerby, 2003). According to the results of this study, the arising polyglutamine-expanded AR fragments inactivate full-length AR in a second step, which leads to an amplification of AR inactivation. In HD, the AR is solely susceptible to the second mechanism, inactivation by polyglutamine-expanded (huntingtin) fragments, because of its polyglutamine stretch in the normal range. Furthermore, the non-pathogenic length of the polyglutamine stretch in AR is between 9 and ~30 repeats (Chamberlain *et al.*, 1994; Sartor *et al.*, 1999) and co-aggregation has been shown to be less efficient as the polyglutamine stretch gets smaller (Figure 37, Figure 41; Schaffar *et al.*, 2004). Indeed, no significant decrease in transactivation capacity of AR containing 27 Q upon expression of polyglutamine-expanded huntingtin exon 1 was observed (data not shown).

Nevertheless, this study and others have shown that proteins with polyglutamine stretches in the non-pathogenic range are recruited into aggregates composed of polyglutamine-expanded huntingtin exon 1 and become inactivated by polyglutamine-expanded species (Figure 41; Cha, 2000; Sakahira *et al.*, 2002b; Schaffar *et al.*, 2004).

This study also addressed the mechanism of AR inactivation by N-terminal polyglutamine fragments. Toxic NLS155-Q102 fragments that caused the greatest AR dysfunction predominantly formed soluble oligomers (Figure 27, Figure 33 and Figure 38). Co-Immunoprecipitation analyses revealed AR

inactivation correlated with enhanced binding of NLS155-Q102 oligomers to full-length AR (Figure 40), suggesting that oligomers are likely the species directly involved in AR inactivation. It may be that small amounts of these oligomers are also present in the 155-Q65 and NLS155-Q65 conditions and cause the mild decrease in AR activity (Figure 38). Such a mild reduction in AR activity could indeed lead to AIS in SBMA patients, especially considering disease duration may span several decades.

This study and others showed that aggregating polyglutamine-expanded fragments have the capacity to induce misfolding of full-length disease proteins (Figure 37; Haacke *et al.*, 2006). Therefore, it is likely that oligomers that bind to full-length AR cause dysfunction by detrimentally altering its conformation although it is possible that other species, such as soluble monomers and detergent insoluble aggregates, also participate to some degree in inactivation of AR.

In summary, data derived from this yeast model system suggests dual mechanisms of cytotoxicity in SBMA. The polyglutamine-expansion mutation in AR promotes a gain-of-function mechanism that results in the formation of toxic oligomers, which in turn cause loss-of-function through direct interaction with full-length AR. Future studies exploiting this yeast model may enrich our understanding of SBMA and associated AIS through the identification of factors that modulate toxic oligomer formation and specifically protect AR from polyglutamine-mediated inactivation.

5.3 Perspective

This study suggests soluble polyglutamine species, and not detergent insoluble fibrils, are the primary toxic agent in polyglutamine diseases. Additionally, this work provides evidence for common structural mechanisms of aggregation in prion and polyglutamine diseases. This leads to the assumption that the toxic species and molecular mechanisms mediating cytotoxicity may be shared among many, if not most, amyloidoses.

Future studies will focus on a further characterization of the toxic species and how they mediate cytotoxicity. It still remains unclear if some form of soluble aggregate or even the misfolded monomer itself causes toxicity. Once identified, it will be only a matter of time until the molecular mechanisms mediating cytotoxicity are resolved. With regard to the common mechanisms underlying the amyloidoses more generally, it seems likely that progress on one disease will be transferable to others, which should accelerate the identification of the basic structural and pathogenic properties of toxic species.

Large scale screens to identify promising compounds should nevertheless continue despite the present lack in knowledge about the nature of the toxic species. Compounds that suppress polyglutamine-mediated cytotoxicity might serve as tools in the analysis of toxic species and toxicity mechanisms. Since so far no promising compound has been developed into an effective drug, the hunt for therapeutical agents is mandatory. It will be important to learn whether suppressing aggregation or enhancing aggregation will be the road to success.

6 References

- Abou-Sleymane, G., Chalmel, F., Helmlinger, D., Lardenois, A., Thibault, C., Weber, C., Merienne, K., Mandel, J.L., Poch, O., Devys, D. and Trottier, Y. (2006) Polyglutamine expansion causes neurodegeneration by altering the neuronal differentiation program. *Human Molecular Genetics*, **15**, 691-703.
- Adachi, H., Katsuno, M., Minamiyama, M., Waza, M., Sang, C., Nakagomi, Y., Kobayashi, Y., Tanaka, F., Doyu, M., Inukai, A., Yoshida, M., Hashizume, Y. and Sobue, G. (2005a) Widespread nuclear and cytoplasmic accumulation of mutant androgen receptor in SBMA patients. *Brain*, **128**, 659-670.
- Adachi, H., Waza, M., Katsuno, M., Tanaka, F., Doyu, M. and Sobue, G. (2007) Pathogenesis and molecular targeted therapy of spinal and bulbar muscular atrophy. *Neuropathol Appl Neurobiol*, **33**, 135-151.
- Aguzzi, A. and Haass, C. (2003) Games played by rogue proteins in prion disorders and Alzheimer's disease. *Science*, **302**, 814-818.
- Alberti, S., Esser, C. and Hohfeld, J. (2003) BAG-1--a nucleotide exchange factor of Hsc70 with multiple cellular functions. *Cell Stress Chaperones*, **8**, 225-231.
- Alexandrescu, A.T. (2005) Amyloid accomplices and enforcers. *Protein Science*, **14**, 1-12.
- Anderson, K.D., Panayotatos, N., Corcoran, T.L., Lindsay, R.M. and Wiegand, S.J. (1996) Ciliary neurotrophic factor protects striatal output neurons in an animal model of Huntington disease. *Proc Natl Acad Sci U S A*, **93**, 7346-7351.
- Anfinsen, C.B. (1973) Principles that govern the folding of protein chains. *Science*, **181**, 223-230.
- Arrasate, M., Mitra, S., Schweitzer, E.S., Segal, M.R. and Finkbeiner, S. (2004) Inclusion body formation reduces levels of mutant huntingtin and the risk of neuronal death. *Nature*, **431**, 805-810.
- Bachoud-Levi, A.C., Maison, P., Bartolomeo, P., Boisse, M.F., Dalla Barba, G., Ergis, A.M., Baudic, S., Degos, J.D., Cesaro, P. and Peschanski, M. (2001) Retest effects and cognitive decline in longitudinal follow-up of patients with early HD. *Neurology*, **56**, 1052-1058.
- Barral, J.M., Broadley, S.A., Schaffar, G. and Hartl, F.U. (2004) Roles of molecular chaperones in protein misfolding diseases. *Seminars in Cell & Developmental Biology*, **15**, 17-29.
- Bates, G. (2000) Huntington's disease. In reverse gear. *Nature*, **404**, 944-945.
- Bates, G. (2003) Huntingtin aggregation and toxicity in Huntington's disease. *Lancet*, **361**, 1642-1644.
- Bauer, H.H., Aebi, U., Haner, M., Hermann, R., Muller, M. and Merkle, H.P. (1995) Architecture and polymorphism of fibrillar supramolecular assemblies produced by in vitro aggregation of human calcitonin. *Journal of Structural Biology*, **115**, 1-15.
- Becher, M.W., Kotzok, J.A., Sharp, A.H., Davies, S.W., Bates, G.P., Price, D.L. and Ross, C.A. (1998) Intranuclear neuronal inclusions in Huntington's disease and dentatorubral and pallidolusian atrophy: correlation between the density of inclusions and IT15 CAG triplet repeat length. *Neurobiol Dis*, **4**, 387-397.

- Behrends, C., Langer, C.A., Boteva, R., Bottcher, U.M., Stemp, M.J., Schaffar, G., Rao, B.V., Giese, A., Kretschmar, H., Siegers, K. and Hartl, F.U. (2006) Chaperonin TRiC promotes the assembly of polyQ expansion proteins into nontoxic oligomers. *Molecular Cell*, **23**, 887-897.
- Bence, N.F., Sampat, R.M. and Kopito, R.R. (2001) Impairment of the ubiquitin-proteasome system by protein aggregation.[see comment]. *Science*, **292**, 1552-1555.
- Bennett, E.J., Bence, N.F., Jayakumar, R. and Kopito, R.R. (2005) Global impairment of the ubiquitin-proteasome system by nuclear or cytoplasmic protein aggregates precedes inclusion body formation. *Molecular Cell*, **17**, 351-365.
- Bennett, E.J., Shaler, T.A., Woodman, B., Ryu, K.Y., Zaitseva, T.S., Becker, C.H., Bates, G.P., Schulman, H. and Kopito, R.R. (2007) Global changes to the ubiquitin system in Huntington's disease. *Nature*, **448**, 704-708.
- Ben-Zvi, A.P. and Goloubinoff, P. (2001) Review: mechanisms of disaggregation and refolding of stable protein aggregates by molecular chaperones. *Journal of Structural Biology*, **135**, 84-93.
- Bertsch, U., Winklhofer, K.F., Hirschberger, T., Bieschke, J., Weber, P., Hartl, F.U., Tavan, P., Tatzelt, J., Kretschmar, H.A. and Giese, A. (2005) Systematic Identification of Antiprion Drugs by High-Throughput Screening Based on Scanning for Intensely Fluorescent Targets. *J. Virol.*, **79**, 7785-7791.
- Bezprozvany, I. and Hayden, M.R. (2004) Deranged neuronal calcium signaling and Huntington disease. *Biochem Biophys Res Commun*, **322**, 1310-1317.
- Blader, P. and Strahle, U. (1998) Casting an eye over cyclopa. *Nature*, **395**, 112-113.
- Boado, R.J., Kazantsev, A., Apostol, B.L., Thompson, L.M. and Pardridge, W.M. (2000) Antisense-mediated down-regulation of the human huntingtin gene. *J Pharmacol Exp Ther*, **295**, 239-243.
- Bodner, R.A., Outeiro, T.F., Altmann, S., Maxwell, M.M., Cho, S.H., Hyman, B.T., McLean, P.J., Young, A.B., Housman, D.E. and Kazantsev, A.G. (2006) Pharmacological promotion of inclusion formation: A therapeutic approach for Huntington's and Parkinson's diseases. *Proceedings of the National Academy of Sciences of the United States of America*, **103**, 4246-4251.
- Bonelli, R.M. and Hofmann, P. (2007) A systematic review of the treatment studies in Huntington's disease since 1990. *Expert Opin Pharmacother*, **8**, 141-153.
- Boorstein, W.R. and Craig, E.A. (1990) Transcriptional regulation of SSA3, an HSP70 gene from *Saccharomyces cerevisiae*. *Molecular & Cellular Biology*, **10**, 3262-3267.
- Borrell-Pages, M., Zala, D., Humbert, S. and Saudou, F. (2006) Huntington's disease: from huntingtin function and dysfunction to therapeutic strategies. *Cell Mol Life Sci*, **63**, 2642-2660.
- Brinkmann, A.O. (2001) Molecular basis of androgen insensitivity. *Molecular & Cellular Endocrinology*, **179**, 105-109.
- Brinkmann, A.O., Faber, P.W., van Rooij, H.C., Kuiper, G.G., Ris, C., Klaassen, P., van der Korput, J.A., Voorhorst, M.M., van Laar, J.H., Mulder, E. and *et al.* (1989) The human

- androgen receptor: domain structure, genomic organization and regulation of expression. *J Steroid Biochem*, **34**, 307-310.
- Brooks, B.P. and Fischbeck, K.H. (1995) Spinal and bulbar muscular atrophy - a trinucleotide-repeat expansion neurodegenerative disease. *Trends in Neurosciences*, **18**, 459-461.
- Brooks, B.P., Paulson, H.L., Merry, D.E., Salazar-Grueso, E.F., Brinkmann, A.O., Wilson, E.M. and Fischbeck, K.H. (1997) Characterization of an expanded glutamine repeat androgen receptor in a neuronal cell culture system. *Neurobiology of Disease*, **3**, 313-323.
- Broome, B.M. and Hecht, M.H. (2000) Nature disfavors sequences of alternating polar and non-polar amino acids: implications for amyloidogenesis. *Journal of Molecular Biology*, **296**, 961-968.
- Bucciantini, M., Giannoni, E., Chiti, F., Baroni, F., Formigli, L., Zurdo, J., Taddei, N., Ramponi, G., Dobson, C.M. and Stefani, M. (2002) Inherent toxicity of aggregates implies a common mechanism for protein misfolding diseases.[see comment]. *Nature*, **416**, 507-511.
- Buchanan, G., Yang, M., Cheong, A., Harris, J.M., Irvine, R.A., Lambert, P.F., Moore, N.L., Raynor, M., Neufing, P.J., Coetzee, G.A. and Tilley, W.D. (2004) Structural and functional consequences of glutamine tract variation in the androgen receptor. *Human Molecular Genetics*, **13**, 1677-1692.
- Butler, R., Leigh, P.N., McPhaul, M.J. and Gallo, J.M. (1998) Truncated forms of the androgen receptor are associated with polyglutamine expansion in X-linked spinal and bulbar muscular atrophy. *Human Molecular Genetics*, **7**, 121-127.
- Canet, D., Last, A.M., Tito, P., Sunde, M., Spencer, A., Archer, D.B., Redfield, C., Robinson, C.V. and Dobson, C.M. (2002) Local cooperativity in the unfolding of an amyloidogenic variant of human lysozyme. *Nature Structural Biology*, **9**, 308-315.
- Caplan, A.J. and Douglas, M.G. (1991) Characterization of YDJ1: a yeast homologue of the bacterial dnaJ protein. *J Cell Biol*, **114**, 609-621.
- Cattaneo, E. (2003) Dysfunction of wild-type huntingtin in Huntington disease. *News Physiol Sci*, **18**, 34-37.
- Cattaneo, E., Rigamonti, D., Goffredo, D., Zuccato, C., Squitieri, F. and Sipione, S. (2001) Loss of normal huntingtin function: new developments in Huntington's disease research. *Trends Neurosci*, **24**, 182-188.
- Ceraline, J., Erdmann, E., Erbs, P., Deslandres-Cruchant, M., Jacqmin, D., Duclos, B., Klein-Soyer, C., Dufour, P. and Bergerat, J.P. (2003) A yeast-based functional assay for the detection of the mutant androgen receptor in prostate cancer. *European Journal of Endocrinology*, **148**, 99-110.
- Cha, J.H. (2000) Transcriptional dysregulation in Huntington's disease. *Trends in Neurosciences*, **23**, 387-392.
- Chai, Y., Shao, J., Miller, V.M., Williams, A. and Paulson, H.L. (2002) Live-cell imaging reveals divergent intracellular dynamics of polyglutamine disease proteins and supports a sequestration model of pathogenesis. *Proceedings of the National Academy of Sciences of the United States of America*, **99**, 9310-9315.

- Chamberlain, N.L., Driver, E.D. and Miesfeld, R.L. (1994) The length and location of CAG trinucleotide repeats in the androgen receptor N-terminal domain affect transactivation function. *Nucleic Acids Research*, **22**, 3181-3186.
- Charrin, B.C., Saudou, F. and Humbert, S. (2005) Axonal transport failure in neurodegenerative disorders: the case of Huntington's disease. *Pathol Biol (Paris)*, **53**, 189-192.
- Chernoff, Y.O., Lindquist, S.L., Ono, B., Inge-Vechtomov, S.G. and Liebman, S.W. (1995) Role of the chaperone protein Hsp104 in propagation of the yeast prion-like factor [psi+]. *Science*, **268**, 880-884.
- Chiti, F., Calamai, M., Taddei, N., Stefani, M., Ramponi, G. and Dobson, C.M. (2002a) Studies of the aggregation of mutant proteins in vitro provide insights into the genetics of amyloid diseases. *Proceedings of the National Academy of Sciences of the United States of America*, **99 Suppl 4**, 16419-16426.
- Chiti, F. and Dobson, C.M. (2006) Protein misfolding, functional amyloid, and human disease. *Annual Review of Biochemistry*, **75**, 333-366.
- Chiti, F., Stefani, M., Taddei, N., Ramponi, G. and Dobson, C.M. (2003) Rationalization of the effects of mutations on peptide and protein aggregation rates. *Nature*, **424**, 805-808.
- Chiti, F., Taddei, N., Baroni, F., Capanni, C., Stefani, M., Ramponi, G. and Dobson, C.M. (2002b) Kinetic partitioning of protein folding and aggregation. *Nature Structural Biology*, **9**, 137-143.
- Choong, C.S., Kempainen, J.A., Zhou, Z.X. and Wilson, E.M. (1996) Reduced androgen receptor gene expression with first exon CAG repeat expansion. *Molecular Endocrinology*, **10**, 1527-1535.
- Chow, M.K., Ellisdon, A.M., Cabrita, L.D. and Bottomley, S.P. (2004) Polyglutamine expansion in ataxin-3 does not affect protein stability: implications for misfolding and disease. *Journal of Biological Chemistry*, **279**, 47643-47651.
- Ciechanover, A. and Brundin, P. (2003) The ubiquitin proteasome system in neurodegenerative diseases: sometimes the chicken, sometimes the egg. *Neuron*, **40**, 427-446.
- Cleary, J.P., Walsh, D.M., Hofmeister, J.J., Shankar, G.M., Kuskowski, M.A., Selkoe, D.J. and Ashe, K.H. (2005) Natural oligomers of the amyloid-beta protein specifically disrupt cognitive function. *Nat Neurosci*, **8**, 79-84.
- Colby, D.W., Chu, Y., Cassady, J.P., Duennwald, M., Zazulak, H., Webster, J.M., Messer, A., Lindquist, S., Ingram, V.M. and Wittrup, K.D. (2004) Potent inhibition of huntingtin aggregation and cytotoxicity by a disulfide bond-free single-domain intracellular antibody. *Proc Natl Acad Sci U S A*, **101**, 17616-17621.
- Conway, K.A., Harper, J.D. and Lansbury, P.T., Jr. (2000) Fibrils formed in vitro from alpha-synuclein and two mutant forms linked to Parkinson's disease are typical amyloid. *Biochemistry*, **39**, 2552-2563.
- Cowan, C.M. and Raymond, L.A. (2006) Selective neuronal degeneration in Huntington's disease. *Current Topics In Developmental Biology*, **75**, 25-71.
- Cowan, K.J., Diamond, M.I. and Welch, W.J. (2003) Polyglutamine protein aggregation and toxicity are linked to the cellular stress response. *Human Molecular Genetics*, **12**, 1377-1391.

- Craufurd, D., Thompson, J.C. and Snowden, J.S. (2001) Behavioral changes in Huntington Disease. *Neuropsychiatry Neuropsychol Behav Neurol*, **14**, 219-226.
- Creighton, T.E. (1990) Protein folding. *Biochemical Journal*, **270**, 1-16.
- Creton, R. (2004) The calcium pump of the endoplasmic reticulum plays a role in midline signaling during early zebrafish development. *Brain Res Dev Brain Res*, **151**, 33-41.
- Cummings, C.J., Mancini, M.A., Antalffy, B., DeFranco, D.B., Orr, H.T. and Zoghbi, H.Y. (1998) Chaperone suppression of aggregation and altered subcellular proteasome localization imply protein misfolding in SCA1. *Nat Genet*, **19**, 148-154.
- Daggett, V. and Fersht, A.R. (2003) Is there a unifying mechanism for protein folding? *Trends in Biochemical Sciences*, **28**, 18-25.
- Danek, A., Witt, T.N., Mann, K., Schweikert, H.U., Romalo, G., La Spada, A.R. and Fischbeck, K.H. (1994) Decrease in androgen binding and effect of androgen treatment in a case of X-linked bulbospinal neuronopathy. *Clinical Investigator*, **72**, 892-897.
- Davies, S.W., Turmaine, M., Cozens, B.A., DiFiglia, M., Sharp, A.H., Ross, C.A., Scherzinger, E., Wanker, E.E., Mangiarini, L. and Bates, G.P. (1997) Formation of neuronal intranuclear inclusions underlies the neurological dysfunction in mice transgenic for the HD mutation. *Cell*, **90**, 537-548.
- Davies, T.H., Ning, Y.M. and Sanchez, E.R. (2002) A new first step in activation of steroid receptors: hormone-induced switching of FKBP51 and FKBP52 immunophilins. *J Biol Chem*, **277**, 4597-4600.
- de Almeida, L.P., Ross, C.A., Zala, D., Aebischer, P. and Deglon, N. (2002) Lentiviral-mediated delivery of mutant huntingtin in the striatum of rats induces a selective neuropathology modulated by polyglutamine repeat size, huntingtin expression levels, and protein length. *J Neurosci*, **22**, 3473-3483.
- De Gendt, K., Swinnen, J.V., Saunders, P.T., Schoonjans, L., Dewerchin, M., Devos, A., Tan, K., Atanassova, N., Claessens, F., Lecureuil, C., Heyns, W., Carmeliet, P., Guillou, F., Sharpe, R.M. and Verhoeven, G. (2004) A Sertoli cell-selective knockout of the androgen receptor causes spermatogenic arrest in meiosis. *Proc Natl Acad Sci U S A*, **101**, 1327-1332.
- Dehay, B. and Bertolotti, A. (2006) Critical role of the proline-rich region in Huntingtin for aggregation and cytotoxicity in yeast. *Journal of Biological Chemistry*, **281**, 35608-35615.
- Dejager, S., Bry-Gauillard, H., Bruckert, E., Eymard, B., Salachas, F., LeGuern, E., Tardieu, S., Chadarevian, R., Giral, P. and Turpin, G. (2002) A comprehensive endocrine description of Kennedy's disease revealing androgen insensitivity linked to CAG repeat length. *Journal of Clinical Endocrinology & Metabolism*, **87**, 3893-3901.
- Di Prospero, N.A. and Fischbeck, K.H. (2005) Therapeutics development for triplet repeat expansion diseases. *Nat Rev Genet.*, **6**, 756-765.
- Difiglia, M., Sapp, E., Chase, K., Schwarz, C., Meloni, A., Young, C., Martin, E., Vonsattel, J.P., Carraway, R., Reeves, S.A., Boyce, F.M. and Aronin, N. (1995) Huntingtin is a cytoplasmic protein associated with vesicles in human and rat brain neurons. *Neuron*, **14**, 1075-1081.

- DiFiglia, M., Sapp, E., Chase, K.O., Davies, S.W., Bates, G.P., Vonsattel, J.P. and Aronin, N. (1997) Aggregation of huntingtin in neuronal intranuclear inclusions and dystrophic neurites in brain. *Science*, **277**, 1990-1993.
- Dobson, C.M. (1999) Protein misfolding, evolution and disease. *Trends in Biochemical Sciences*, **24**, 329-332.
- Dobson, C.M. (2003) Protein folding and misfolding. *Nature*, **426**, 884-890.
- Dragatsis, I., Levine, M.S. and Zeitlin, S. (2000) Inactivation of Hdh in the brain and testis results in progressive neurodegeneration and sterility in mice. *Nat Genet*, **26**, 300-306.
- Drubin, D. (1989) The yeast *Saccharomyces cerevisiae* as a model organism for the cytoskeleton and cell biology. *Cell Motil Cytoskeleton*, **14**, 42-49.
- Duennwald, M.L., Jagadish, S., Muchowski, P.J. and Lindquist, S. (2006a) Flanking sequences profoundly alter polyglutamine toxicity in yeast. *Proceedings of the National Academy of Sciences of the United States of America*, **103**, 11045-11050.
- Duennwald, M.L., Jagadish, S., Muchowski, P.J. and Lindquist, S. (2006b) Flanking sequences profoundly alter polyglutamine toxicity in yeast. *Proceedings of the National Academy of Sciences of the United States of America*, **103**, 11045-11050.
- Eacker, S.M., Shima, J.E., Connolly, C.M., Sharma, M., Holdcraft, R.W., Griswold, M.D. and Braun, R.E. (2007) Transcriptional profiling of androgen receptor (AR) mutants suggests instructive and permissive roles of AR signaling in germ cell development. *Mol Endocrinol*, **21**, 895-907.
- Ecker, D.J., Khan, M.I., Marsh, J., Butt, T.R. and Crooke, S.T. (1987) Chemical synthesis and expression of a cassette adapted ubiquitin gene. *J Biol Chem*, **262**, 3524-3527.
- Ellerby, L.M., Hackam, A.S., Propp, S.S., Ellerby, H.M., Rabizadeh, S., Cashman, N.R., Trifiro, M.A., Pinsky, L., Wellington, C.L., Salvesen, G.S., Hayden, M.R. and Bredesen, D.E. (1999) Kennedy's disease: caspase cleavage of the androgen receptor is a crucial event in cytotoxicity. *Journal of Neurochemistry*, **72**, 185-195.
- Ellis, R.J. (2001) Macromolecular crowding: obvious but underappreciated. *Trends in Biochemical Sciences*, **26**, 597-604.
- Ellis, R.J. and Hartl, F.U. (1996) Protein folding in the cell: competing models of chaperonin function. *FASEB Journal*, **10**, 20-26.
- Evans, T.G., Yamamoto, Y., Jeffery, W.R. and Krone, P.H. (2005) Zebrafish Hsp70 is required for embryonic lens formation. *Cell Stress Chaperones*, **10**, 66-78.
- Faber, P.W., Kuiper, G.G., van Rooij, H.C., van der Korput, J.A., Brinkmann, A.O. and Trapman, J. (1989) The N-terminal domain of the human androgen receptor is encoded by one, large exon. *Mol Cell Endocrinol*, **61**, 257-262.
- Fan, C.Y., Ren, H.Y., Lee, P., Caplan, A.J. and Cyr, D.M. (2005) The type I Hsp40 zinc finger-like region is required for Hsp70 to capture non-native polypeptides from Ydj1. *J Biol Chem*, **280**, 695-702.
- Fandrich, M. and Dobson, C.M. (2002) The behaviour of polyamino acids reveals an inverse side chain effect in amyloid structure formation. *EMBO Journal*, **21**, 5682-5690.

- Faux, N.G., Bottomley, S.P., Lesk, A.M., Irving, J.A., Morrison, J.R., de la Banda, M.G. and Whisstock, J.C. (2005) Functional insights from the distribution and role of homopeptide repeat-containing proteins. *Genome Research*, **15**, 537-551.
- Fedoroff, J.P., Peyser, C., Franz, M.L. and Folstein, S.E. (1994) Sexual disorders in Huntington's disease. *J Neuropsychiatry Clin Neurosci*, **6**, 147-153.
- Ferrao-Gonzales, A.D., Souto, S.O., Silva, J.L. and Foguel, D. (2000) The preaggregated state of an amyloidogenic protein: hydrostatic pressure converts native transthyretin into the amyloidogenic state. *Proceedings of the National Academy of Sciences of the United States of America*, **97**, 6445-6450.
- Fersht, A.R. (2000) Transition-state structure as a unifying basis in protein-folding mechanisms: contact order, chain topology, stability, and the extended nucleus mechanism. *Proceedings of the National Academy of Sciences of the United States of America*, **97**, 1525-1529.
- Folstein, S.E., Leigh, R.J., Parhad, I.M. and Folstein, M.F. (1986) The diagnosis of Huntington's disease. *Neurology*, **36**, 1279-1283.
- Freeman, B.C., Felts, S.J., Toft, D.O. and Yamamoto, K.R. (2000) The p23 molecular chaperones act at a late step in intracellular receptor action to differentially affect ligand efficacies. *Genes Dev*, **14**, 422-434.
- Freeman, B.C. and Yamamoto, K.R. (2001) Continuous recycling: a mechanism for modulatory signal transduction. *Trends Biochem Sci*, **26**, 285-290.
- Froesch, B.A., Takayama, S. and Reed, J.C. (1998) BAG-1L protein enhances androgen receptor function. *J Biol Chem*, **273**, 11660-11666.
- Frydman, J. and Hartl, F.U. (1996) Principles of chaperone-assisted protein folding: differences between in vitro and in vivo mechanisms.[see comment]. *Science*, **272**, 1497-1502.
- Frydman, J. and Hohfeld, J. (1997) Chaperones get in touch: the Hip-Hop connection. *Trends Biochem Sci*, **22**, 87-92.
- Fusco, F.R., Chen, Q., Lamoreaux, W.J., Figueredo-Cardenas, G., Jiao, Y., Coffman, J.A., Surmeier, D.J., Honig, M.G., Carlock, L.R. and Reiner, A. (1999) Cellular localization of huntingtin in striatal and cortical neurons in rats: lack of correlation with neuronal vulnerability in Huntington's disease. *J Neurosci*, **19**, 1189-1202.
- Gari, E., Piedrafita, L., Aldea, M. and Herrero, E. (1997) A set of vectors with a tetracycline-regulatable promoter system for modulated gene expression in *Saccharomyces cerevisiae*. *Yeast*, **13**, 837-848.
- Gatchel, J.R. and Zoghbi, H.Y. (2005) Diseases of unstable repeat expansion: mechanisms and common principles. *Nature Reviews Genetics*, **6**, 743-755.
- Gauthier, L.R., Charrin, B.C., Borrell-Pages, M., Dompierre, J.P., Rangone, H., Cordelieres, F.P., De Mey, J., MacDonald, M.E., Lessmann, V., Humbert, S. and Saudou, F. (2004) Huntingtin controls neurotrophic support and survival of neurons by enhancing BDNF vesicular transport along microtubules. *Cell*, **118**, 127-138.
- Geissler, S., Siegers, K. and Schiebel, E. (1998) A novel protein complex promoting formation of functional alpha- and gamma-tubulin. *EMBO Journal*, **17**, 952-966.

- Gelmann, E.P. (2002) Molecular biology of the androgen receptor. *Journal of Clinical Oncology*, **20**, 3001-3015.
- Georget, V., Terouanne, B., Nicolas, J.C. and Sultan, C. (2002) Mechanism of antiandrogen action: key role of hsp90 in conformational change and transcriptional activity of the androgen receptor. *Biochemistry*, **41**, 11824-11831.
- Gerber, H.P., Seipel, K., Georgiev, O., Hofferer, M., Hug, M., Rusconi, S. and Schaffner, W. (1994) Transcriptional activation modulated by homopolymeric glutamine and proline stretches. *Science*, **263**, 808-811.
- Gervais, F.G., Singaraja, R., Xanthoudakis, S., Gutekunst, C.A., Leavitt, B.R., Metzler, M., Hackam, A.S., Tam, J., Vaillancourt, J.P., Houtzager, V., Rasper, D.M., Roy, S., Hayden, M.R. and Nicholson, D.W. (2002) Recruitment and activation of caspase-8 by the Huntingtin-interacting protein Hip-1 and a novel partner Hip1. *Nat Cell Biol*, **4**, 95-105.
- Goldberg, A.L. (2003) Protein degradation and protection against misfolded or damaged proteins. *Nature*, **426**, 895-899.
- Gonzalez-Alegre, P. (2007) Therapeutic RNA interference for neurodegenerative diseases: From promise to progress. *Pharmacol Ther*, **114**, 34-55.
- Govaerts, C., Wille, H., Prusiner, S.B. and Cohen, F.E. (2004) Evidence for assembly of prions with left-handed beta-helices into trimers. *Proc Natl Acad Sci U S A*, **101**, 8342-8347.
- Graham, R.K., Deng, Y., Slow, E.J., Haigh, B., Bissada, N., Lu, G., Pearson, J., Shehadeh, J., Bertram, L., Murphy, Z., Warby, S.C., Doty, C.N., Roy, S., Wellington, C.L., Leavitt, B.R., Raymond, L.A., Nicholson, D.W. and Hayden, M.R. (2006) Cleavage at the caspase-6 site is required for neuronal dysfunction and degeneration due to mutant huntingtin. *Cell*, **125**, 1179-1191.
- Greer, L.F., 3rd and Szalay, A.A. (2002) Imaging of light emission from the expression of luciferases in living cells and organisms: a review. *Luminescence*, **17**, 43-74.
- Guarente, L. (1983) Yeast promoters and lacZ fusions designed to study expression of cloned genes in yeast. *Methods in Enzymology*, **101**, 181-191.
- Guijarro, J.I., Sunde, M., Jones, J.A., Campbell, I.D. and Dobson, C.M. (1998) Amyloid fibril formation by an SH3 domain. *Proceedings of the National Academy of Sciences of the United States of America*, **95**, 4224-4228.
- Guo, J., Zhu, P., Wu, C., Yu, L., Zhao, S. and Gu, X. (2003) In silico analysis indicates a similar gene expression pattern between human brain and testis. *Cytogenet Genome Res*, **103**, 58-62.
- Gutekunst, C.A., Levey, A.I., Heilman, C.J., Whaley, W.L., Yi, H., Nash, N.R., Rees, H.D., Madden, J.J. and Hersch, S.M. (1995) Identification and localization of huntingtin in brain and human lymphoblastoid cell lines with anti-fusion protein antibodies. *Proceedings of the National Academy of Sciences of the United States of America*, **92**, 8710-8714.
- Haacke, A., Broadley, S.A., Boteva, R., Tzvetkov, N., Hartl, F.U. and Breuer, P. (2006) Proteolytic cleavage of polyglutamine-expanded ataxin-3 is critical for aggregation and sequestration of non-expanded ataxin-3. *Human Molecular Genetics*, **15**, 555-568.

- Hackam, A.S., Yassa, A.S., Singaraja, R., Metzler, M., Gutekunst, C.A., Gan, L., Warby, S., Wellington, C.L., Vaillancourt, J., Chen, N., Gervais, F.G., Raymond, L., Nicholson, D.W. and Hayden, M.R. (2000) Huntingtin interacting protein 1 induces apoptosis via a novel caspase-dependent death effector domain. *J Biol Chem*, **275**, 41299-41308.
- Haque, N. and Isacson, O. (1997) Antisense gene therapy for neurodegenerative disease? *Exp Neurol*, **144**, 139-146.
- Haque, N.S., Borghesani, P. and Isacson, O. (1997) Therapeutic strategies for Huntington's disease based on a molecular understanding of the disorder. *Mol Med Today*, **3**, 175-183.
- Hardy, J. and Orr, H. (2006) The genetics of neurodegenerative diseases. *Journal of Neurochemistry*, **97**, 1690-1699.
- Harjes, P. and Wanker, E.E. (2003) The hunt for huntingtin function: interaction partners tell many different stories. *Trends Biochem Sci*, **28**, 425-433.
- Harper, J.D., Lieber, C.M. and Lansbury, P.T., Jr. (1997a) Atomic force microscopic imaging of seeded fibril formation and fibril branching by the Alzheimer's disease amyloid-beta protein. *Chemistry & Biology*, **4**, 951-959.
- Harper, J.D., Wong, S.S., Lieber, C.M. and Lansbury, P.T. (1997b) Observation of metastable A β amyloid protofibrils by atomic force microscopy. *Chemistry & Biology*, **4**, 119-125.
- Hartl, F.U. and Hayer-Hartl, M. (2002) Molecular chaperones in the cytosol: from nascent chain to folded protein. *Science*, **295**, 1852-1858.
- Hasholt, L., Abell, K., Norremolle, A., Nellemann, C., Fenger, K. and Sorensen, S.A. (2003) Antisense downregulation of mutant huntingtin in a cell model. *J Gene Med*, **5**, 528-538.
- Hazeki, N., Tukamoto, T., Goto, J. and Kanazawa, I. (2000) Formic acid dissolves aggregates of an N-terminal huntingtin fragment containing an expanded polyglutamine tract: applying to quantification of protein components of the aggregates. *Biochem Biophys Res Commun*, **277**, 386-393.
- He, B., Bai, S., Hnat, A.T., Kalman, R.I., Minges, J.T., Patterson, C. and Wilson, E.M. (2004) An androgen receptor NH₂-terminal conserved motif interacts with the COOH terminus of the Hsp70-interacting protein (CHIP). *J Biol Chem*, **279**, 30643-30653.
- Heiser, V., Engemann, S., Brocker, W., Dunkel, I., Boeddrich, A., Waelter, S., Nordhoff, E., Lurz, R., Schugardt, N., Rautenberg, S., Herhaus, C., Barnickel, G., Bottcher, H., Lehrach, H. and Wanker, E.E. (2002) Identification of benzothiazoles as potential polyglutamine aggregation inhibitors of Huntington's disease by using an automated filter retardation assay. *Proc Natl Acad Sci U S A.*, **99**, 16400-16406.
- Hersch, S.M. and Ferrante, R.J. (2004) Translating therapies for Huntington's disease from genetic animal models to clinical trials. *NeuroRx*, **1**, 298-306.
- Hershko, A. and Ciechanover, A. (1998) The ubiquitin system. *Annual Review of Biochemistry*, **67**, 425-479.
- Hirakura, Y., Azimov, R., Azimova, R. and Kagan, B.L. (2000) Polyglutamine-induced ion channels: a possible mechanism for the neurotoxicity of Huntington and other CAG repeat diseases. *J Neurosci Res*, **60**, 490-494.

- Hirschfield, G.M. and Hawkins, P.N. (2003) Amyloidosis: new strategies for treatment. *International Journal of Biochemistry & Cell Biology*, **35**, 1608-1613.
- Ho, L.W., Brown, R., Maxwell, M., Wyttenbach, A. and Rubinsztein, D.C. (2001) Wild type Huntingtin reduces the cellular toxicity of mutant Huntingtin in mammalian cell models of Huntington's disease. *J Med Genet*, **38**, 450-452.
- Hockly, E., Tse, J., Barker, A.L., Moolman, D.L., Beunard, J.L., Revington, A.P., Holt, K., Sunshine, S., Moffitt, H., Sathasivam, K., Woodman, B., Wanker, E.E., Lowden, P.A. and Bates, G.P. (2006) Evaluation of the benzothiazole aggregation inhibitors riluzole and PGL-135 as therapeutics for Huntington's disease. *Neurobiol Dis.*, **21**, 228-236.
- Hohfeld, J., Minami, Y. and Hartl, F.U. (1995) Hip, a novel cochaperone involved in the eukaryotic Hsc70/Hsp40 reaction cycle. *Cell*, **83**, 589-598.
- Hoogeveen, A.T., Willemsen, R., Meyer, N., Derooij, K.E., Roos, R.A.C., Vanommen, G.J.B. and Galjaard, H. (1993) Characterization and localization of the huntington disease gene product. *Human Molecular Genetics*, **2**, 2069-2073.
- Hsiao, P.W., Lin, D.L., Nakao, R. and Chang, C. (1999) The linkage of Kennedy's neuron disease to ARA24, the first identified androgen receptor polyglutamine region-associated coactivator. *Journal of Biological Chemistry*, **274**, 20229-20234.
- Irvine, R.A., Ma, H., Yu, M.C., Ross, R.K., Stallcup, M.R. and Coetzee, G.A. (2000) Inhibition of p160-mediated coactivation with increasing androgen receptor polyglutamine length. *Human Molecular Genetics*, **9**, 267-274.
- Jackson, G.R., Salecker, I., Dong, X., Yao, X., Arnheim, N., Faber, P.W., MacDonald, M.E. and Zipursky, S.L. (1998) Polyglutamine-expanded human huntingtin transgenes induce degeneration of Drosophila photoreceptor neurons. *Neuron*, **21**, 633-642.
- Jaenicke, R. (1991) Protein folding: local structures, domains, subunits, and assemblies. *Biochemistry*, **30**, 3147-3161.
- Jahn, T.R. and Radford, S.E. (2005) The Yin and Yang of protein folding. *FEBS Journal*, **272**, 5962-5970.
- Jakob, U. and Buchner, J. (1994) Assisting spontaneity: the role of Hsp90 and small Hsps as molecular chaperones. *Trends Biochem Sci*, **19**, 205-211.
- Janknecht, R. (2002) The versatile functions of the transcriptional coactivators p300 and CBP and their roles in disease. *Histol Histopathol*, **17**, 657-668.
- Jia, K., Hart, A.C. and Levine, B. (2007) Autophagy genes protect against disease caused by polyglutamine expansion proteins in *Caenorhabditis elegans*. *Autophagy*, **3**, 21-25.
- Johansen, K.L. (2004) Testosterone metabolism and replacement therapy in patients with end-stage renal disease. *Semin Dial*, **17**, 202-208.
- Kalchman, M.A., Koide, H.B., McCutcheon, K., Graham, R.K., Nichol, K., Nishiyama, K., Kazemi-Esfarjani, P., Lynn, F.C., Wellington, C., Metzler, M., Goldberg, Y.P., Kanazawa, I., Gietz, R.D. and Hayden, M.R. (1997) HIP1, a human homologue of *S. cerevisiae* Sla2p, interacts with membrane-associated huntingtin in the brain. *Nat Genet*, **16**, 44-53.

- Karlovich, C.A., John, R.M., Ramirez, L., Stainier, D.Y. and Myers, R.M. (1998) Characterization of the Huntington's disease (HD) gene homologue in the zebrafish *Danio rerio*. *Gene*, **217**, 117-125.
- Karplus, M. (1997) The Levinthal paradox: yesterday and today. *Folding & Design*, **2**, S69-75.
- Katsuno, M., Adachi, H., Tanaka, F. and Sobue, G. (2004) Spinal and bulbar muscular atrophy: ligand-dependent pathogenesis and therapeutic perspectives. *J Mol Med*, **82**, 298-307.
- Katsuno, M., Adachi, H., Waza, M., Banno, H., Suzuki, K., Tanaka, F., Doyu, M. and Sobue, G. (2006) Pathogenesis, animal models and therapeutics in spinal and bulbar muscular atrophy (SBMA). *Experimental Neurology*, **200**, 8-18.
- Kayed, R., Head, E., Thompson, J.L., McIntire, T.M., Milton, S.C., Cotman, C.W. and Glabe, C.G. (2003) Common structure of soluble amyloid oligomers implies common mechanism of pathogenesis.[see comment]. *Science*, **300**, 486-489.
- Kayed, R., Sokolov, Y., Edmonds, B., McIntire, T.M., Milton, S.C., Hall, J.E. and Glabe, C.G. (2004) Permeabilization of lipid bilayers is a common conformation-dependent activity of soluble amyloid oligomers in protein misfolding diseases. *Journal of Biological Chemistry*, **279**, 46363-46366.
- Kazemi-Esfarjani, P., Trifiro, M.A. and Pinsky, L. (1995) Evidence for a repressive function of the long polyglutamine tract in the human androgen receptor: possible pathogenetic relevance for the (CAG)_n-expanded neuronopathies. *Human Molecular Genetics*, **4**, 523-527.
- Kegel, K.B., Meloni, A.R., Yi, Y., Kim, Y.J., Doyle, E., Cuiffo, B.G., Sapp, E., Wang, Y., Qin, Z.H., Chen, J.D., Nevins, J.R., Aronin, N. and DiFiglia, M. (2002) Huntingtin is present in the nucleus, interacts with the transcriptional corepressor C-terminal binding protein, and represses transcription. *J Biol Chem*, **277**, 7466-7476.
- Kegel, K.B., Sapp, E., Yoder, J., Cuiffo, B., Sobin, L., Kim, Y.J., Qin, Z.H., Hayden, M.R., Aronin, N., Scott, D.L., Isenberg, F., Goldmann, W.H. and DiFiglia, M. (2005) Huntingtin associates with acidic phospholipids at the plasma membrane. *Journal of Biological Chemistry*, **280**, 36464-36473.
- Kelly, J.W. (1998) The alternative conformations of amyloidogenic proteins and their multi-step assembly pathways. *Current Opinion in Structural Biology*, **8**, 101-106.
- Kennedy, W.R., Alter, M. and Sung, J.H. (1968) Progressive proximal spinal and bulbar muscular atrophy of late onset. A sex-linked recessive trait. *Neurology*, **18**, 671-680.
- Kim, M., Lee, H.S., LaForet, G., McIntyre, C., Martin, E.J., Chang, P., Kim, T.W., Williams, M., Reddy, P.H., Tagle, D., Boyce, F.M., Won, L., Heller, A., Aronin, N. and DiFiglia, M. (1999) Mutant huntingtin expression in clonal striatal cells: dissociation of inclusion formation and neuronal survival by caspase inhibition. *J Neurosci*, **19**, 964-973.
- Kim, S., Nollen, E.A., Kitagawa, K., Bindokas, V.P. and Morimoto, R.I. (2002) Polyglutamine protein aggregates are dynamic. *Nature Cell Biology*, **4**, 826-831.
- Kimmel, C.B., Ballard, W.W., Kimmel, S.R., Ullmann, B. and Schilling, T.F. (1995) Stages of embryonic development of the zebrafish. *Dev Dyn*, **203**, 253-310.
- Kisselev, A.F., Akopian, T.N., Woo, K.M. and Goldberg, A.L. (1999) The sizes of peptides generated from protein by mammalian 26 and 20 S proteasomes. Implications for

- understanding the degradative mechanism and antigen presentation. *Journal of Biological Chemistry*, **274**, 3363-3371.
- Kitada, T., Asakawa, S., Hattori, N., Matsumine, H., Yamamura, Y., Minoshima, S., Yokochi, M., Mizuno, Y. and Shimizu, N. (1998) Mutations in the parkin gene cause autosomal recessive juvenile parkinsonism.[see comment]. *Nature*, **392**, 605-608.
- Kleizen, B. and Braakman, I. (2004) Protein folding and quality control in the endoplasmic reticulum.[erratum appears in *Curr Opin Cell Biol.* 2004 Oct;16(5):597]. *Current Opinion in Cell Biology*, **16**, 343-349.
- Kobayashi, Y., Kume, A., Li, M., Doyu, M., Hata, M., Ohtsuka, K. and Sobue, G. (2000) Chaperones Hsp70 and Hsp40 suppress aggregate formation and apoptosis in cultured neuronal cells expressing truncated androgen receptor protein with expanded polyglutamine tract. *J Biol Chem*, **275**, 8772-8778.
- Kobayashi, Y., Miwa, S., Merry, D.E., Kume, A., Mei, L., Doyu, M. and Sobue, G. (1998) Caspase-3 cleaves the expanded androgen receptor protein of spinal and bulbar muscular atrophy in a polyglutamine repeat length-dependent manner. *Biochemical & Biophysical Research Communications*, **252**, 145-150.
- Kopito, R.R. (2000) Aggresomes, inclusion bodies and protein aggregation. *Trends Cell Biol*, **10**, 524-530.
- Krobitsch, S. and Lindquist, S. (2000) Aggregation of huntingtin in yeast varies with the length of the polyglutamine expansion and the expression of chaperone proteins. *Proc Natl Acad Sci U S A*, **97**, 1589-1594.
- Kuemmerle, S., Gutekunst, C.A., Klein, A.M., Li, X.J., Li, S.H., Beal, M.F., Hersch, S.M. and Ferrante, R.J. (1999) Huntington aggregates may not predict neuronal death in Huntington's disease. *Ann Neurol*, **46**, 842-849.
- La Spada, A.R., Wilson, E.M., Lubahn, D.B., Harding, A.E. and Fischbeck, K.H. (1991) Androgen receptor gene mutations in X-linked spinal and bulbar muscular atrophy. *Nature*, **352**, 77-79.
- Laemmli, U.K. (1970) Cleavage of structural proteins during the assembly of the head of bacteriophage T4. *Nature*, **227**, 680-685.
- LaFevre-Bernt, M.A. and Ellerby, L.M. (2003) Kennedy's disease. Phosphorylation of the polyglutamine-expanded form of androgen receptor regulates its cleavage by caspase-3 and enhances cell death. *Journal of Biological Chemistry*, **278**, 34918-34924.
- Langer, T., Lu, C., Echols, H., Flanagan, J., Hayer, M.K. and Hartl, F.U. (1992) Successive action of DnaK, DnaJ and GroEL along the pathway of chaperone-mediated protein folding. *Nature*, **356**, 683-689.
- Larson, J., Lynch, G., Games, D. and Seubert, P. (1999) Alterations in synaptic transmission and long-term potentiation in hippocampal slices from young and aged PDAPP mice. *Brain Research*, **840**, 23-35.
- Leavitt, B.R., Guttman, J.A., Hodgson, J.G., Kimel, G.H., Singaraja, R., Vogl, A.W. and Hayden, M.R. (2001) Wild-type huntingtin reduces the cellular toxicity of mutant huntingtin in vivo. *Am J Hum Genet*, **68**, 313-324.

- Leavitt, B.R., van Raamsdonk, J.M., Shehadeh, J., Fernandes, H., Murphy, Z., Graham, R.K., Wellington, C.L., Raymond, L.A. and Hayden, M.R. (2006a) Wild-type huntingtin protects neurons from excitotoxicity. *Journal of Neurochemistry*, **96**, 1121-1129.
- Leavitt, B.R., van Raamsdonk, J.M., Shehadeh, J., Fernandes, H., Murphy, Z., Graham, R.K., Wellington, C.L., Raymond, L.A. and Hayden, M.R. (2006b) Wild-type huntingtin protects neurons from excitotoxicity. *J Neurochem*, **96**, 1121-1129.
- Lee, W.C., Yoshihara, M. and Littleton, J.T. (2004) Cytoplasmic aggregates trap polyglutamine-containing proteins and block axonal transport in a Drosophila model of Huntington's disease. *Proc Natl Acad Sci U S A*, **101**, 3224-3229.
- Levine, B. and Klionsky, D.J. (2004) Development by self-digestion: molecular mechanisms and biological functions of autophagy. *Developmental Cell*, **6**, 463-477.
- Levinthal, C. (1969) How to Fold Graciously. In DeBrunner, J.T.P. and Munck, E. (eds.), *Mossbauer Spectroscopy in Biological Systems: Proceedings of a meeting held at Allerton House*. University of Illinois Press, Monticello, Illinois, pp. 22-24.
- Li, M., Chevalier-Larsen, E.S., Merry, D.E. and Diamond, M.I. (2007) Soluble androgen receptor oligomers underlie pathology in a mouse model of spinobulbar muscular atrophy. *J Biol Chem*, **282**, 3157-3164.
- Li, M., Miwa, S., Kobayashi, Y., Merry, D.E., Yamamoto, M., Tanaka, F., Doyu, M., Hashizume, Y., Fischbeck, K.H. and Sobue, G. (1998a) Nuclear inclusions of the androgen receptor protein in spinal and bulbar muscular atrophy. *Annals of Neurology*, **44**, 249-254.
- Li, M., Nakagomi, Y., Kobayashi, Y., Merry, D.E., Tanaka, F., Doyu, M., Mitsuma, T., Hashizume, Y., Fischbeck, K.H. and Sobue, G. (1998b) Nonneural nuclear inclusions of androgen receptor protein in spinal and bulbar muscular atrophy. *American Journal of Pathology*, **153**, 695-701.
- Li, S.H. and Li, X.J. (2004) Huntingtin-protein interactions and the pathogenesis of Huntington's disease. *Trends Genet*, **20**, 146-154.
- Li, X.J., Li, S.H., Sharp, A.H., Nucifora, F.C., Schilling, G., Lanahan, A., Worley, P., Snyder, S.H. and Ross, C.A. (1995) A huntingtin-associated protein enriched in brain with implications for pathology. *Nature*, **378**, 398-402.
- Lipinski, C.A., Lombardo, F., Dominy, B.W. and Feeney, P.J. (2001) Experimental and computational approaches to estimate solubility and permeability in drug discovery and development settings. *Adv Drug Deliv Rev*, **46**, 3-26.
- Lubahn, D.B., Joseph, D.R., Sullivan, P.M., Willard, H.F., French, F.S. and Wilson, E.M. (1988) Cloning of human androgen receptor complementary DNA and localization to the X chromosome. *Science*, **240**, 327-330.
- Lunkes, A., Lindenberg, K.S., Ben-Haiem, L., Weber, C., Devys, D., Landwehrmeyer, G.B., Mandel, J.L. and Trottier, Y. (2002) Proteases acting on mutant huntingtin generate cleaved products that differentially build up cytoplasmic and nuclear inclusions. *Mol Cell*, **10**, 259-269.
- Lyon, M.F. and Hawkes, S.G. (1970) X-linked gene for testicular feminization in the mouse. *Nature*, **227**, 1217-1219.
- Ma, D. (2001) Applications of yeast in drug discovery. *Prog Drug Res*, **57**, 117-162.

- MacLean, H.E., Choi, W.T., Rekaris, G., Warne, G.L. and Zajac, J.D. (1995) Abnormal androgen receptor binding affinity in subjects with Kennedy's disease (spinal and bulbar muscular atrophy). *Journal of Clinical Endocrinology & Metabolism*, **80**, 508-516.
- Madeo, F., Herker, E., Maldener, C., Wissing, S., Lachelt, S., Herlan, M., Fehr, M., Lauber, K., Sigrist, S.J., Wesselborg, S. and Frohlich, K.U. (2002) A caspase-related protease regulates apoptosis in yeast. *Molecular Cell*, **9**, 911-917.
- Maier, T., Ferbitz, L., Deuerling, E. and Ban, N. (2005) A cradle for new proteins: trigger factor at the ribosome. *Current Opinion in Structural Biology*, **15**, 204-212.
- Malisaukas, M., Ostman, J., Darinskas, A., Zamotin, V., Liutkevicius, E., Lundgren, E. and Morozova-Roche, L.A. (2005) Does the cytotoxic effect of transient amyloid oligomers from common equine lysozyme in vitro imply innate amyloid toxicity? *Journal of Biological Chemistry*, **280**, 6269-6275.
- Mangiarini, L., Sathasivam, K., Seller, M., Cozens, B., Harper, A., Hetherington, C., Lawton, M., Trotter, Y., Lehrach, H., Davies, S.W. and Bates, G.P. (1996) Exon 1 of the HD gene with an expanded CAG repeat is sufficient to cause a progressive neurological phenotype in transgenic mice. *Cell*, **87**, 493-506.
- Martin, J.B. and Gusella, J.F. (1986) Huntington's disease. Pathogenesis and management. *N Engl J Med*, **315**, 1267-1276.
- Martin-Benito, J., Boskovic, J., Gomez-Puertas, P., Carrascosa, J.L., Simons, C.T., Lewis, S.A., Bartolini, F., Cowan, N.J. and Valpuesta, J.M. (2002) Structure of eukaryotic prefoldin and of its complexes with unfolded actin and the cytosolic chaperonin CCT. *EMBO Journal*, **21**, 6377-6386.
- McCampbell, A., Taylor, J.P., Taye, A.A., Robitschek, J., Li, M., Walcott, J., Merry, D., Chai, Y., Paulson, H., Sobue, G. and Fischbeck, K.H. (2000) CREB-binding protein sequestration by expanded polyglutamine. *Human Molecular Genetics*, **9**, 2197-2202.
- Meriin, A.B., Zhang, X., He, X., Newnam, G.P., Chernoff, Y.O. and Sherman, M.Y. (2002) Huntington toxicity in yeast model depends on polyglutamine aggregation mediated by a prion-like protein Rnq1. [erratum appears in J Cell Biol 2002 Aug 5;158(3):591]. *Journal of Cell Biology*, **157**, 997-1004.
- Merry, D.E., Kobayashi, Y., Bailey, C.K., Taye, A.A. and Fischbeck, K.H. (1998) Cleavage, aggregation and toxicity of the expanded androgen receptor in spinal and bulbar muscular atrophy. *Human Molecular Genetics*, **7**, 693-701.
- Meyer, A.S., Gillespie, J.R., Walther, D., Millet, I.S., Doniach, S. and Frydman, J. (2003) Closing the folding chamber of the eukaryotic chaperonin requires the transition state of ATP hydrolysis. *Cell*, **113**, 369-381.
- Michalik, A. and Van Broeckhoven, C. (2003) Pathogenesis of polyglutamine disorders: aggregation revisited. *Hum Mol Genet*, **12 Spec No 2**, R173-186.
- Miller, V.M., Nelson, R.F., Gouvion, C.M., Williams, A., Rodriguez-Lebron, E., Harper, S.Q., Davidson, B.L., Rebagliati, M.R. and Paulson, H.L. (2005) CHIP suppresses polyglutamine aggregation and toxicity in vitro and in vivo. *Journal of Neuroscience*, **25**, 9152-9161.

- Minton, A.P. (2001) The influence of macromolecular crowding and macromolecular confinement on biochemical reactions in physiological media. *Journal of Biological Chemistry*, **276**, 10577-10580.
- Modregger, J., DiProspero, N.A., Charles, V., Tagle, D.A. and Plomann, M. (2002) PACSIN 1 interacts with huntingtin and is absent from synaptic varicosities in presymptomatic Huntington's disease brains. *Hum Mol Genet*, **11**, 2547-2558.
- Moechars, D., Dewachter, I., Lorent, K., Reverse, D., Baekelandt, V., Naidu, A., Tesseur, I., Spittaels, K., Haute, C.V., Checler, F., Godaux, E., Cordell, B. and Van Leuven, F. (1999) Early phenotypic changes in transgenic mice that overexpress different mutants of amyloid precursor protein in brain. *Journal of Biological Chemistry*, **274**, 6483-6492.
- Monoï, H., Futaki, S., Kugimiya, S., Minakata, H. and Yoshihara, K. (2000) Poly-L-glutamine forms cation channels: relevance to the pathogenesis of the polyglutamine diseases. *Biophys J*, **78**, 2892-2899.
- Mooradian, A.D., Morley, J.E. and Korenman, S.G. (1987) Biological actions of androgens. *Endocrine Reviews*, **8**, 1-28.
- Muchowski, P.J., Schaffar, G., Sittler, A., Wanker, E.E., Hayer-Hartl, M.K. and Hartl, F.U. (2000) Hsp70 and hsp40 chaperones can inhibit self-assembly of polyglutamine proteins into amyloid-like fibrils. *Proc Natl Acad Sci U S A*, **97**, 7841-7846.
- Muchowski, P.J. and Wacker, J.L. (2005) Modulation of neurodegeneration by molecular chaperones. *Nat Rev Neurosci*, **6**, 11-22.
- Mullins, M.C., Hammerschmidt, M., Haffter, P. and Nusslein-Volhard, C. (1994) Large-scale mutagenesis in the zebrafish: in search of genes controlling development in a vertebrate. *Curr Biol*, **4**, 189-202.
- Mumberg, D., Muller, R. and Funk, M. (1994) Regulatable promoters of *Saccharomyces cerevisiae*: comparison of transcriptional activity and their use for heterologous expression. *Nucleic Acids Research*, **22**, 5767-5768.
- Nagai, Y., Fujikake, N., Ohno, K., Higashiyama, H., Popiel, H.A., Rahadian, J., Yamaguchi, M., Strittmatter, W.J., Burke, J.R. and Toda, T. (2003) Prevention of polyglutamine oligomerization and neurodegeneration by the peptide inhibitor QBP1 in *Drosophila*. *Hum Mol Genet*, **12**, 1253-1259.
- Nagai, Y., Inui, T., Popiel, H.A., Fujikake, N., Hasegawa, K., Urade, Y., Goto, Y., Naiki, H. and Toda, T. (2007) A toxic monomeric conformer of the polyglutamine protein. *Nat Struct Mol Biol*, **14**, 332-340.
- Naiki, H., Gejyo, F. and Nakakuki, K. (1997) Concentration-dependent inhibitory effects of apolipoprotein E on Alzheimer's beta-amyloid fibril formation in vitro. *Biochemistry*, **36**, 6243-6250.
- Nellemann, C., Abell, K., Norremolle, A., Lokkegaard, T., Naver, B., Ropke, C., Rygaard, J., Sorensen, S.A. and Hasholt, L. (2000) Inhibition of Huntington synthesis by antisense oligodeoxynucleotides. *Mol Cell Neurosci*, **16**, 313-323.
- Nguyen, H.D. and Hall, C.K. (2004) Molecular dynamics simulations of spontaneous fibril formation by random-coil peptides. *Proceedings of the National Academy of Sciences of the United States of America*, **101**, 16180-16185.

- Nucifora, F.C., Jr., Sasaki, M., Peters, M.F., Huang, H., Cooper, J.K., Yamada, M., Takahashi, H., Tsuji, S., Troncoso, J., Dawson, V.L., Dawson, T.M. and Ross, C.A. (2001) Interference by huntingtin and atrophin-1 with cbp-mediated transcription leading to cellular toxicity. *Science*, **291**, 2423-2428.
- Oliveira, J.M.A., Chen, S., Almeida, S., Riley, R., Goncalves, J., Oliveira, C.R., Hayden, M.R., Nicholls, D.G., Ellerby, L.M. and Rego, A.C. (2006) Mitochondrial-dependent Ca²⁺ handling in Huntington's disease striatal cells: Effect of histone deacetylase inhibitors. *Journal of Neuroscience*, **26**, 11174-11186.
- Oliveira, J.M.A., Jekabsons, M.B., Chen, S., Lin, A., Rego, A.C., Goncalves, J., Ellerby, L.M. and Nicholls, D.G. (2007) Mitochondrial dysfunction in Huntington's disease: the bioenergetics of isolated and in situ mitochondria from transgenic mice. *Journal of Neurochemistry*, **101**, 241-249.
- Orr, H.T. and Zoghbi, H.Y. (2001) SCA1 molecular genetics: a history of a 13 year collaboration against glutamines. *Human Molecular Genetics*, **10**, 2307-2311.
- Otzen, D.E., Kristensen, O. and Oliveberg, M. (2000) Designed protein tetramer zipped together with a hydrophobic Alzheimer homology: a structural clue to amyloid assembly. *Proceedings of the National Academy of Sciences of the United States of America*, **97**, 9907-9912.
- Pandey, U.B., Nie, Z., Batlevi, Y., McCray, B.A., Ritson, G.P., Nedelsky, N.B., Schwartz, S.L., DiProspero, N.A., Knight, M.A., Schuldiner, O., Padmanabhan, R., Hild, M., Berry, D.L., Garza, D., Hubbert, C.C., Yao, T.P., Baehrecke, E.H. and Taylor, J.P. (2007) HDAC6 rescues neurodegeneration and provides an essential link between autophagy and the UPS. *Nature*, **447**, 860-864.
- Papalexi, E., Persson, A., Bjorkqvist, M., Petersen, A., Woodman, B., Bates, G.P., Sundler, F., Mulder, H., Brundin, P. and Popovic, N. (2005) Reduction of GnRH and infertility in the R6/2 mouse model of Huntington's disease. *Eur J Neurosci*, **22**, 1541-1546.
- Pedersen, J.S., Christensen, G. and Otzen, D.E. (2004) Modulation of S6 fibrillation by unfolding rates and gatekeeper residues. *Journal of Molecular Biology*, **341**, 575-588.
- Pedersen, J.S., Dikov, D., Flink, J.L., Hjuler, H.A., Christiansen, G. and Otzen, D.E. (2006) The changing face of glucagon fibrillation: structural polymorphism and conformational imprinting. *Journal of Molecular Biology*, **355**, 501-523.
- Perez, M.K., Paulson, H.L., Pendse, S.J., Saionz, S.J., Bonini, N.M. and Pittman, R.N. (1998) Recruitment and the role of nuclear localization in polyglutamine-mediated aggregation. *Journal of Cell Biology*, **143**, 1457-1470.
- Perez-Navarro, E., Akerud, P., Marco, S., Canals, J.M., Tolosa, E., Arenas, E. and Alberch, J. (2000) Neurturin protects striatal projection neurons but not interneurons in a rat model of Huntington's disease. *Neuroscience*, **98**, 89-96.
- Peters, M.F., Nucifora, F.C., Jr., Kushi, J., Seaman, H.C., Cooper, J.K., Herring, W.J., Dawson, V.L., Dawson, T.M. and Ross, C.A. (1999) Nuclear targeting of mutant Huntingtin increases toxicity. *Mol Cell Neurosci*, **14**, 121-128.
- Petersen, A. and Brundin, P. (1999) Effects of ciliary neurotrophic factor on excitotoxicity and calcium-ionophore A23187-induced cell death in cultured embryonic striatal neurons. *Exp Neurol*, **160**, 402-412.

- Petty, S.A., Adalsteinsson, T. and Decatur, S.M. (2005) Correlations among morphology, beta-sheet stability, and molecular structure in prion peptide aggregates. *Biochemistry*, **44**, 4720-4726.
- Picard, D. (2006) Chaperoning steroid hormone action. *Trends in Endocrinology & Metabolism*, **17**, 229-235.
- Piccioni, F., Pinton, P., Simeoni, S., Pozzi, P., Fascio, U., Vismara, G., Martini, L., Rizzuto, R. and Poletti, A. (2002) Androgen receptor with elongated polyglutamine tract forms aggregates that alter axonal trafficking and mitochondrial distribution in motor neuronal processes. *Faseb J*, **16**, 1418-1420.
- Piccioni, F., Simeoni, S., Andriola, I., Armatura, E., Bassanini, S., Pozzi, P. and Poletti, A. (2001) Polyglutamine tract expansion of the androgen receptor in a motoneuronal model of spinal and bulbar muscular atrophy. *Brain Research Bulletin*, **56**, 215-220.
- Pickart, C.M. and Cohen, R.E. (2004) Proteasomes and their kin: proteases in the machine age. *Nature Reviews Molecular Cell Biology*, **5**, 177-187.
- Pinsky, L., Trifiro, M., Kaufman, M., Beitel, L.K., Mhatre, A., Kazemi-Esfarjani, P., Sabbaghian, N., Lumbroso, R., Alvarado, C. and Vasiliou, M. (1992) Androgen resistance due to mutation of the androgen receptor. *Clinical & Investigative Medicine - Medecine Clinique et Experimentale*, **15**, 456-472.
- Plakoutsi, G., Bemporad, F., Calamai, M., Taddei, N., Dobson, C.M. and Chiti, F. (2005) Evidence for a mechanism of amyloid formation involving molecular reorganisation within native-like precursor aggregates. *Journal of Molecular Biology*, **351**, 910-922.
- Poirier, M.A., Li, H., Macosko, J., Cai, S., Amzel, M. and Ross, C.A. (2002) Huntingtin spheroids and protofibrils as precursors in polyglutamine fibrilization. *J Biol Chem*, **277**, 41032-41037.
- Pratt, W.B., Galigniana, M.D., Morishima, Y. and Murphy, P.J. (2004) Role of molecular chaperones in steroid receptor action. *Essays Biochem*, **40**, 41-58.
- Pratt, W.B. and Toft, D.O. (1997) Steroid receptor interactions with heat shock protein and immunophilin chaperones. *Endocr Rev*, **18**, 306-360.
- Preisinger, E., Jordan, B.M., Kazantsev, A. and Housman, D. (1999) Evidence for a recruitment and sequestration mechanism in Huntington's disease. *Philosophical Transactions of the Royal Society of London - Series B: Biological Sciences*, **354**, 1029-1034.
- Prescott, J. and Coetzee, G.A. (2006) Molecular chaperones throughout the life cycle of the androgen receptor. *Cancer Letters*, **231**, 12-19.
- Radford, S.E., Dobson, C.M. and Evans, P.A. (1992) The folding of hen lysozyme involves partially structured intermediates and multiple pathways.[see comment]. *Nature*, **358**, 302-307.
- Raffen, R., Dieckman, L.J., Szpunar, M., Wunschl, C., Pokkuluri, P.R., Dave, P., Wilkins Stevens, P., Cai, X., Schiffer, M. and Stevens, F.J. (1999) Physicochemical consequences of amino acid variations that contribute to fibril formation by immunoglobulin light chains. *Protein Science*, **8**, 509-517.

- Rajan, R.S., Illing, M.E., Bence, N.F. and Kopito, R.R. (2001) Specificity in intracellular protein aggregation and inclusion body formation. *Proceedings of the National Academy of Sciences of the United States of America*, **98**, 13060-13065.
- Rajender, S., Singh, L. and Thangaraj, K. (2007) Phenotypic heterogeneity of mutations in androgen receptor gene. *Asian J Androl*, **9**, 147-179.
- Rassow, J., Voos, W. and Pfanner, N. (1995) Partner proteins determine multiple functions of Hsp70. *Trends Cell Biol*, **5**, 207-212.
- Ravikumar, B., Duden, R. and Rubinsztein, D.C. (2002) Aggregate-prone proteins with polyglutamine and polyalanine expansions are degraded by autophagy. *Human Molecular Genetics*, **11**, 1107-1117.
- Ravikumar, B., Vacher, C., Berger, Z., Davies, J.E., Luo, S.Q., Oroz, L.G., Scaravilli, F., Easton, D.F., Duden, R., O'Kane, C.J. and Rubinsztein, D.C. (2004) Inhibition of mTOR induces autophagy and reduces toxicity of polyglutamine expansions in fly and mouse models of Huntington disease. *Nature Genetics*, **36**, 585-595.
- Richter, K. and Buchner, J. (2001) Hsp90: chaperoning signal transduction. *Journal of Cellular Physiology*, **188**, 281-290.
- Rigamonti, D., Bauer, J.H., De-Fraja, C., Conti, L., Sipione, S., Sciorati, C., Clementi, E., Hackam, A., Hayden, M.R., Li, Y., Cooper, J.K., Ross, C.A., Govoni, S., Vincenz, C. and Cattaneo, E. (2000) Wild-type huntingtin protects from apoptosis upstream of caspase-3. *J Neurosci*, **20**, 3705-3713.
- Riley, B.E. and Orr, H.T. (2006) Polyglutamine neurodegenerative diseases and regulation of transcription: assembling the puzzle. *Genes & Development*, **20**, 2183-2192.
- Romisch, K. (2005) Endoplasmic reticulum-associated degradation. *Annual Review of Cell & Developmental Biology*, **21**, 435-456.
- Ross, C.A. and Poirier, M.A. (2005) Opinion: What is the role of protein aggregation in neurodegeneration? *Nat Rev Mol Cell Biol*, **6**, 891-898.
- Rubinstein, A.L. (2003) Zebrafish: from disease modeling to drug discovery. *Curr Opin Drug Discov Devel*, **6**, 218-223.
- Rubinsztein, D.C. (2002) Lessons from animal models of Huntington's disease. *Trends Genet*, **18**, 202-209.
- Rubinsztein, D.C., Gestwicki, J.E., Murphy, L.O. and Klionsky, D.J. (2007) Potential therapeutic applications of autophagy. *Nature Reviews, Drug Discovery*, **6**, 304-312.
- Rudiger, S., Schneider-Mergener, J. and Bukau, B. (2001) Its substrate specificity characterizes the DnaJ co-chaperone as a scanning factor for the DnaK chaperone. *EMBO Journal*, **20**, 1042-1050.
- Saiki, M., Honda, S., Kawasaki, K., Zhou, D., Kaito, A., Konakahara, T. and Morii, H. (2005) Higher-order molecular packing in amyloid-like fibrils constructed with linear arrangements of hydrophobic and hydrogen-bonding side-chains. *Journal of Molecular Biology*, **348**, 983-998.

- Sakahira, H., Breuer, P., Hayer-Hartl, M.K. and Hartl, F.U. (2002a) Molecular chaperones as modulators of polyglutamine protein aggregation and toxicity. *Proc Natl Acad Sci U S A*, **99 Suppl 4**, 16412-16418.
- Sakahira, H., Breuer, P., Hayer-Hartl, M.K. and Hartl, F.U. (2002b) Molecular chaperones as modulators of polyglutamine protein aggregation and toxicity. *Proceedings of the National Academy of Sciences of the United States of America*, **99 Suppl 4**, 16412-16418.
- Sanchez, I., Mahlke, C. and Yuan, J. (2003) Pivotal role of oligomerization in expanded polyglutamine neurodegenerative disorders. *Nature*, **421**, 373-379.
- Saric, T., Graef, C.I. and Goldberg, A.L. (2004) Pathway for degradation of peptides generated by proteasomes: a key role for thimet oligopeptidase and other metallopeptidases. *Journal of Biological Chemistry*, **279**, 46723-46732.
- Sartor, O., Zheng, Q. and Eastham, J.A. (1999) Androgen receptor gene CAG repeat length varies in a race-specific fashion in men without prostate cancer. *Urology*, **53**, 378-380.
- Sathasivam, K., Hobbs, C., Mangiarini, L., Mahal, A., Turmaine, M., Doherty, P., Davies, S.W. and Bates, G.P. (1999) Transgenic models of Huntington's disease. *Philos Trans R Soc Lond B Biol Sci*, **354**, 963-969.
- Satyal, S.H., Schmidt, E., Kitagawa, K., Sondheimer, N., Lindquist, S., Kramer, J.M. and Morimoto, R.I. (2000) Polyglutamine aggregates alter protein folding homeostasis in *Caenorhabditis elegans*. *Proc Natl Acad Sci U S A*, **97**, 5750-5755.
- Saudou, F., Finkbeiner, S., Devys, D. and Greenberg, M.E. (1998) Huntingtin acts in the nucleus to induce apoptosis but death does not correlate with the formation of intranuclear inclusions. *Cell*, **95**, 55-66.
- Schaffar, G., Breuer, P., Boteva, R., Behrends, C., Tzvetkov, N., Strippel, N., Sakahira, H., Siegers, K., Hayer-Hartl, M. and Hartl, F.U. (2004) Cellular toxicity of polyglutamine expansion proteins: Mechanism of transcription factor deactivation. *Molecular Cell*, **15**, 95-105.
- Scherzinger, E., Lurz, R., Turmaine, M., Mangiarini, L., Hollenbach, B., Hasenbank, R., Bates, G.P., Davies, S.W., Lehrach, H. and Wanker, E.E. (1997) Huntingtin-encoded polyglutamine expansions form amyloid-like protein aggregates in vitro and in vivo. *Cell*, **90**, 549-558.
- Schmidt, B.J., Greenberg, C.R., Allingham-Hawkins, D.J. and Spriggs, E.L. (2002) Expression of X-linked bulbospinal muscular atrophy (Kennedy disease) in two homozygous women. *Neurology*, **59**, 770-772.
- Schmittschmitt, J.P. and Scholtz, J.M. (2003) The role of protein stability, solubility, and net charge in amyloid fibril formation. *Protein Science*, **12**, 2374-2378.
- Schroder, M. and Kaufman, R.J. (2005) The mammalian unfolded protein response. *Annual Review of Biochemistry*, **74**, 739-789.
- Seo, H., Sonntag, K.C., Kim, W., Cattaneo, E. and Isacson, O. (2007) Proteasome Activator Enhances Survival of Huntington's Disease Neuronal Model Cells. *PLoS ONE*, **2**, e238.
- Serio, T.R., Cashikar, A.G., Kowal, A.S., Sawicki, G.J., Moslehi, J.J., Serpell, L., Arnsdorf, M.F. and Lindquist, S.L. (2000) Nucleated conformational conversion and the replication of conformational information by a prion determinant. *Science*, **289**, 1317-1321.

- Serpell, L.C., Sunde, M., Benson, M.D., Tennent, G.A., Pepys, M.B. and Fraser, P.E. (2000) The protofilament substructure of amyloid fibrils. *Journal of Molecular Biology*, **300**, 1033-1039.
- Sha, B., Lee, S. and Cyr, D.M. (2000) The crystal structure of the peptide-binding fragment from the yeast Hsp40 protein Sis1.[see comment]. *Structure*, **8**, 799-807.
- Shatkina, L., Mink, S., Rogatsch, H., Klocker, H., Langer, G., Nestl, A. and Cato, A.C. (2003) The cochaperone Bag-1L enhances androgen receptor action via interaction with the NH2-terminal region of the receptor. *Mol Cell Biol*, **23**, 7189-7197.
- Shimohata, M., Shimohata, T., Igarashi, S., Naruse, S. and Tsuji, S. (2005) Interference of CREB-dependent transcriptional activation by expanded polyglutamine stretches--augmentation of transcriptional activation as a potential therapeutic strategy for polyglutamine diseases. *J Neurochem*, **93**, 654-663.
- Sikorski, R.S. and Hieter, P. (1989) A system of shuttle vectors and yeast host strains designed for efficient manipulation of DNA in *Saccharomyces cerevisiae*. *Genetics*, **122**, 19-27.
- Simental, J.A., Sar, M., Lane, M.V., French, F.S. and Wilson, E.M. (1991) Transcriptional activation and nuclear targeting signals of the human androgen receptor. *J Biol Chem*, **266**, 510-518.
- Singaraja, R.R., Hadano, S., Metzler, M., Givan, S., Wellington, C.L., Warby, S., Yanai, A., Gutekunst, C.A., Leavitt, B.R., Yi, H., Fichter, K., Gan, L., McCutcheon, K., Chopra, V., Michel, J., Hersch, S.M., Ikeda, J.E. and Hayden, M.R. (2002) HIP14, a novel ankyrin domain-containing protein, links huntingtin to intracellular trafficking and endocytosis. *Hum Mol Genet*, **11**, 2815-2828.
- Singh, R., Artaza, J.N., Taylor, W.E., Braga, M., Yuan, X., Gonzalez-Cadavid, N.F. and Bhasin, S. (2006) Testosterone inhibits adipogenic differentiation in 3T3-L1 cells: nuclear translocation of androgen receptor complex with beta-catenin and T-cell factor 4 may bypass canonical Wnt signaling to down-regulate adipogenic transcription factors. *Endocrinology*, **147**, 141-154.
- Sipe, J.D. and Cohen, A.S. (2000) Review: history of the amyloid fibril. *Journal of Structural Biology*, **130**, 88-98.
- Sirangelo, I., Malmo, C., Iannuzzi, C., Mezzogiorno, A., Bianco, M.R., Papa, M. and Irace, G. (2004) Fibrillogenesis and cytotoxic activity of the amyloid-forming apomyoglobin mutant W7FW14F. *Journal of Biological Chemistry*, **279**, 13183-13189.
- Slow, E.J., Graham, R.K., Osmand, A.P., Devon, R.S., Lu, G., Deng, Y., Pearson, J., Vaid, K., Bissada, N., Wetzel, R., Leavitt, B.R. and Hayden, M.R. (2005) Absence of behavioral abnormalities and neurodegeneration in vivo despite widespread neuronal huntingtin inclusions. *Proceedings of the National Academy of Sciences of the United States of America*, **102**, 11402-11407.
- Smith, D.F. (1993) Dynamics of heat shock protein 90-progesterone receptor binding and the disactivation loop model for steroid receptor complexes. *Mol Endocrinol*, **7**, 1418-1429.
- Smith, D.F. and Toft, D.O. (1993) Steroid receptors and their associated proteins. *Mol Endocrinol*, **7**, 4-11.

- Sobue, G., Doyu, M., Kachi, T., Yasuda, T., Mukai, E., Kumagai, T. and Mitsuma, T. (1993) Subclinical phenotypic expressions in heterozygous females of X-linked recessive bulbospinal neuronopathy. *Journal of the Neurological Sciences*, **117**, 74-78.
- Sobue, G., Hashizume, Y., Mukai, E., Hirayama, M., Mitsuma, T. and Takahashi, A. (1989) X-linked recessive bulbospinal neuronopathy. A clinicopathological study. *Brain*, **112** (Pt 1), 209-232.
- Sopher, B.L., Thomas, P.S., Jr., LaFevre-Bernt, M.A., Holm, I.E., Wilke, S.A., Ware, C.B., Jin, L.W., Libby, R.T., Ellerby, L.M. and La Spada, A.R. (2004) Androgen receptor YAC transgenic mice recapitulate SBMA motor neuronopathy and implicate VEGF164 in the motor neuron degeneration.[see comment]. *Neuron*, **41**, 687-699.
- Stefani, M. (2004) Protein misfolding and aggregation: new examples in medicine and biology of the dark side of the protein world. *Biochimica et Biophysica Acta*, **1739**, 5-25.
- Stenoien, D.L., Cummings, C.J., Adams, H.P., Mancini, M.G., Patel, K., DeMartino, G.N., Marcelli, M., Weigel, N.L. and Mancini, M.A. (1999) Polyglutamine-expanded androgen receptors form aggregates that sequester heat shock proteins, proteasome components and SRC-1, and are suppressed by the HDJ-2 chaperone. *Human Molecular Genetics*, **8**, 731-741.
- Stork, M., Giese, A., Kretschmar, H.A. and Tavan, P. (2005) Molecular dynamics simulations indicate a possible role of parallel beta-helices in seeded aggregation of poly-Gln. *Biophys J.*, **88**, 2442-2451.
- Strong, T.V., Tagle, D.A., Valdes, J.M., Elmer, L.W., Boehm, K., Swaroop, M., Kaatz, K.W., Collins, F.S. and Albin, R.L. (1993) Widespread expression of the human and rat Huntington's disease gene in brain and nonneural tissues. *Nat Genet*, **5**, 259-265.
- Sugars, K.L. and Rubinsztein, D.C. (2003) Transcriptional abnormalities in Huntington disease. *Trends Genet*, **19**, 233-238.
- Sunde, M. and Blake, C. (1997) The structure of amyloid fibrils by electron microscopy and X-ray diffraction. *Advances in Protein Chemistry*, **50**, 123-159.
- Takahashi, Y., Okamoto, Y., Popiel, H.A., Fujikake, N., Toda, T., Kinjo, M. and Nagai, Y. (2007) Detection of polyglutamine protein oligomers in cells by fluorescence correlation spectroscopy. *J Biol Chem*, **282**, 24039-24048.
- Takeyama, K., Ito, S., Yamamoto, A., Tanimoto, H., Furutani, T., Kanuka, H., Miura, M., Tabata, T. and Kato, S. (2002) Androgen-dependent neurodegeneration by polyglutamine-expanded human androgen receptor in *Drosophila*. *Neuron*, **35**, 855-864.
- Thomas, P.S., Fraley, G.S., Damien, V., Woodke, L.B., Zapata, F., Sopher, B.L., Plymate, S.R. and La Spada, A.R. (2006) Loss of endogenous androgen receptor protein accelerates motor neuron degeneration and accentuates androgen insensitivity in a mouse model of X-linked spinal and bulbar muscular atrophy. *Human Molecular Genetics*, **15**, 2225-2238.
- Towbin, H., Staehelin, T. and Gordon, J. (1979) Electrophoretic transfer of proteins from polyacrylamide gels to nitrocellulose sheets: procedure and some applications. *Proc Natl Acad Sci U S A*, **76**, 4350-4354.
- Trottier, Y., Devys, D., Imbert, G., Saudou, F., An, I., Lutz, Y., Weber, C., Agid, Y., Hirsch, E.C. and Mandel, J.L. (1995) Cellular localization of the huntingtons disease protein and discrimination of the normal and mutated form. *Nature Genetics*, **10**, 104-110.

- Truant, R., Atwal, R.S. and Burtnik, A. (2007) Nucleocytoplasmic trafficking and transcription effects of huntingtin in Huntington's disease. *Prog Neurobiol*, **83**, 211-227.
- Trushina, E. and McMurray, C.T. (2007) Oxidative stress and mitochondrial dysfunction in neurodegenerative diseases. *Neuroscience*, **145**, 1233-1248.
- Tut, T.G., Ghadessy, F.J., Trifiro, M.A., Pinsky, L. and Yong, E.L. (1997) Long polyglutamine tracts in the androgen receptor are associated with reduced trans-activation, impaired sperm production, and male infertility. *Journal of Clinical Endocrinology & Metabolism*, **82**, 3777-3782.
- Tycko, R. (2004) Progress towards a molecular-level structural understanding of amyloid fibrils. *Current Opinion in Structural Biology*, **14**, 96-103.
- Uversky, V.N. and Fink, A.L. (2004) Conformational constraints for amyloid fibrillation: the importance of being unfolded. *Biochimica et Biophysica Acta*, **1698**, 131-153.
- Uversky, V.N., Li, J., Souillac, P., Millett, I.S., Doniach, S., Jakes, R., Goedert, M. and Fink, A.L. (2002) Biophysical properties of the synucleins and their propensities to fibrillate: inhibition of alpha-synuclein assembly by beta- and gamma-synucleins. *Journal of Biological Chemistry*, **277**, 11970-11978.
- Vainberg, I.E., Lewis, S.A., Rommelaere, H., Ampe, C., Vandekerckhove, J., Klein, H.L. and Cowan, N.J. (1998) Prefoldin, a chaperone that delivers unfolded proteins to cytosolic chaperonin. *Cell*, **93**, 863-873.
- van Anken, E. and Braakman, I. (2005a) Endoplasmic reticulum stress and the making of a professional secretory cell. *Critical Reviews in Biochemistry & Molecular Biology*, **40**, 269-283.
- van Anken, E. and Braakman, I. (2005b) Versatility of the endoplasmic reticulum protein folding factory. *Critical Reviews in Biochemistry & Molecular Biology*, **40**, 191-228.
- van der Sar, A.M., Appelmelk, B.J., Vandenbroucke-Grauls, C.M. and Bitter, W. (2004) A star with stripes: zebrafish as an infection model. *Trends Microbiol*, **12**, 451-457.
- Van Raamsdonk, J.M., Gibson, W.T., Pearson, J., Murphy, Z., Lu, G., Leavitt, B.R. and Hayden, M.R. (2006) Body weight is modulated by levels of full-length Huntingtin. *Human Molecular Genetics*, **15**, 1513-1523.
- Van Raamsdonk, J.M., Murphy, Z., Selva, D.M., Hamidizadeh, R., Pearson, J., Petersen, A., Bjorkqvist, M., Muir, C., Mackenzie, I.R., Hammond, G.L., Vogl, A.W., Hayden, M.R. and Leavitt, B.R. (2007) Testicular degeneration in Huntington disease. *Neurobiol Dis*, **26**, 512-520.
- Van Raamsdonk, J.M., Murphy, Z., Slow, E.J., Leavitt, B.R. and Hayden, M.R. (2005) Selective degeneration and nuclear localization of mutant huntingtin in the YAC128 mouse model of Huntington disease. *Human Molecular Genetics*, **14**, 3823-3835.
- Venkatraman, P., Wetzel, R., Tanaka, M., Nukina, N. and Goldberg, A.L. (2004) Eukaryotic proteasomes cannot digest polyglutamine sequences and release them during degradation of polyglutamine-containing proteins. *Molecular Cell*, **14**, 95-104.
- Ventimiglia, R., Mather, P.E., Jones, B.E. and Lindsay, R.M. (1995) The neurotrophins BDNF, NT-3 and NT-4/5 promote survival and morphological and biochemical differentiation of striatal neurons in vitro. *Eur J Neurosci*, **7**, 213-222.

- Vonsattel, J.P., Myers, R.H., Stevens, T.J., Ferrante, R.J., Bird, E.D. and Richardson, E.P., Jr. (1985) Neuropathological classification of Huntington's disease. *J Neuropathol Exp Neurol*, **44**, 559-577.
- Walsh, D.M., Hartley, D.M., Kusumoto, Y., Fezoui, Y., Condron, M.M., Lomakin, A., Benedek, G.B., Selkoe, D.J. and Teplow, D.B. (1999) Amyloid beta-protein fibrillogenesis. Structure and biological activity of protofibrillar intermediates. *Journal of Biological Chemistry*, **274**, 25945-25952.
- Walsh, D.M., Klyubin, I., Fadeeva, J.V., Cullen, W.K., Anwyl, R., Wolfe, M.S., Rowan, M.J. and Selkoe, D.J. (2002) Naturally secreted oligomers of amyloid beta protein potently inhibit hippocampal long-term potentiation in vivo. *Nature*, **416**, 535-539.
- Walsh, D.M., Lomakin, A., Benedek, G.B., Condron, M.M. and Teplow, D.B. (1997) Amyloid beta-protein fibrillogenesis. Detection of a protofibrillar intermediate. *Journal of Biological Chemistry*, **272**, 22364-22372.
- Wang, W., Duan, W.Z., Igarashi, S., Morita, H., Nakamura, M. and Ross, C.A. (2005) Compounds blocking mutant huntingtin toxicity identified using a Huntington's disease neuronal cell model. *Neurobiology of Disease*, **20**, 500-508.
- Wanker, E.E., Rovira, C., Scherzinger, E., Hasenbank, R., Walter, S., Tait, D., Colicelli, J. and Lehrach, H. (1997) HIP-1: a huntingtin interacting protein isolated by the yeast two-hybrid system. *Hum Mol Genet*, **6**, 487-495.
- Warner, C.L., Griffin, J.E., Wilson, J.D., Jacobs, L.D., Murray, K.R., Fischbeck, K.H., Dickoff, D. and Griggs, R.C. (1992) X-linked spinomuscular atrophy: a kindred with associated abnormal androgen receptor binding. *Neurology*, **42**, 2181-2184.
- Warrick, J.M., Chan, H.Y., Gray-Board, G.L., Chai, Y., Paulson, H.L. and Bonini, N.M. (1999) Suppression of polyglutamine-mediated neurodegeneration in *Drosophila* by the molecular chaperone HSP70. *Nat Genet*, **23**, 425-428.
- Waza, M., Adachi, H., Katsuno, M., Minamiyama, M., Sang, C., Tanaka, F., Inukai, A., Doyu, M. and Sobue, G. (2005) 17-AAG, an Hsp90 inhibitor, ameliorates polyglutamine-mediated motor neuron degeneration. *Nature Medicine*, **11**, 1088-1095.
- Webb, J.L., Ravikumar, B., Atkins, J., Skepper, J.N. and Rubinsztein, D.C. (2003) Alpha-Synuclein is degraded by both autophagy and the proteasome. *Journal of Biological Chemistry*, **278**, 25009-25013.
- Wellington, C.L., Ellerby, L.M., Hackam, A.S., Margolis, R.L., Trifiro, M.A., Singaraja, R., McCutcheon, K., Salvesen, G.S., Propp, S.S., Bromm, M., Rowland, K.J., Zhang, T., Rasper, D., Roy, S., Thornberry, N., Pinsky, L., Kakizuka, A., Ross, C.A., Nicholson, D.W., Bredesen, D.E. and Hayden, M.R. (1998) Caspase cleavage of gene products associated with triplet expansion disorders generates truncated fragments containing the polyglutamine tract. *Journal of Biological Chemistry*, **273**, 9158-9167.
- Wellington, C.L. and Hayden, M.R. (2000) Caspases and neurodegeneration: on the cutting edge of new therapeutic approaches. *Clin Genet*, **57**, 1-10.
- Wellington, C.L., Singaraja, R., Ellerby, L., Savill, J., Roy, S., Leavitt, B., Cattaneo, E., Hackam, A., Sharp, A., Thornberry, N., Nicholson, D.W., Bredesen, D.E. and Hayden, M.R. (2000) Inhibiting caspase cleavage of huntingtin reduces toxicity and aggregate formation in neuronal and nonneuronal cells. *J Biol Chem*, **275**, 19831-19838.

- Westermarck, P., Benson, M.D., Buxbaum, J.N., Cohen, A.S., Frangione, B., Ikeda, S., Masters, C.L., Merlini, G., Saraiva, M.J., Sipe, J.D. and Nomenclature Committee of the International Society of, A. (2005) Amyloid: toward terminology clarification. Report from the Nomenclature Committee of the International Society of Amyloidosis. *Amyloid*, **12**, 1-4.
- Wolfgang, W.J., Miller, T.W., Webster, J.M., Huston, J.S., Thompson, L.M., Marsh, J.L. and Messer, A. (2005) Suppression of Huntington's disease pathology in *Drosophila* by human single-chain Fv antibodies. *Proceedings of the National Academy of Sciences of the United States of America*, **102**, 11563-11568.
- Wood, N.I., Pallier, P.N., Wanderer, J. and Morton, A.J. (2007) Systemic administration of Congo red does not improve motor or cognitive function in R6/2 mice. *Neurobiol Dis*, **25**, 342-353.
- Wurth, C., Guimard, N.K. and Hecht, M.H. (2002) Mutations that reduce aggregation of the Alzheimer's A β 42 peptide: an unbiased search for the sequence determinants of A β amyloidogenesis. *Journal of Molecular Biology*, **319**, 1279-1290.
- Wytenbach, A. (2004) Role of heat shock proteins during polyglutamine neurodegeneration: mechanisms and hypothesis. *J Mol Neurosci*, **23**, 69-96.
- Wytenbach, A., Carmichael, J., Swartz, J., Furlong, R.A., Narain, Y., Rankin, J. and Rubinsztein, D.C. (2000) Effects of heat shock, heat shock protein 40 (HDJ-2), and proteasome inhibition on protein aggregation in cellular models of Huntington's disease. *Proc Natl Acad Sci U S A*, **97**, 2898-2903.
- Yaffe, K., Edwards, E.R., Lui, L.Y., Zmuda, J.M., Ferrell, R.E. and Cauley, J.A. (2003) Androgen receptor CAG repeat polymorphism is associated with cognitive function in older men. *Biological Psychiatry*, **54**, 943-946.
- Yamamoto, A., Lucas, J.J. and Hen, R. (2000) Reversal of neuropathology and motor dysfunction in a conditional model of Huntington's disease.[see comment]. *Cell*, **101**, 57-66.
- Yang, H., Zhong, X., Ballar, P., Luo, S., Shen, Y., Rubinsztein, D.C., Monteiro, M.J. and Fang, S. (2007) Ubiquitin ligase Hrd1 enhances the degradation and suppresses the toxicity of polyglutamine-expanded huntingtin. *Exp Cell Res*, **313**, 538-550.
- Yen, L., Strittmatter, S.M. and Kalb, R.G. (1999) Sequence-specific cleavage of Huntingtin mRNA by catalytic DNA. *Ann Neurol*, **46**, 366-373.
- Young, J.C., Agashe, V.R., Siegers, K. and Hartl, F.U. (2004) Pathways of chaperone-mediated protein folding in the cytosol. *Nature Reviews Molecular Cell Biology*, **5**, 781-791.
- Young, J.C. and Hartl, F.U. (2000) Polypeptide release by Hsp90 involves ATP hydrolysis and is enhanced by the co-chaperone p23. *EMBO Journal*, **19**, 5930-5940.
- Young, J.C., Moarefi, I. and Hartl, F.U. (2001) Hsp90: a specialized but essential protein-folding tool. *Journal of Cell Biology*, **154**, 267-273.
- Zhang, Y., Li, M., Drozda, M., Chen, M., Ren, S., Mejia Sanchez, R.O., Leavitt, B.R., Cattaneo, E., Ferrante, R.J., Hayden, M.R. and Friedlander, R.M. (2003) Depletion of wild-type huntingtin in mouse models of neurologic diseases. *J Neurochem*, **87**, 101-106.

-
- Zimmerman, S.B. and Trach, S.O. (1991) Estimation of macromolecule concentrations and excluded volume effects for the cytoplasm of *Escherichia coli*. *Journal of Molecular Biology*, **222**, 599-620.
- Zoghbi, H.Y. and Orr, H.T. (2000) Glutamine repeats and neurodegeneration. *Annual Review of Neuroscience*, **23**, 217-247.
- Zon, L.I. and Peterson, R.T. (2005) In vivo drug discovery in the zebrafish. *Nat Rev Drug Discov*, **4**, 35-44.
- Zuccato, C., Tartari, M., Crotti, A., Goffredo, D., Valenza, M., Conti, L., Cataudella, T., Leavitt, B.R., Hayden, M.R., Timmusk, T., Rigamonti, D. and Cattaneo, E. (2003) Huntingtin interacts with REST/NRSF to modulate the transcription of NRSE-controlled neuronal genes. *Nat Genet*, **35**, 76-83.

7 Appendix

7.1 Abbreviations

Units are expressed according to the international system of units (SI), including outside units accepted for use with the SI. Amino acids are abbreviated with their one or three letter symbols. Protein and gene names are abbreviated according to their SWISSPROT database entries.

ADP	adenosine 5'-diphosphate
AF	activation function
AIS	androgen insensitivity syndrome
AO	Acridine Orange
AR	androgen receptor
ARE	androgen response elements
APS	ammonium peroxodisulfate
ATP	adenosine 5'-triphosphate
BAG1	BCL2-associated athanogene-1
bp	base pair
CAIS	complete androgen insensitivity syndrome
<i>C. elegans</i>	<i>Caenorhabditis elegans</i>
CHIP	carboxyl terminus of HSP70-interacting protein
CMV	cytomegalovirus immediate-early promoter
CIP	calf intestine alkaline phosphatase
Da	Dalton
DBD	DNA-binding domain
ddH ₂ O	double distilled water
DAPI	4,6-diamidin-2-phenylindol
DNA	deoxyribonucleic acid
dNTP	didesoxy-nucleoside triphosphate
DHT	dihydrotestosterone
DMSO	dimethylsulfoxid
<i>D. rerio</i>	<i>Danio rerio</i>
DTT	dithiothreitol

DMEM	Dulbecco's Modified Eagle's Medium
Dox	doxycycline
DRPLA	Dentatorubral-pallidoluysian atrophy
ECL	enhance chemiluminescence
<i>E.coli</i>	<i>Escherichia coli</i>
EDTA	ethylenediaminetetraacetic acid
ER	endoplasmic reticulum
ERAD	ER-associated degradation
FCS	fetal calf serum
FITC	fluorescein-isothiocyanate
FPLC	fast performance liquid chromatography
g	acceleration of gravity, 9.81 m/s ²
Gal	galactose
GFP	green fluorescent protein
Glu	glucose
GuHCL	guanidinium hydrochloride
HD	Huntington's disease
Hip	hsc70 interacting protein
Hop	Hsp-organizing protein
hr	hours
Hsp	heat shock protein
htt	huntingtin
IB	inclusion body
LB	Luria-Bertani
LBD	C-terminal ligand-binding domain
Luc	luciferase
min	minutes
MTT	3-(4,5-Dimethylthiazol-2-yl)-2,5-diphenyltetrazolium bromide
NAC	nascent chain-associated complex
NBB	<i>N'</i> -benzylidene-benzohydrazide
NLS	nuclear localization signal
OD	optical density
P _i	inorganic Phosphate
PBS	phosphate-buffered saline

PEG	polyethylene glycol
PMSF	phenylmethylsulfonyl fluoride
pH	reverse logarithm of relative hydrogen proton (H ⁺) concentration
RAC	ribosome-associated complex
RT	room temperature
SBMA	Spinal bulbar muscular atrophy, Kennedy's disease
<i>S. cerevisiae</i>	<i>Saccharomyces cerevisiae</i>
S.D.	standard deviation
SDS	sodium dodecylsulfate
TAD	N-terminal transactivation domain
TCA	trichloroacetic acid
TEM	transmission electron microscopy
TEMED	N,N,N',N'-tetramethylethylenediamine
tPSA	total polar surface area
Tris	Tris(hydroxymethyl)aminomethane
Triton X-100	octyl phenol ethoxylate
TRP	tetradricopeptide repeat
U	unit
Ub	ubiquitin polypeptide
UPR	unfolded protein response
UPS	ubiquitin-proteasome system
U.S.	United States of America
Tween 20	polyoxyethylen-sorbitan-monolaurate
w/o	without
YFP	yellow fluorescent protein

7.2 Publications and Conference abstracts

7.2.1 Publications

Schiffer, N.W., Broadley, S.A., Hirschberger, T., Tavan, P., Kretzschmar, H.A., Giese, A., Haass, C., Hartl, F.U. and Schmid, B. (2007) Identification of anti-prion compounds as efficient inhibitors of polyglutamine protein aggregation in a zebrafish model. *Journal of Biological Chemistry*, 282, 9195-9203.

7.2.2 Conference abstracts

Schiffer, N. W., Broadley, S. A. and Hartl, F. U.

"N-terminal polyglutamine-containing fragments inhibit androgen receptor transactivation capacity in a yeast model of spinal and bulbar muscular atrophy." The 7. Eibsee Meeting of Alzheimer's Disease ' , November 2007, Eibsee.

Schiffer, N. W., Broadley, S. A. and Hartl, F. U.

"N-terminal polyglutamine-containing fragments inhibit androgen receptor transactivation capacity in a yeast model of spinal and bulbar muscular atrophy." EMBO-FEBS WorksHop on 'Chaperones in Normal & Aberrant Protein Folding, Aging & Cancer', June 2007, Tomar, Portugal.

Schiffer, N. W., Broadley, S. A. and Hartl, F. U.

"A novel yeast model for understanding the molecular mechanism of androgen receptor inactivation in spinal and bulbar muscular atrophy." SFB 594 '2nd International Symposium', May 2007, München.

Schiffer, N. W., Broadley, S. A., Hirschberger, T., Tavan, P., Kretschmar, H. A., Giese, A., Haass C., Hartl, F. U. and Schmid, B. "Identification of anti-prion compounds as efficient inhibitors of polyglutamine protein aggregation in a zebrafish model." 'Neurodegenerative Diseases: Molecular Mechanisms in a Functional Genomics Framework', September 2006, Berlin.

Schiffer, N. W., Broadley, S. A., Hirschberger, T., Tavan, P., Kretschmar, H. A., Giese, A., Haass C., Hartl, F. U. and Schmid, B. "Identification of N'-benzylidene benzohydrazides as inhibitors of aggregation in a zebrafish model of polyglutamine disease." SFB 596 'Molecular mechanisms of neurodegeneration', March 2006, München.

7.3 Curriculum vitae

7.3.1 Personal details

Name	Niclas Wilhelm Schiffer
Date of Birth	January 30, 1978
Place of Birth	Bad Hersfeld
Nationality	German

7.3.2 Education

2003-2008	Graduate Research at the Max-Planck-Institute, Martinsried, Germany: Investigation of the mechanism of toxicity in newly established models of polyglutamine diseases
2003	'Diplom' in Biochemistry, Graduated with honors; University of Bayreuth, Bayreuth, Germany
1998-2003	Undergraduate Research at the University of Bayreuth, Bayreuth, Germany: Analysis of the anti-sigma factor RsiW of <i>Bacillus subtilis</i>
2002	Internship at the University of Granada, Granada, Spain (ERASMUS fellowship): Effects on the stability of <i>Escherichia coli</i> thioredoxin by replacing various glutamate residues by aspartate residues
2002	Internship at Dept. of Microbiology and Analytical Development, B.BRAUN Medical, Rubí, Spain
1997-1998	Military service, Breitenburg and Fritzlar, Germany
1997	Abitur (High School Diploma), Jakob-Grimm-Schule, Rotenburg/F, Germany